Estimation of Soil Shear Strength Parameters from Index Properties Using Artificial Neural Network

Eyael Tenaye Habte

A Thesis Submitted to department of Civil Engineering,
School of Civil Engineering and Architecture

Presented in Partial Fulfillment of the Requirement for the Degree of Master's in Civil Engineering (Geotechnical Engineering)

Office of Graduate Studies
Adama Science and Technology University

June, 2023
Adama, Ethiopia

Estimation of Soil Shear Strength Parameters from Index Properties Using Artificial Neural Network

Eyael Tenaye Habte
Advisor: Dr. Srikanth Vadlamudi (PhD)

A Thesis Submitted to the department of Civil Engineering,
School of Civil Engineering and Architecture

Presented in Partial Fulfillment of the Requirement for the Degree of
Master's in Civil Engineering (Geotechnical Engineering)

Office of Graduate Studies
Adama Science and Technology University

June, 2023

Adama, Ethiopia

DECLARATION

I hereby declare that this Master Thesis entitled "**Estimation of soil shear strength parameters from index properties using Artificial Neural Network**" is my original work. That is, it has not been submitted for the award of any academic degree, diploma or certificate in any other university. All sources of materials that are used for this thesis have been duly acknowledged through citation.

______________________________ ________________________ ______________________

Name of the student Signature Date

RECOMMENDATION

I, the advisor of this thesis, hereby certify that I have read the revised version of the thesis entitled'**Estimation of soil shear strength parameters from index properties using Artificial Neural Network** prepared under my guidance by Eyael Tenaye Habte submitted in partial fulfillment of the requirements for the degree of Master's of Science in Civil Engineering (Geotechnical Engineering) .

Therefore, I recommend the submission of revised version of the thesis to the department following the applicable procedures.

______________________	______________________	______________________
Major Advisor	Signature	Date
______________________	______________________	______________________
Co-advisor	Signature	Date

APPROVAL OF ADVISOR

I, the advisor of the thesis entitled "**Estimation of soil shear strength parameters from index properties using Artificial Neural Network**" and developed by Eyael Tenaye Habte; hereby certify that the recommendation and suggestions made by the board of examiners are appropriately incorporated into the final version of the thesis.

____________________________ ______________________ ____________________

Major Advisor Signature Date

_________________________ ______________________ ____________________

Co-advisor Signature Date

APPROVAL OF THE BOARD OF EXAMINERS

We, the undersigned, members of the Board of Examiners of the thesis by Eyael Tenaye Habte have read and evaluated the thesis entitled **Estimation of soil shear strength parameters from index properties using Artificial Neural Network** and examined the candidate during open defense. This is, therefore, to certify that the thesis is accepted for partial fulfillment of the requirement of the degree of Master of Science in Civil Engineering (Geotechnical Engineering).

______________________	______________________	______________________
Chairperson	Signature	Date
______________________	______________________	______________________
Internal Examiner	Signature	Date
______________________	______________________	______________________
External Examiner	Signature	Date

Finally, approval and acceptance of the thesis is contingent upon submission of its final copy to the Office of Postgraduate Studies (OPGS) through the Department Graduate Council (DGC) and School Graduate Committee (SGC).

______________________	______________________	______________________
Department Head	Signature	Date
______________________	______________________	______________________
School Dean	Signature	Date
______________________	______________________	______________________
Office of Postgraduate Studies, Dean	Signature	Date

AKNOWLEDGEMENT

First and foremost, I would like to express my deepest gratitude to God for guiding me throughout this thesis endeavor. The unwavering faith, strength, and providence I have received from Him have been instrumental in every aspect of this study.

I would like to express my sincere appreciation and gratitude to my advisor Dr. Srikanth Vadlamudi, for his invaluable guidance, support, and expertise throughout the entire study process. His insightful feedback and constructive comment have greatly contributed to the quality and rigor of this study.

I would also like to acknowledge Adama Science and Technology University, Bishoftu Construction Office, Grace and Pier Design Build PLCs of Bishoftu town, and ARCON Design Build PLC who have contributed significantly to the collection of necessary data and also the laboratory work for my study.

Finally, I am grateful to my mother, friends, and colleagues who have supported me throughout this thesis journey. Their encouragement and belief in my abilities have been a constant source of motivation.

TABLE OF CONTENTS

LIST OF TABLES

LIST OF FIGURES

ABBREVIATIONS

AASHTO	American Association of States Highway and Transportation Officials
AI	Artificial Intelligence
ANN	Artificial Neural Network
ASTM	American Society of Testing and Materials
ASTU	Adama Science and Technology University
BD	Bulk Density
BP	Back Propagation
c	Cohesion
Fine %	Fine grained soil content percentage
Gs	Specific gravity
LGP	Linear Genetic Programming
LL	Liquid limit
LLSR	Linear Least Square Regression
MAE	Mean Absolute Error
MLP	Multilayer Perceptron Network
MSE	Mean Squared Error
NN	Neural Network
PI	Plastic index
PL	Plastic limit
R	Correlation coefficient
R^2	Coefficient of determination
RMSE	Root Mean Squared Error
Sand %	Sand sized soil content percentage
USCS	Unified Soil Classification System
ϕ	Internal friction angle
τ	Shear stress
σ_n	Normal stress

ABSTRACT

Shear strength parameters (angle of internal friction and cohesion) are the key engineering properties of soil. In every situation finding these parameters by laboratory testing or by using advanced equipment may be uneconomical for clients during the preliminary design phase. This study is about developing models for predicting the shear strength parameters (cohesion and angle of friction) of soils in Bishoftu town by using artificial neural network modeling technique; with a view to reducing time, effort and cost usually incurred in determining these shear strength parameters in the laboratory for future planning, design and construction projects in the study area. This is done by developing separate neural network models for c and ϕ from the index properties of soil consisting of Sand % (S), Fines % (F), Liquid limit (LL), Plastic limit (PL), and Plasticity Index (PI) as input parameters. A multi-layer perceptron network with feed forward back propagation is used to model varying the number of hidden layers. For this purpose, 316 both primary and secondary soil test result data of index properties and shear strength parameters was used. The geotechnical soil properties are done in accordance with ASTM Standards. Direct shear box method is used to determine soil cohesion and soil internal friction angle. During the testing phase, it was discovered that the developed models were quite successful at predicting shear strength parameters, with correlation values of roughly 0.99 and 0.98 for cohesion and angle of internal friction, respectively. The models are examined using existing correlation techniques and cross validated using primary soil test data. The results have shown that for predicting shear strength parameters, the artificial neural network method provided a better fit and accuracy than the selected empirical methods.

Keywords: ANN, Shear Strength, Cohesion, Friction Angle, Prediction, Index Properties.

1 INTRODUCTION

1.1 Background

Numerous projects must be carried out on or in soils due to the interest in urban area development in plains. Therefore, it is essential for engineering projects to determine the shear strength parameters of soils, such as cohesion and internal friction angle. For instance, it is necessary to determine the bearing capacity for foundation analysis while designing various engineering projects that are executed on soils. These shear strength parameters serve as the basis for the most common bearing capacity estimation techniques, such as the Vesic and Hansen methods (Khanlari et al., 2012). Furthermore, the ability of soil to prevent sliding along internal surfaces within a mass is one of the most important engineering characteristics. The stability of structures built on soil depends on the shearing resistance obtainable by the soil along probable surfaces of slippage. It is quite essential that an engineer has to safeguard the structure is safe against shear catastrophe in the soil that supports it and does not undergo excessive settlement (Bakala et al., 2021). The shearing resistance of the soil along possible slippage surfaces will determine the stability of any building built on soil. Assessment of slope stability, design of retaining walls, embankment dams, bridges, tunnel linings, pavement, and the resistance traction and tillage tools in agricultural applications are all accompanied with the understanding of shear strength of materials (Lyeke et al., 2016).

Shear strength determined on either undisturbed specimens of fine grained soils or disturbed and remolded specimens of fine or coarse grained soils. There are varieties of shear strength tests that can be conducted on soils in the laboratory or field. The triaxial compression test and direct shear test are the two most common tests used for determining the angle of internal friction and cohesion values in the laboratory (Khanlari et al., 2012). Measurement of shear strength parameters both at field and laboratory conditions are cumbersome, expensive, time consuming and labor intensive. Obtaining accurate undisturbed soil samples from the field is also difficult; due to handling, transportation, release of overburden pressure and poor laboratory conditions. In addition, the laboratory equipment and field instruments are not sufficient in developing countries to obtain soil engineering properties, especially strength properties. Thus, Geotechnical engineers usually endeavor to develop statistical models that best fit a particular area and soil type, especially for analysis and design purposes. It is often necessary for the geotechnical engineer to quickly characterize the soil and determine its engineering properties to estimate the soil's appropriateness for any industrial practices (Bakala et al., 2021).

In order to cope with the difficulty of experimental investigation, engineering design models are needed. Correlations and empirical relationships are principally useful in preliminary studies, or when due to time and/or financial constraints that a thorough geotechnical examination cannot to be conducted. This is most relevant in third world countries where up-to-date testing equipment is lacking together with the trained manpower needed to operate them. Empirical correlations are widely used in geotechnical engineering practice as a tool to estimate the engineering properties of soils. Useful correlations exist between the index properties obtained from simple routine testing and the strength properties of soils among others. Several empirical procedures have been developed over the years to estimate the shear strength parameters for soils (Lyeke et al., 2016).

The ability to derive shear strength parameters from the simple index properties of soil has become a persistent demand and area of research interest.As a result, there is currently a global trend toward developing correlation equations between shear strength and index properties of soil (Alves et al.,2016) .Geotechnical engineers usually endeavor to develop statistical models that best fit a particular area and soil type, especially for analysis and design purposes. Many empirical and hyperbolic functions have already been employed for estimating shear strength parametersused statistical approach to determine the shear strength parameters (Lee et al., 2003). Although these methods to some extent are able to predict the soil shear strength, they have certain limitations to predict shear strength parameters for soil mixtures in which it presents both shear resistance parts. For that matter, Artificial Neural Network (ANN) was proposed on shear strength parameters prediction because of the generalization and capacity on modeling complex problems (Sarat Kumar Das, 2013)(Shooshpasha et al., 2015). These days artificial intelligence is playing an important role in the field of engineering, medical science, estimating, planning, credit evaluation, business and marketing etc. Artificial Neural Networks which works on the principle of biological neuron is one of those methods of artificial intelligence. ANN works by learning or training as human mind do (Abdulabbas, A. A.., & Bind, 2014).

1.2 Statement of the Problem

In order to evaluate the soil's suitability for any industrial processes, the geotechnical engineer frequently needs to properly analyze the soil and determine its engineering properties. Most of the time, engineers use other methods in addition to conducting a useful study of a subsurface incident that may have caused the destruction of structures on it when they need to analyze and design engineering structures. The required strength parameters must be determined experimentally, which is time-consuming, costly, and labor-intensive. The laboratory equipment and field instruments are not sufficient in developing countries to obtain soil engineering properties, especially strength properties. Experimental determination of the strength parameters used for design purposes is widespread, challenging to perform, and costly compared to index properties of soils. The difficulty in accurately determining these parameters lies in designing and conducting appropriate laboratory tests that simulate the behavior of the material in real-world conditions. The tests must be designed so that the shear stress response of the material is accurately measured and that the outcomes are representative of the material's behavior in situ. This requires careful selection of testing equipment, test conditions, and sample preparation methods. Due to various factors such as soil type, depth, and location, getting undisturbed samples might be difficult. Larger soil samples ideally yield more reliable results, but obtaining large, undisturbed samples can be challenging and costly. And also it's possible that the testing tools used to measure shear strength parameters aren't always suitable for the specific soil type and conditions. When direct testing is unfeasible or there is a lack of data, empirical correlations are frequently employed to predict shear strength values. Empirical correlations might not always be accurate or applicable to various soil types and conditions. Relying solely on empirical correlations without proper validation and understanding of the underlying soil behavior can lead to inaccurate shear strength parameter estimation. Overall, while determining index properties of soil can be relatively straightforward, accurately estimating shear strength parameters can be more complex and require specialized knowledge and equipment. Engineering design models must be created and used as a tool to estimate the engineering properties of soils in order to overcome such practical challenges. The research aims to overcome the limitations of traditional methods and provide a practical and efficient tool by the development of an accurate and reliable ANN modelfor geotechnical engineers to estimate the shear strength parameters of soils, particularly when direct measurement is not feasible or easy. In addition, this study seeks to develop a relationship between soil index properties and shear strength parameters, which can be used to minimize cost, effort, and time for any geotechnical practice to analyze and design conditions of the study area. In conclusion, it is essential to carefully consider these challenges and use appropriate techniques and methods to ensure accurate and reliable estimation of soil shear strength parameters in geotechnical engineering practice.

1.3 Objective

1.3.1 General Objective

The general objective of this study is to estimate the shear strength parameters of soils from index properties of soil by using Artificial Neural Network (ANN).

1.3.2 Specific Objectives

The specific objectives of this study are:

- To predict the shear strength parameters of soil based on index properties by the developed Artificial Neural Network (ANN) model
- To determine index properties and shear strength parameters of soils of the study area
- To investigate the relationship between index properties and shear strength parameters of soils test results and to identify the most influential index properties for shear strength parameters prediction
- To collect and compile a comprehensive database of soil samples with corresponding index properties and shear strength parameters for training and validation of the ANN model
- To evaluate the performance of the developed ANN model in comparison with existing empirical models and regression methods of estimating shear strength parameters from index properties

1.4 Research Questions

1. What are the key index properties that significantly influence the estimation of soil shear strength parameters?

2. Can artificial neural networks (ANN) accurately predict soil shear strength parameters from index properties?

3. How does the performance of ANN model compare to traditional methods for estimating soil shear strength parameters from index properties?

4. How do the prediction capabilities of ANN compare to other empirical and traditional methods for estimating soil shear strength parameters from index properties?

1.5 Scope of the Study

A broad range of experimental data will be gathered from various Bishoftu construction projects in order to build neural network-based soil models. The soil index properties, which include the liquid limit (LL), plastic limit (PL), plasticity index (PI), sand % (S), and fine% (silt& clay) will be taken into consideration when determining the shear strength parameters. To estimate the internal friction angle and cohesion of soil from the index properties, two distinct neural network models will be created. The American Society for Testing and Materials (ASTM) standards are followed in all transportation and testing procedures.

1.6 Limitation of the study

The limitation of this study was the data availability and quality. The availability and quality of the data used for training and validation determine the reliability and accuracy of ANN-based estimations. The accuracy and generalizability of the ANN model may be impacted by limited or incomplete datasets, inconsistent data quality, or biased data. And also the actual application of ANN-based estimations in geotechnical engineering practice in the real world may have limitations of its own, such as the availability of software, computational resources, and ANN modeling expertise.

1.7 Significance of the study

In determining shear strength parameters for soil's bearing capacity, slope stability, and embankment works, engineers will be benefited by an understanding of the relationship between soil index properties and shear strength parameters. It is possible to develop geotechnical designs that are safer and more reliable by accurately estimating the soil shear strength parameters, which are essential to the design of geotechnical structures including slopes, retaining walls, and foundations. ANN-based estimation methods have the potential to enhance the accuracy of shear strength parameter estimation, providing valuable tools for geotechnical engineers to make informed decisions in design and analysis. Before doing a thorough analysis of the geotechnical properties of the soil, it might be a significant information source for engineers and public building officials. This study will contribute to the advancement of ANN as a powerful computational tool in geotechnical engineering and it provides insights into the potential and limitations of ANN for geotechnical applications and help establish ANN as a reliable and efficient tool in the field. This study developed an artificial neural network model that helped to forecast the shear strength parameters (c and ϕ) from soils' index properties in order to give simple and accurate response for various soil types. Since index properties can be obtained simply with low-cost equipment when compared to strength properties equipment.Consequently, soft computing methods like artificial neural networks (ANN) are a crucial method to predict soils' engineering properties, especially for developing countries like Ethiopia, where there is a financial limitation, lack of test equipment, and limited time, which is used for design purposes. By providing insights on the application of ANN for estimating soil shear strength parameters from index properties, the study can add to the body of knowledge in geotechnical engineering. It can aid in understanding the relationships between index properties and shear strength parameters, the accuracy and limitations of ANN-based methods, and the potential benefits of ANN use in geotechnical engineering practice. The findings from this study can be a useful tool for researchers, practitioners, and other parties with an interest in soil mechanics and geotechnical engineering.

1.8 Organization of the study

The thesis is organized into five chapters and each chapter effectively examines the content and data of the study accordingly.

Chapter One: This section provides the introduction, background and context of the study, presents the research problems, research questions, and outlines the significance and objectives for the study.

Chapter Two: Literature review is a chapter that discusses key definitions of soil's shear strength, shear strength parameters and ANN model. It includes both empirical and theoretical methods about the estimation of shear strength parameters from soil index properties. It is a section for a review of relevant literature and highlights the current knowledge gap or research need.

Chapter Three: This section describes the methodology and approach used in the research, including details on the description of study area, data collection, data preprocessing and analysis, ANN model development, and evaluation procedures.

Chapter Four: Result and discussion is a chapter that discusses the results of quantitative data findings. This section presents the findings of the research, including the performance and accuracy of the ANN model in estimating the soil shear strength parameters from index properties. And it includes tables and figures to illustrate the results. And also it compares the results with traditional methods or previous studies, and discusses the implications of the findings for geotechnical engineering practice.

Chapter Five: Conclusion and recommendation is the concluding part of the research. It made a conclusion based on the findings from the data collected and the ANN model. This section summarizes the main findings of the research, restates the research objectives and research questions, and provides recommendations for future research or practical applications.

2 LITERATURE REVIEW

2.1 Shear strength of soil

Shear strength is the amount of internal resistance per unit area a soil mass can provide to withstand failure and sliding along any internal plane. The highest shearing resistance that a material is capable of attaining is referred to as shearing strength. The shearing resistance that the soil provides along the probable surfaces of slippage determines the stability of a cut, the slope of an earth dam, the foundations of structures, the natural slopes of hillsides, and other structures constructed on soil. There is hardly an issue in engineering that does not in some way include the shear properties of the soil (Gopal Ranjan. A S R Rao, 2011).

Geotechnical engineering project designs must take into account the mechanical behavior of soils since it affects how structures will respond to loads placed on them by the mass. Some constitutive models were proposed in this regard, with the Mohr-Coulomb criterion being the most widely employed in Geotechnics due to its precise and practical modeling theory. According to this theory, the soil's shear strength varies linearly with applied stress via the cohesion intercept and angle of shearing resistance, two shear strength parameters. The Mohr-Coulomb equation, as given in Equation (2.1), can be used to calculate the force acting on a failure surface in the soil body. If the cohesion intercept and angle of shearing resistance are determined using the total stresses, they are named as total or undrained cohesion intercept (c) and angle of shearing resistance (ϕ). The difference between the total stress and the excess pore water pressure is the effective stress. The effective circles can be plotted and the effective strength parameters (c' and ϕ') can be derived if the pore water pressures are monitored during the test (Mollahasani et al., 2011). The Mohr circles and failure envelopes are shown in the Figure 1.

$$\tau = c + \sigma_n \tan\phi \qquad \text{Equation 2.1}$$

Where, τ is the shear (tangential) stress, σ_n is the normal stress, c is the cohesion of soil, and ϕ is the internal friction angle of soil.

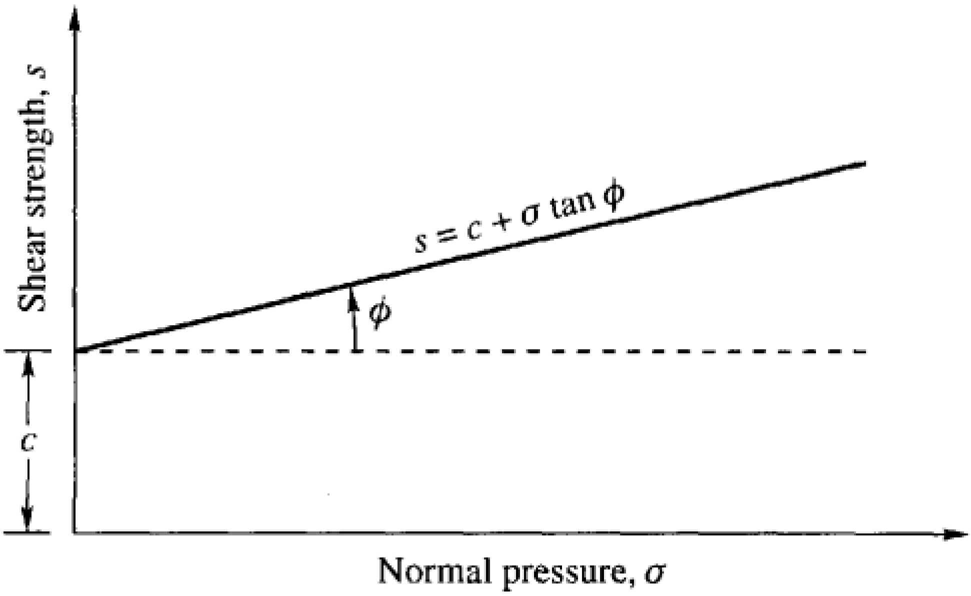

Figure 1: Coulomb's law (Murthy, 2002)

2.2 Soil shear strength parameters

Soil shear strength parameters are key parameters used to characterize the resistance of soil to deformation or failure under the action of shear forces. They are essential in geotechnical engineering for assessing the stability and performance of soil slopes, foundations, retaining walls, and other geotechnical structures. The two primary shear strength parameters commonly used in geotechnical practice are cohesion (c) and angle of internal friction (ϕ).

Cohesion (c): is the resistance of soil particles to displacement due to intermolecular attraction and surface tension of the held water. The soil cohesion is the intercept on the shear axis of the Mohr–Coulomb shear resistance line in the stress plane of the shear effect on normal stress (Mollahasani et al., 2011). Because of the size and polarity of grains, cohesion is extremely appropriate in fine-grained soils. Cohesion represents the shear strength of soil particles due to the electrochemical and cementation forces, and it is typically applied to cohesive soils such as clays, which have fine particles that can stick together due to chemical bonding or electrostatic forces. Cohesion is usually expressed in units of force per unit area (e.g. kPa, psi) and represents the shear strength of soil in the absence of any shear deformation or normal stress. True cohesion, on the other hand, can be seen in coarse-grained soils when particles stay in touch for long periods of time, resulting in contact cementing, as seen in the formation of sandstone from the sand.

In soils, the factors responsible for true cohesion are electrostatic forces in stiff over consolidated clays (which may be lost through weathering), and cementing (by Fe_2O_3, $CaCO_3$, NaCl, etc). However, apparent cohesion can also occur, mainly caused due to negative capillary pressure (which generally disappears upon wetting), pore pressure response during un drained loading (which fades away with time), and root cohesion (which may be lost through logging or fire of the contributing plants, or through the solution) (Murthy, 2002).

Internal Friction Angle (ϕ): The shear resistance of a soil in the presence of normal effective stress at which shear failure occurs is described by its friction angle. The angle of internal friction is a measure of the resistance of soil particles to shear deformation due to friction between particles. It represents the maximum angle that can be formed between the normal stress (vertical stress) and the shear stress (horizontal stress) before the soil starts to deform or fail. The angle of internal friction is typically applicable to cohesion less soils, such as sands and gravels, which do not possess any significant cohesive properties. The angle of internal friction is usually expressed in degrees and is a critical parameter in determining the shear strength and stability of cohesion less soils. The mechanical behavior of coarse-grained soils is primarily determined by particle-to-particle contact, which implies that the frictional component of shear strength is more visible (Gopal Ranjan. A S R Rao, 2011).

The values of these parameters for any soil depend on several factors; such as the soil textural properties, past history of the soil, initial state of the soil (i.e. whether it is saturated or unsaturated), permeability characteristics of the soil and the conditions of drainage allowed to take place during the test (Murthy, 2002).

2.3 Methods of determining shear strength parameters

Direct shear test: This test, also called the shear box test, is the oldest shear test used and is also quite simple to perform. The direct shear test has the advantage of being quick, inexpensive, and simple. In the case of sands, the ease of sample preparation is also plus point. The test, however, suffers from many serious disadvantages. Drainage conditions cannot be controlled and pore water pressure cannot be measured. This means that it is not of much use for fine-grained soils where drainage conditions play an important role in influencing the shear strength. Its usefulness is limited to freely-draining soils when the effective stress parameters of shear strength are to be determined(Murthy, 2002).

Triaxial Test: The triaxial test is the most versatile of the entire shear testing methods, even if a trifle complicated. Drainage conditions can be controlled, whatever be the type of soil. In the triaxial tests, pore water pressure measurements can be made accurately. Volume changes can also be measured. There's no rotation of the principal stresses during the test. The failure plane is not forced. The specimens can fail on any weak plane or can simply bulge. The stress distribution on the failure plane is fairly uniform. Three types of triaxial tests can be conducted with different combinations of drainage conditions. They are unconsolidated un drained (UU), Consolidated Un drained (CU), and Consolidated Drained (CD) (Gopal Ranjan. ASR Rao, 2011).

Unconfined Compression Test: It is a quick and simple test and is often used to determine the in situ strength of soft, saturated, fine-grained soil deposits. The test is also frequently used to determine the sensitivity of clay soils. It is a special case of the triaxial test carried out at zero cell pressure, that is, σ_c=0 or σ_3=0. The test is conducted in the laboratory using a triaxial set-up or a modified triaxial apparatus (Gopal Ranjan. ASR Rao, 2011).

Vane Shear Test: A difficulty often encountered in the determining the shearing resistance of soft, saturated clay deposits in the field is in obtaining undisturbed samples. The shear strength of such sensitive clays may be significantly altered during the process of sampling and handling. The Vane shear test offers a method of overcoming this problem.

Other common tests are the static cone penetrometer test, the standard penetration test, the borehole shear test, the pressure meter, and the screw plate test (Murthy, 2002)(Gopal Ranjan. A S R Rao, 2011).

2.4 Effect of index properties on the shear strength parameters

In nature, soil occurs in a large variety. However, soil exhibiting approximately similar behavior can be put together to form a particular group. The soil can also be put into major and minor groups. Various classification systems in practice place these soil in different categories based on certain properties of soil. The tests carried out in order to classify a soil are termed classification tests. The numerical results obtained on the basis of such tests are termed index properties of soil. The index properties of soil can be divided into two categories, namely, soil grain properties, and soil aggregate properties. Soil grain properties are those properties that are dependent on the individual grains of the soil and are independent of the manner of soil formation. The properties in this category are mineralogical composition, the specific gravity of solids, size, and shape of grains. Soil aggregate properties are those properties that are dependent on the soil mass as a whole and, thus, represent the collective behavior of a soil. Soil aggregate properties are influenced by soil stress history, mode of soil formation, and the soil structure. Soil aggregate properties are of greater significance in engineering practice, since engineering structures are founded on undisturbed, natural soil deposits(Gopal Ranjan. A S R Rao, 2011).

2.5 Review on Artificial Neural Network

An artificial neural network is an advanced computational tool categorized under machine learning. Machine learning, as the name suggests, is a modeling technique that uses a learning process to generate models by analyzing data. These data can be any kind of information that can be presented in the form of documents, audio, images or others. Pattern recognition, image and audio recognition, natural language processing, recommendation systems, and prediction modeling are just a few of the many applications for which ANNs are frequently employed in machine learning and data mining. Geotechnical engineering, like other science and engineering disciplines, uses ANNs to solve complicated issues and make predictions based on input data. The process of learning is a key behavior in artificial neural networks. It is a method of providing the network with experience in that particular field to aid in their development of knowledge-based decision-making abilities. Using this learning capability, neural networks can construct a model that can resolve a given problem. The artificial neural network has emerged as a superior alternative to traditional modeling tools for addressing a number of real-world problems across several fields (Vanneschi & Silva, 2023).

2.5.1 Biological and Artificial Neural Network

Much is still unknown about how the brain trains itself to process information, so theories abound. In the human brain, a typical neuron collects signals from others through a host of fine structures called dendrites. The neuron sends out spikes of electrical activity through a long, thin stand known as an axon, which splits into thousands of branches. At the end of each branch, a structure called a synapse converts the activity from the axon into electrical effects that inhibit or excite activity from the axon into electrical effects that inhibit or excite activity in the connected neurons. When a neuron receives excitatory input that is sufficiently large compared with its inhibitory input, it sends a spike of electrical activity down its axon. Learning occurs by changing the effectiveness of the synapses so that the influences of one neuron on another change (Abdulabbas, A. A.., & Bind, 2014).

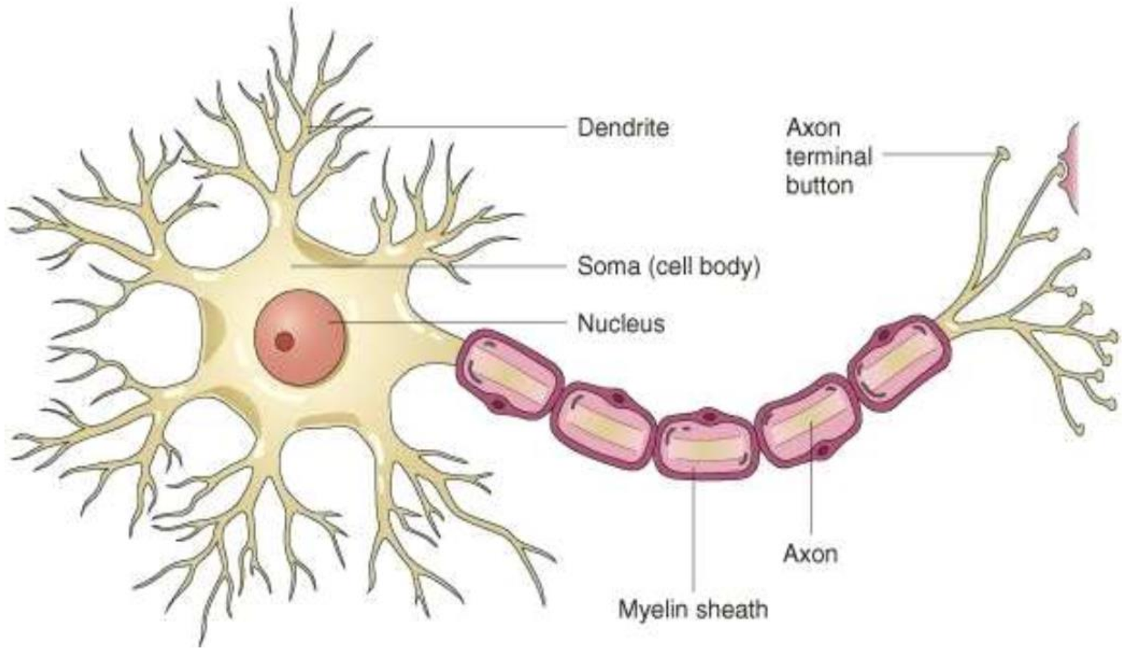

Figure 2: Neurobiological Background (Abdulabbas, A. A.., & Bind, 2014)

We conduct these neural networks by first trying to deduce the essential features of neurons and their interconnections. We then typically program a computer to simulate these features. However because our knowledge of neurons is incomplete and our computing power is limited, our models are necessarily gross idealizations of real networks of neurons (Abdulabbas, A. A.., & Bind, 2014).

Artificial neural networks are imitators of the human brain, even though their approximation is highly oversimplified in terms of size and capacity. The human brain has a remarkable ability to learn and adapt to new situations. Artificial neural networks, unlike traditional computers that only accomplish a certain task based on the instructions loaded by the programmer, also can learn and adapt to new data. These are the major characteristics that an artificial neural network inherited from biological neural networks(Gallo, 2018).

Following the same fashion as the biological neuron, a multi-layer neural network has three layers known as the input, output, and hidden layers. The Input layer receives initial data to the neural network whereas the output layer presents the results to the external environment. The intermediate layer between the two is called a hidden layer. The hidden layer is the layer where all computations are performed while training the network. In an Artificial neural network, nodes are linked to each other using weight. The magnitude of weight determines the effect of input variables on the corresponding output values (Vanneschi & Silva, 2023).

Table 1: Contrasts between Biological and Artificial Neural Network (Dipo Theophilus Akomalfe, 2013)

Biological Neural Network	Artificial Neural Network
Cell body	Node
Dendrite	Input
Axon	Transfer function
Terminal Axon	Output
Synapses	Weight

Artificial Neural Networks (ANNs) are computational models that mimic the functioning of the human brain to process information and make predictions or decisions. ANNs consist of interconnected nodes or neurons organized in layers, and each neuron performs a mathematical operation on input data and produces an output. Recent development in the field of computer-based modeling had provided an alternative to the hectic and tedious work of developing analytical and computational models in the field of engineering and science, one of them is Artificial Neural Network based models which are not only capable of developing models but also contains predicting capacity. Artificial neural networks can be most adequately characterized as computational models with particular properties such as the ability to adapt or lean, to generalize, or to cluster or organize the data, and which operations are based on parallel processing (Abdulabbas, A. A.., & Bind, 2014).

ANN can be described as a computational tool devised on the basic behavior of neural architecture of biological system and focused to model the human brain. Nowadays ANN can be applied to problems that cannot be easily solved with an algorithm or are very complex to describe. ANN formulates a mathematical model for a system in which no clear relationship is available between the inputs and outputs. Unlike the majority of the conventional statistical methods, ANNs use the data alone to determine the structure of the model and the unknown model parameters. It does not have to explicitly assume a model form, which is prerequisite in the parametric approach. The ANN is a powerful tool bestowed with capability to establish the relationship between different examples being presented to them. This technique also gives flexible solution in wider domain and has been used in many tasks such as pattern recognition, forecasting, optimization and simulation etc. The ANN exhibits the massive parallelism as neurons are organized by layers which are mutually interconnected by synaptic weights. Despite all these characteristics of ANN it has also been quoted as black box because of its disability to explain the interrelation between input and output parameter, However availability of different methodologies such as Connection weight approach**,** Garson's algorithm**,** Input Perturbation**,** Sensitivity analysis have changed this notion of not assessing variable importance in neural network(Olden & Jackson, 2002)(Gevrey et al., 2003)(Michele Scardi, Lawerence W, 1999)(Lek et al., 1996).

ANN advantages include:

Adaptive Learning: An ability to learn how to do tasks based on the data given for training or initial experience.

Self - Organization: An ANN can create its own organization or representation of the information it receives during learning time.

Real Time Operation: ANN computation may be carried out in parallel, and special hardware devices are being designed and manufactured which take advantage of this capability.

Fault Tolerance via Redundant Information Coding: Partial destruction of network leads to the corresponding degradation of performance. However, some network capabilities may be retained even with major network damage.

2.5.2 Types of Neural Networks

There are several types of neural networks used in machine learning and artificial intelligence. Some of the most common types are discussed below (Vanneschi & Silva, 2023).

1. **Feedforward Neural Networks:** is a type of neural network in which the information flows in only one direction, from input to output, with no feedback loops. These neural networks are used for supervised learning tasks, such as classification and regression tasks. In a feedforward neural network, each neuron in a layer is connected to all the neurons in the next layer. The input layer receives the input data, and each neuron in the input layer is connected to a neuron in the first hidden layer. Each neuron in the hidden layer receives inputs from all the neurons in the previous layer and applies an activation function to produce an output, which is then passed to the next layer. The final layer is the output layer, which produces the output of the network. The activation function of a neuron in a feedforward neural network determines whether the neuron should be "activated" or "not activated" based on the input it receives. The weights and biases of the neurons in a feedforward neural network are learned during the training process, using a method such as back propagation. Feedforward neural networks are relatively simple and easy to implement, making them a popular choice for many applications. However, they can struggle with tasks that require the network to remember information from previous inputs or to handle complex input data, such as images. Based on the number of layers it consists, a feed-forward neural network can be classified as a single-layer and a multi-layer neural network. A single-layer neural network only contains one input and one output layer. Multi-layer neural networks on the other hand consist of one or more hidden layers in addition to the input and output layers.

2. **Recurrent Neural Networks(RNNs)**: are types of artificial neural network that can handle sequential data and make predictions based on it. Unlike feedforward neural networks, RNNs have loops within the network, which allow the network to retain information about previous inputs and use that information to make predictions about future inputs. It allows signals to travel in both forward and backward directions, forming a loop. In an RNN, each neuron in the network has a hidden state that represents its "memory" of the previous inputs. The hidden state is updated at each time step by taking a weighted sum of the current input and the

previous hidden state, and passing it through an activation function. The output of the RNN at each time step is produced by applying another activation function to the current hidden state. RNNs are particularly well-suited for tasks that involve sequences of data, such as natural language processing and speech recognition. They can be used for tasks such as predicting the next word in a sentence, generating text, and even translating between languages(Gallo, 2018)(Dipo Theophilus Akomalfe, 2013).

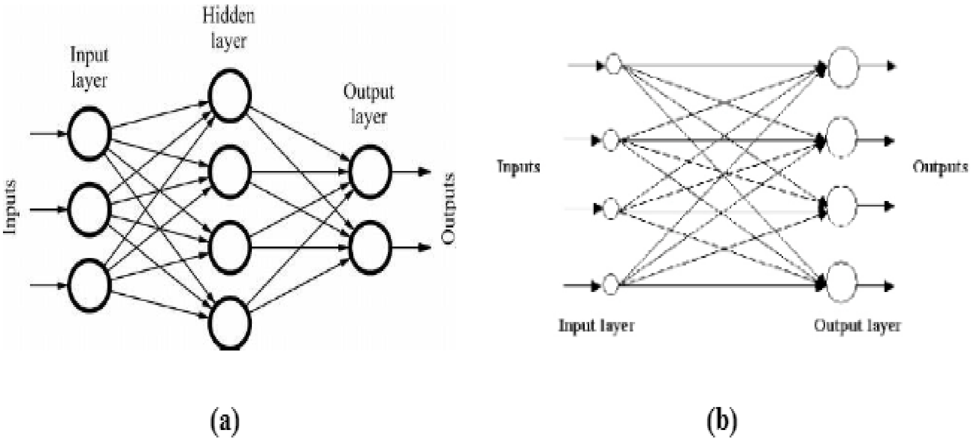

Figure 3: A Single-Layer Neural Network (b) A Multi-Layer Neural Network (a) (Vanneschi & Silva, 2023)

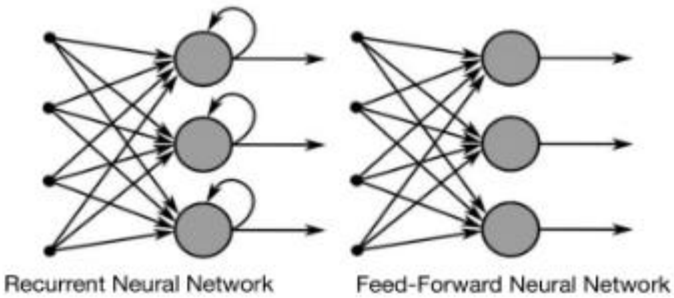

Figure 4: Recurrent Neural Network

3. **Convolution Neural Networks (CNNs):** are a type of artificial neural network that are particularly well-suited for processing images and other two-dimensional data. CNNs are often used for image recognition tasks, for example, because they are better suited to handling the complex input data. CNNs use a special type of layer

called a convolution layer that allows the network to automatically learn local features from the input data. In a CNN, the input data is typically a two-dimensional image with multiple channels (e.g., red, green, and blue channels for a color image). The first layer in the network is a convolution layer that applies a set of filters to the input image. The filters are learned during the training process and can detect different patterns in the input data, such as edges and corners. After the convolution layer, the output is typically passed through a pooling layer, which reduces the dimensionality of the output by down sampling it. This helps to make the network more efficient and reduce the risk of over fitting. The output of the pooling layer is then passed through one or more fully connected layers, which are similar to the layers in a feedforward neural network (Gallo, 2018).

2.5.3 Artificial Neural Network Computation

ANN (Artificial Neural Network) computations involve the process of feeding input data into a neural network, performing mathematical computations at each neuron, and producing an output.

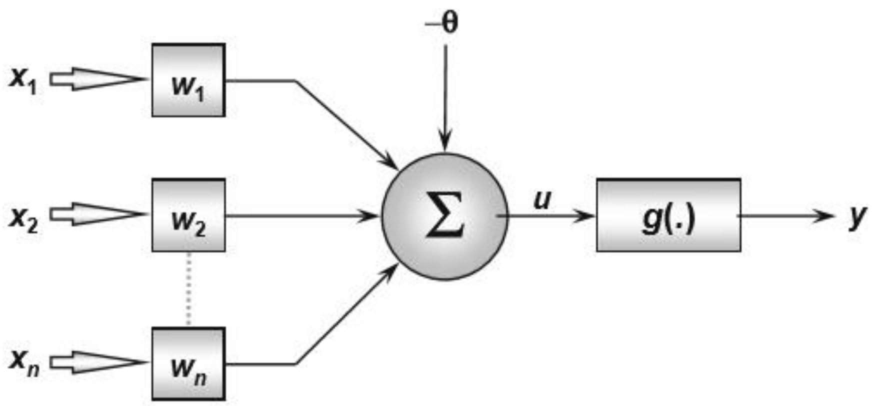

Figure 5: Simplified overview of the Artificial neuron (Vanneschi & Silva, 2023)

The variables {x_1, x_2, x_3… x_n}, {w_1, w_2, w_3... w_n}, and “y” represent the input, the weight, and the output values respectively. As inputs travel from neurons of the input layer to the next layer neurons they will be multiplied by the weights. Then their summation will be computed when they reach the next neuron or node. Lastly, b which stands for bias will be added to the inputs’ weighted sum. The weighted sum then will be entered into the activation function to give the output value.(P. Kim, 2017).

1. **Inputs**

The inputs are defined as data from outside a neuron, which can come from an external neuron or the neuron itself. Input is the foundation of network training(Aslay, F., & Ustun, 2013). They are the signals or samples coming from the external environment and representing the values assumed by the variables of a particular application. The input signals are usually normalized in order to enhance the computational efficiency of learning algorithms. The input data can be in a wide variety of formats, depending on the specific application and type of network architecture being used such as number, image, audio, and text data.

2. **Weights**

Synaptic weights are the values used to weights each one of the input variables, which enables the quantification of their relevance with respect to the functionality of the neuron. They are used to show how the neural nerve's input data affects the nerve cell. There is a weight assigned to each input. The input is important, and the effective rate is high, as indicated by the high weight value. Low weight levels imply that the input is unimportant. In the connection between input and output values, weights are used(Harsh Kukreja, 2016a).

3. **Linear aggregator (∑)**

This function gathers all input signals weighted by the synaptic weights to produce an activation voltage. It is a summing function that estimates the net input from the neuron, and different functions to do so. The linear combiner is defined by the total of the entries weighted by each individual weight in this segment. Depending on the problem, the summing function may be chosen differently. The perfect summing function is determined using the trial and error method (Hamzacebi, 2011).

4. **Activation threshold or bias (ϕ)**

It is a variable used to specify the proper threshold that the result produced by the linear aggregator should have to generate a trigger value toward the neuron output.

5. **Activation potential (u)**

It is the result produced by the difference between the linear aggregator and the activation threshold. If this value is positive, i.e. if u ≥ ϴ, then the neuron produces an excitatory potential; otherwise, it will be inhibitory.

6. **Activation function (g)**

Its goal is limiting the neuron output within a reasonable range of values, assumed by its own functional image. It's the function that keeps the neuron's output value in a specified range when compared to its net input value. It creates a link between the neuron's input and output values. It analyzes the cell's total input and creates the appropriate output (Haykin, S., & Network, 2004). The activation functions can be categorized into two fundamental groups, partially differentiable functions, and fully differentiable functions when considering their complete definition domains. Partially differentiable activation functions are functions with points whose first order derivatives are nonexistent. The three main functions of this category are step function, bipolar step function, and symmetric ramp function. Fully differentiable activation functions are those whose first order derivatives exist for all points of their definition domain. The four main functions of this category, which can be employed on artificial neural networks, are the logistic function, hyperbolic tangent, Gaussian function, and linear function.

(a) Logistic function

The output result produced by the logistic function will always assume real values between zero and one. The sigmoid or logistic activation function is a continuous and derivative function. Because of its non-linearity, it is one of the most commonly employed functions in ANN applications. For each of the supplied input values, this function generates a value between zero and one. Its mathematical expression is given by:

$$g(u) = \frac{1}{1+e^{-\beta \cdot u}} ,$$

Equation 2.2

Where "**β**" is a real constant associated with the function slope in its inflection point.

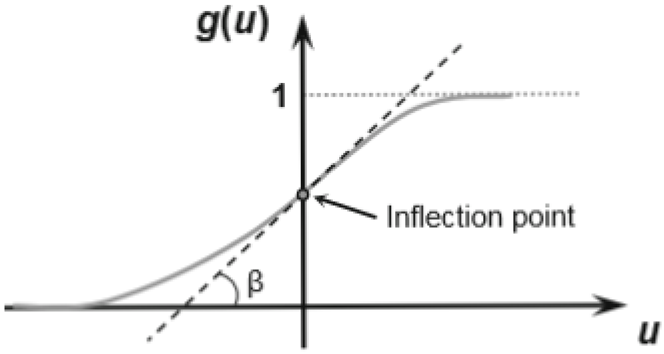

Figure 6: The logistic activation function

(b) Hyperbolic tangent function

The output result, unlike the case of the logistic function, will always assume real values between −1 and 1, and it shows a non-linear change in this range based on the neuron's total input neuron. Its mathematical expression is

$$g(u) = \frac{1 - e^{-\beta \cdot u}}{1 + e^{-\beta \cdot u}} \quad , \qquad \text{Equation 2.3}$$

where "β" is also associated with the slope of the hyperbolic tangent function in its inflection point.

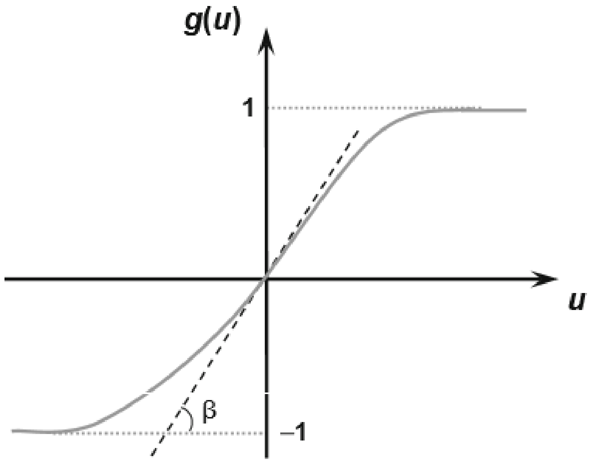

Figure 7: The hyperbolic tangent activation function

It is important to note that both logistic and hyperbolic tangent functions belong to a family of functions called sigmoid.

(c) Gaussian function

In the case of Gaussian activation functions, the neuron output will produce equal results for those activation potential values {u} placed at the same distance from its center (average). The curve is symmetric to this center and the Gaussian function is given by:

$$g(u) = e^{-\frac{(u-c)^2}{2\sigma^2}}, \qquad \text{Equation 2.4}$$

Where c is the parameter that defines the center of the Gaussian function and r denotes the associated standard deviation, that is, how scattered (dispersed) is the curve in relation to its center. The graphical representation of this function is illustrated by Fig. 2.4.

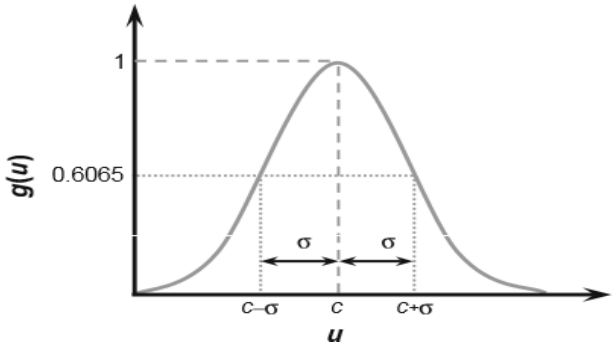

Figure 8: The Gaussian activation function

(d) Linear function

The linear activation function, or identity function, produces output results equal to the activation potential {u}, having its mathematical expression given by:

$$g(u)= u \qquad \text{Equation 2.5}$$

One application of the linear activation functions is in artificial neural networks performing universal curve fitting (function approximation), to map the behavior of the input/output variables of a particular process.

7. Outputs (y)

It consists of the final value produced by the neuron given a particular set of input signals, and can also be used as input for other sequentially interconnected neurons.

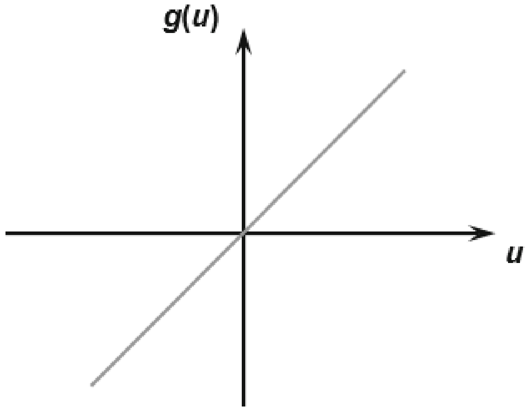

Figure 9: The linear activation function

2.5.4 Artificial Neural Network Architectures

The architecture of an artificial neural network is defines how its several neurons are arranged, or placed, in relation to each other. These arrangements are structured essentially by directing the synaptic connections of the neurons. The topology of a given neural network, within a particular architecture, can be defined as the different structural compositions it can assume. In other words, it is possible to have two topologies belonging to the same architecture, where the first topology is composed of 10 neurons, and the second is composed of 20 neurons. Moreover, one can consist of neurons with a logistic activation function, while the other one can consist of neurons with the hyperbolic tangent as the activation function. In general, an artificial neural network can be divided into three parts, named layers(Vanneschi & Silva, 2023).

(a) Input layer: this layer is responsible for receiving information (data), signals, features, or measurements from the external environment. These inputs (samples or patterns) are usually normalized within the limit values produced by activation functions. This normalization results in better numerical precision for the mathematical operations performed by the network.

(b) Hidden, intermediate, or invisible layers: these layers are composed of neurons which are responsible for extracting patterns associated with the process or system being analyzed. These layers perform most of the internal processing from a network.

(c) Output layer: this layer is also composed of neurons, and thus is responsible for producing and presenting the final network outputs, which result from the processing performed by the neurons in the previous layers.

The main architectures of artificial neural networks, considering the neuron disposition, as well as how they are interconnected and how its layers are composed, can be divided as follows: (i) single-layer feedforward network, (ii) multilayer feedforward networks, (iii) recurrent networks and (iv) mesh networks (Gallo, 2018).

(i) Single-layer feedforward architecture

This artificial neural network has just one input layer and a single neural layer, which is also the output layer. The information is always flows in a single direction (thus, unidirectional), which is from the input layer to the output layer. These networks are usually employed in pattern classification and linear filtering problems.

(ii) Multilayer feedforward architecture

Differently from networks belonging to the previous architecture, feedforward networks with multiple layers are composed of one or more hidden neural layers. They are employed in the solution of diverse problems, like those related to function approximation, pattern classification, system identification, process control, optimization, robotics, and so on. The amount of neurons composing the first hidden layer is usually different from the number of signals composing the input layer of the network. In fact, the number of hidden layers and their respective amount of neurons depend on the nature and complexity of the problem being mapped by the network, as well as the quantity and quality of the available data about the problem. Nonetheless, likewise, for simple-layer feed forward networks, the amount of output signals will always coincide with the number of neurons from that respective layer(Vanneschi & Silva, 2023).

2.5.5 Training Processes and Properties of Learning

One of the most relevant features of artificial neural networks is their capability of learning from the presentation of samples (patterns), which expresses the system behavior. Hence, after the network has learned the relationship between inputs and outputs, it can generalize solutions, meaning that the network can produce an output which is close to the expected (or desired) output of any given input values. The set of ordinate steps used for training the network is called learning algorithm. During its execution, the network will thus be able to extract discriminant features about the system being mapped from samples acquired from the system. There are three learning data sets in Artificial Neural Networks (Vanneschi & Silva, 2023).

1. Training Data Set: A set of samples used to learn how to fit the network's parameters (i.e. weights). On the training set, one approach comprises one full training cycle. The training process is presented to the network during training, and the network is adjusted according to its error.

An artificial neural network is trained through a learning process(Foram S. Panchal & Mahesh Panchal, 2014). There are five types of learning methods in artificial neural networks, these are:

a. Supervised Learning

b. Unsupervised Learning

c. Reinforcement Learning

2. Test data Set: A set of examples is used only to assess the performance (generalization) of a fully specified network or apply successfully to predict output whose input is known. These have no effect on training and so provide an independent measure of network performance during and after training. This data set will be used to verify if the network capabilities of generalizing solutions are within acceptable levels, thus allowing the validation of a given topology. Nonetheless, when dimensioning these subsets, statistical features of the data must also be considered.

3. Validation data Set: A set of examples used to tune the parameters (i.e. architecture) of the network. It is used to choose the number of hidden units in a Neural Network. On the other hand, once the weights have been corrected, the network is validated using an additional set of known samples that has not yet been used. This process is called validation and aims to verify the generalization capacity of the ANN from data not used in the training process(Gallo, 2018).

2.5.6 Steps for Training an Artificial Neural Network

Training an artificial neural network (ANN) involves a series of steps that are aimed at optimizing the weights and biases of the network so that it can accurately predict outcomes from input data. Here are the general steps for training an ANN in detail:

2.5.6.1 Data Preprocessing

The first step is to preprocess the input data to ensure that it is in a format that can be easily used by the ANN. Data preprocessing is a data mining technique for converting raw data into more suitable forms for machine learning. Raw data sometimes can be noisy with some outliers, have missing information, and be inconsistent because of their huge quantity and variety of sources. As data quality decreases, the results of machine learning will decrease as well. Therefore, to get an efficient neural network it is important to implement data preprocessing techniques. There are different data preprocessing techniques such as data cleaning, data reduction, data transformation, normalization, feature scaling, splitting the data into training, and others. Data cleaning is used to remove noise from the data and improve its consistency while data reduction is used to eliminate redundancy in the data set. Data transformation is a way to scale data into the same and smaller range and is important in giving all data with different measurement units an equal weight (Jiawei Han, 2012).

2.5.6.2 Data Division

After data preprocessing, the data sets are divided into three categories called training, validation and test set with different proportions. There are several suggestions on how to divide input data into these three categories but not a single fixed way. In supervised learning, a training set is a set of data with known inputs and actual outputs that are used to train the network. A validation set is a data set that is not used in the training process. They are reserved from the training set to know when to stop training the neural network and prevent over fitting (Shahin et al., 2004). A model is said to be over-fitted when it has poor performance on the validation set while performing well on the training set. This is because the model gets very customized by the training set that it lacks generalization ability on other data sets. This is one of the problems faced in training neural network models. A test set is a new data set not included in both the training and validation sets. Now the network is given only the input values without the actual output values. The network is required to provide the output values of the new test data. A test set is used to measure the network performance and its generalization ability on new data (P. Kim, 2017)(S. Karsoliya, 2012).

2.5.6.3 Define the Architecture of the Neural Network

Defining the architecture of an artificial neural network includes fixing the number of input, output and hidden neurons in each layer. The number of input neurons in an input layer is equal to the number of input variables used to train the neural network and the number of neurons in the output layer is equal to the desired number of output variables.

The most controversial part is however to determine the number of hidden layers and a number of hidden neurons in that layer. The number of hidden layer requirements depends on the number of training data used and the complexity of the problem under consideration. In most cases, two hidden layers are enough to solve any non-linear complex problems. Multiple hidden layers can be used in the application where accuracy is the first major criteria and if the time for training the network is not limited (Adugna, 2021). Among the suggested methods by many researchers, a structured trial and error method is found to be the most commonly used approach(S. Karsoliya, 2012)(Vanneschi & Silva, 2023).

2.5.6.4 Back Propagation

Back propagation is a widely used algorithm for training artificial neural networks (ANNs). The goal of back propagation is to adjust the weights and biases of the neurons in the network to minimize the difference between the predicted output of the network and the actual output. Back propagation works by returning the error from the input layer to the output layer of the network. The output of the network is compared to the desired output at each iteration of the algorithm, and the difference between the two is utilized to calculate the error signal. The weights and biases of each neuron are then modified using the error signal, which is subsequently sent backward through the network layer by layer. The partial derivative of the error proportional to each weight or bias, which is calculated using the chain rule of calculus, determines how much adjustment is made to each weight or bias. he weights and biases of the neurons are typically updated via the back propagation algorithm using the gradient descent technique. To minimize the error, this entails computing the gradient of the error for each weight and bias and modifying them in the direction of the negative gradient. A variety of neural network designs, including feed forward networks, recurrent networks, and convolution networks, have been trained using the powerful algorithm(Harsh Kukreja, 2016b).

2.6 Applications of ANN

Recently, artificial neural networks have become applicable for a variety of applications in different fields. ANNs are effective for tasks like object detection, facial recognition, and audio-to-text transcription because they can be trained to identify patterns in speech and image data. ANNs can be used for tasks including sentiment analysis, language translation, and text categorization in natural language processing (NLP). For instance, Google Translate uses ANNs to translate text between languages. And also ANNs can be used for predictive modeling, which uses historical data to forecast future outcomes. They can be applied, for instance, to forecast stock prices, disease diagnosis, or customer turnover. By analyzing sensor data and taking prompt judgments, ANNs can be utilized to control robotic systems, such as autonomous automobiles. ANNs can be used to assess financial data, including economic indicators, and to make investment decisions (Shahin, M. A., Jaksa, M. B., & Maier, 2001)(P. Kim, 2017).

2.6.1 Application of ANN in Geotechnical Engineering

Geotechnical engineering is the basis for the various engineering project construction which deals with materials like soil and rock. Traditional methods in geotechnical engineering cannot predict the non-linear and plastic properties of rock and soil accurately. Machine learning techniques are able to deal with non-linear and plastic issues of rock and soil effectively and avoid the flaws that older methods might produce. ANN algorithm is a popular machine learning algorithm that is widely applied in geotechnical engineering (Shahin, M. A., Jaksa, M. B., & Maier, 2001)(S. K Das, 2013)(Juwaied, 2018). Artificial neural networks (ANNs) are well suited to model the complex behavior of most geotechnical engineering materials which, by their very nature, exhibit extreme variability. ANNs have also demonstrated superior predictive ability when compared with traditional methods (Shahin et al., 2009). The researchers have presented the state of art and the uses of ANN that have been applied in Geotechnical Engineering (Shahin, 2013)(Juwaied, 2018)(S. K Das, 2013)(Shahin, M. A., Jaksa, M. B., & Maier, 2001). Some of the applications of ANN in geotechnical engineering are listed below in the table.

Table 2: Applications of ANN in Geotechnical Engineering

Site characterization	Prediction of the behavior of foundations
Earth retaining structures, Dams, Mining	Prediction of soil properties and behavior
Design of tunnels and underground openings	Modeling the axial and lateral load capacities of pile foundations
Settlement of foundations	Soil composition and classification
Pile capacity Prediction	Deep excavation
Slope stability and landslides	Prediction of soil shear strength parameters
Compaction characteristics prediction	Rock mechanics

2.7 Prediction models of soil shear strength parameters

In geotechnical engineering, empirical correlations are commonly employed to estimate the engineering parameters of soils. There are useful relationships between index parameters acquired from routine testing and soil strength properties. The most often utilized approaches for developing relationships between material properties are regression analysis and artificial neural networks (Harini, H., & Naagesh, 2014).

2.7.1 Existing Regression Approach

Regression analysis is a statistical method to model the relationship between a dependent (target) and independent (predictor) variables with one or more independent variables. It also helps us to understand how the value of the dependent variable is changing corresponding to an independent variable when other independent variables are held fixed. Some of the regression analysis models developed for prediction of shear strength parameters are illustrated below.

According to a study**,** soils with high plasticity have lower angle of shearing resistance and higher cohesion. This study was aimed at obtaining meaningful linear genetic programming (LGP) based relationships between the undrained cohesion intercept (c) and angle of shearing resistance (ϕ) and the soil physical properties. In contrast, when the size of the soil grains increases, the internal friction angle of the soil also increases, and its cohesion decreases. The soil unit weight and liquid limit were determined to have the greatest influence on c and ϕ. As a result, the study came to the sensible conclusion that the soil type, soil plasticity, and soil density are the main factors that influence soil strength parameters(Mousavi & Alavi, 2011).

A study showed that the value of soil cohesion varies depending on soil moisture content, grain size, and compaction. In the study, laboratory experiments were carried out with the help of a direct shear device. To determine the relation between soil strength parameters and both soil moisture content and soil bulk density linear regression equations were developed. The results indicate that both angle of internal friction and soil cohesion were inversely proportional to soil moisture content and were directly proportional to soil bulk density(El-Maksoud, 2006).

Multiple regression models are developed in the equations below for the prediction of shear strength parameters. They conducted a thorough investigation in Sirsa, India. The impact of geotechnical variables on shear strength parameters was investigated, including bulk density, dry density, natural moisture content, specific gravity, particle size, liquid limit, plastic limit, and plasticity index. The most influencing variables were chosen using a stepwise regression technique (Roy, 2014).

$$c = -0.525 + 0.241\ Gs \qquad 2.6$$

$$\phi = -29.604 + 34.220\ BD \qquad 2.7$$

Where c is cohesion (kPa), ϕ is internal friction angle (°), Gs is specific gravity, and BD is soil bulk density (g/cm3).

In study, empirical equations were given utilizing statistical and multi criteria analysis based techniques for the prediction of strength parameters as a function of the index qualities of clayey soils. According to the results of multiple regression analysis and analytical hierarchy process, the correlations characterized by the regression coefficient of 0.80 were determined among the friction angle, cohesion and plasticity properties. The study indicates that cohesion and the friction angle can be estimated from their plasticity properties with mathematical relations as shown in Equations below (Ersoy et al., 2013).

$$c = 0.265(PI/LL)^{2.78} \qquad 2.8$$

$$\phi = -204.5(PI/LL) + 56.3(PI/LL) + 31 \qquad 2.9$$

Where, c is cohesion in (kPa), ϕ is internal friction angle (°), PI is plasticity index (%) and LL is liquid limit (%).

2.7.2 ANN Prediction Models of Shear Strength Parameters

There are developed models for predicting the shear strength parameters (cohesion and angle of friction) of lateritic soils in central and southern areas of Delta State using artificial neural network modeling technique. A total of eighty-three soil samples were collected. The input factors considered were plasticity index, percentage of particles passing sieve No.200, specific gravity, liquid limit, plastic limit. A Pearson correlation analysis was carried out to study the relative relationship of the factors that affect shear strength parameters. The correlation analysis indicated a high level of relationship between plastic limit, liquid limit and plasticity index. Hence only the plasticity index was used in the modeling exercise. The results between the predicted and measured shear strength parameters obtained by utilizing ANNs were compared with three traditional methods. The results obtained demonstrated that the ANN method outperforms the empirical methods considered(Lyeke et al., 2016).

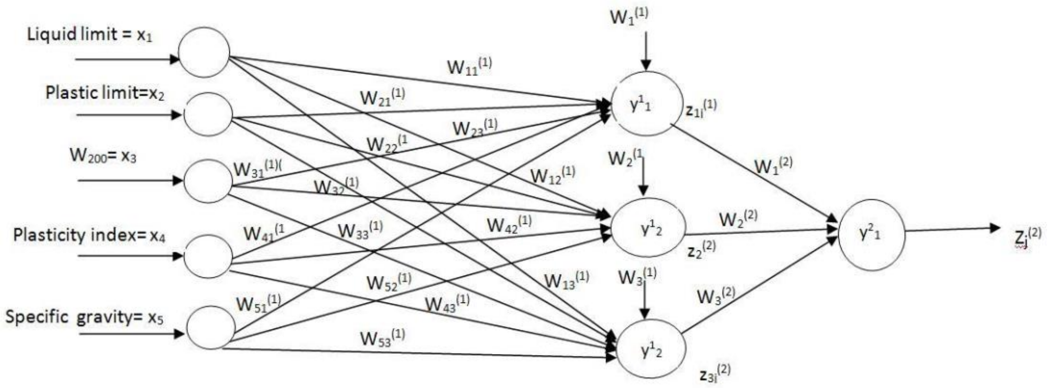

Figure 10: Proposed Model structure Architecture (Lyeke et al., 2016)

One study developed an Artificial Neural Network as prediction tool for determination of internal friction angle "ϕ" and cohesion "c". With this context, an attempt has been made to develop a neural model from the index properties of soil consisting of water content (w), Plasticity Index (PI), Bulk density (BD), Sand % (SP), Silt%(STP), and Clay% (CP) as input parameter. A comprehensive set of experimental data obtained from Bihar were used in developing models of neural network based soil models. According to this analysis clay% (CP) and silt% (STP) are the most significant variables contributing in estimation of strength parameter "c". However plasticity Index (PI) and dry density (DD) affects considerably in prediction of internal friction angle "ϕ"(Kiran & Lal, 2016).

A published study on the residual shear strength prediction is developed for clays with ANN. Since soil cohesion in a residual state is very low or inexistent, and its resistance is described in terms of residual friction angle (ϕr). In fact, an artificial neural network was built using 54 samples of volcanic ash clay (39 for training and 15 for testing), as well as triaxial and soil characterization test results. They developed four distinct MLP models based on LL, CF (clay fraction), PI and ΔPI. It showed the proposed models and their results, with Model 4 being chosen as the best for achieving the highest coefficients of correlation during both training (R= 0.906) and testing (R= 0.942)(Sarat Kumar Das & Basudhar, 2008).

Later, researchers conducted a study on friction angle correlation using a GMDH (Group Method for Data Handling) artificial neural network. They collected 195 soil samples (120 for training, 50 for testing, and 25 for model validation).Then, using GMDH, several ANN were constructed one after the other, resulting in increasingly complicated networks at each level. The predicted to measured values adjustment was excellent, and the correlations achieved were high, with 0.998 for training and 0.997 for testing. The model was then validated by comparing the findings of regularly used correlations to the outcomes of unanticipated data(Shooshpasha et al., 2015).

The focus of the study is on creating artificial neural network (ANN) models for predicting soil cohesion and angle of shearing resistance, both of which are important parameters of shear strength. Two applicable output parameters of shear strength have been estimated using relevant input parameters such as depth, SPT-N value, liquid limit, and plastic limit. There were 72 datasets from site A in the total number of datasets gathered for the soil geotechnical investigation region. For the purpose of predicting the parameters of shear strength, cohesion-less soils were excluded. Each site's ANN models were created. In contrast to the third model, which includes both cohesion and angle of internal friction as output parameters, the first two models output cohesion and angle of internal friction separately? Nearly all of the sites had accurate predictions for the shear strength parameters cohesion (c) and angle of internal friction (ϕ). The findings show that back-propagation neural networks can predict cohesive cohesiveness (c) with a respectable level of accuracy. Cohesion and angle of friction, however, had very little effect on combined model regression, indicating that it may be challenging to get better results from a multidimensional output system. The analysis of the network architecture of all models revealed that models with a combination of six neurons in the second layer performed better than those with other combinations of neurons (Abdulabbas, A. A.., & Bind, 2014).

In order to reduce the time, effort, and expense typically associated with determining shear strength parameters in the laboratory for future planning, design, and construction projects, a research developed models for predicting the shear strength parameters (cohesion and angle of friction) of soils in Addis Ababa city using ANN modeling technique. With the soil index properties of sand percentage (SP), fines percentage (FP), liquid limit (LL), plasticity index (PI), water content (w), and bulk density (BD) as input parameters, distinct neural network models for c and have been made an approach to create. For the purposes of varying the number of hidden layers, a multi-layer perceptron network with feed-forward back propagation is used. And the collected data were 284 to develop the model. The developed models were found to be quite satisfactory in predicting shear strength parameters with correlation coefficients of about 0.98 and 0.92 for cohesion and angle of internal friction, respectively during the testing phase (Yoseph, 2022).

2.8 Comparison between Regression and ANN Prediction Models

A research proposed linear and non-linear regression, and artificial neural networks to estimate shear strength characteristics of clays from ω and PI. They performed 79 CU triaxial tests on normally consolidated plastic clays from the Antalya region in Turkey for the research. The results of the linear regression analysis are shown in equations illustrated below, where ε denotes the errors. The equations produced for predicting c' and ϕ' had coefficients of correlation of 0.72 and 0.87, respectively (Goktepe et al., 2008).

$$\phi' = -6.38 + 0.58\,\omega + 0.05\,PI + \varepsilon \qquad 2.10$$

$$c' = 1.61 - 0.03\,\omega - 0.01\,PI + \varepsilon \qquad 2.11$$

The results of non-linear multiple regression correlations were marginally better than those of linear regression analysis. Equations stated below for cohesion and friction angle presented R^2 equal to 0.73 and 0.90, respectively, which are already satisfactory.

$$\phi' = 0.0077\,\omega^2 + 0.1305\,\omega - 0.0125PI^2 + 0.4242\,PI - 0.0012\,\omega\,PI + \varepsilon \qquad 2.12$$

$$c' = 0.0006\,\omega^2 - 0.0737\,\omega - 0.0002\,PI^2 - 0.0282PI + 0.001\,\omega\,PI + \varepsilon \qquad 2.13$$

However, the researchers used feed-forward multilayer perceptrons to achieve new results on estimating these parameters (MLP). To this goal, the authors provided models for two types of learning algorithms: gradient descent and the Lavenberg-Marquardt technique, both of which use the hyperbolic tangent as an activation function. In conclusion, the ANN model trained with the Lavenberg-Marquardt method achieved a significantly good performance in Antalya normally consolidated clays with architecture 2 x 30 x 2 and R^2 = 0.99 (Goktepe et al., 2008).

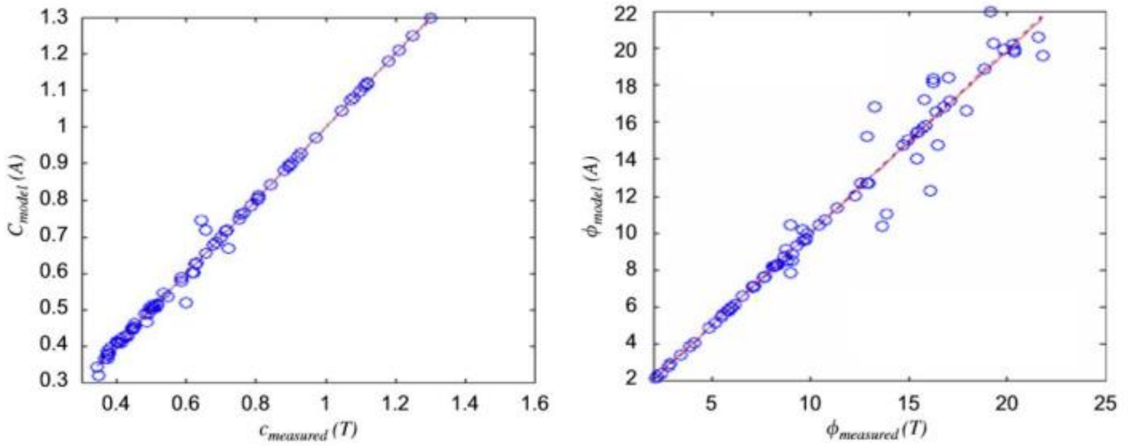

Figure 11: Scatter Graphs of ANN Models for C and Φ Using Lavenberg-Marquardt Algorithm (Goktepe et al, 2008)

A study developed an Artificial Neural Network as a prediction tool for determination of internal friction angle and cohesion. In this regard, an attempt was made to create a neural model using the index properties of soil as input parameters, which included water content (ω), Plasticity Index (PI), Bulk density (BD), Sand % (SP), Silt%(STP), and Clay % (CP). The development of neural network based soil models was based on a large set of experimental data collected in Bihar. According to this investigation, the most significant variables contributing to the estimation of the strength parameter c were clay percent (CP) and silt percent (STP). However, the plasticity index (PI) and dry density (DD) showed a significant impact on internal friction angle prediction. Multivariable linear least square regression (LLSR) and non-linear least square regression were used in a regression analysis (NLSR). (Kiran & Lal, 2016):

The LLSR based equations used for formulation of c and ϕ are given as:

$$c = 0.216 - 0.00091\ PI - 0.0092\ SP - 0.008\ STP + 0.143\ CP - 2.14\ BD + 0.0347\ \omega + \varepsilon \qquad 2.14$$

$$\phi = 5.481 + 0.057\ PI + 0.238\ SP + 0.1066\ STP - 0.489\ CP - 1.21\ BD + 0.079\ \omega + \varepsilon \qquad 2.15$$

The NLSR based equations used for formulation of c and ϕ are as follows:

$$c = 0.0077\ PI^{1.58} - 0.005\ SP^{0.0076} + 0.008\ STP^{0.001} + 0.001\ CP^{0.0112} - 0.006\ BD^{0.89} \qquad 2.16$$

$$\phi = 0.009\ PI^{0.008} + 0.9695\ SP^{0.7808} + 0.0055\ STP^{1.663} - 0.009\ CP^{0.0196} + 0.0014\ BD^{8.08} + 0.00078\ w^{0.243} + \varepsilon \qquad 2.17$$

For the ANN MLP model 7-3-2 architecture gave the best result with the single hidden layer and 7-1-6-2 for the double hidden layers. From the result the author concluded that developed ANN model using MLPs, the back propagation training algorithm, and weight biases can be used with reasonable accuracy to model shear strength parameters. In ANN solution the equation results derived from weight and biases are closer to laboratory results with very less percentage of error.

Many empirical methods for shear strength parameters prediction of soils are presented in literature. Among these, four have been chosen for the purpose of assessing the relative performance of the ANN model (Goktepe et al., 2008)(Ersoy et al., 2013)(Yoseph, 2022)(Korayem, A., Ismail, K., & Sehari, 1996)(Roy, 2014). These methods are chosen as the database used in the work contains most parameters required to calculate shear strength parameters by these methods and also the models are developed for fine grained soils. The performance of the existing correlation methods and the ANN model on the validation set are given in Tables below for cohesion and internal friction angle respectively; also the graphical comparison of the models are shown in Figure below (Yoseph, 2022).

From the above models comparison, one can see that there is much variation of prediction values between the models. This indicates that correlation developed for a certain soil is not applicable for other soil. The reason for this variation may be due to the difference in test procedures and also the unique properties of the geological material where this correlation was developed (Yoseph, 2022).

Table 3: Summary of Literature Review

ANN Models	Sample size	Soil type	Input parameters	Correlation coefficient(R)
Lyeke et al,2016	83	Tropical lateritic soils	PI,Gs, LL,PL & %passing No.200	= 0.861 for c & 0.805 for ϕ
Kiran& Lal,2016	200	Clay soil	w, PI, BD, Sand %, Silt %,and Clay %	=0.942 for c & 0.981 for ϕ
Sarat Kumar Das & Basudhar, 2008	54	Clay soil	LL, Clay fraction, PI, and Change in PI	=0.906 for training & 0.942 for testing
Shoshpasha et al, 2015	195	Fine grained soils	N60, effective stress, and Fine content	=0.998 for training & 0.997 for testing
Abdulabbas,A.A & Bind, 2014	72	Cohesive soils	Depth, SPT-N value, LL, and PL	=0.8318 for c % 0.8033 for ϕ
Yoseph,2022	284	Fine grained soil	Sand%, Fine%, LL, PI, w, and BD	=0.98 for c & 0.92 for ϕ
Goktepe et al, 2008	79	Clay soils	w, LL, PL, Natural unit wieght & Dry unit weight	=0.93 for c & 0.85 for ϕ

2.9 Research Gaps

From the review of literature under related works, research gaps are identified for further study to improve the results and create a better understanding of the application of estimation of shear strength parameters. Here are the research gaps identified.

1. There is no research on using ANN software to solve any engineering problems in many towns other than Addis Ababa.
2. There is no specific equation developed to determine shear strength parameters from index properties for Bishoftu town.
3. There is also a need to estimate the shear strength parameters of soil easily.
4. There is no developed ANN model with large number of dataset.
5. While many studies have shown the potential of ANN models in predicting soil shear strength parameters, there is a need for comparison with traditional empirical methods. This could help to assess the accuracy and effectiveness of the ANN models in practical applications.

3 MATERIALS AND METHODS

The following section will explain the steps taken in this study, revealing the difficulties encountered throughout the research. Also, the stages of the work done, which were designed to obtain soil strength parameters cohesion and friction angle by developing and validating an artificial neural network model based on the primary and secondary data of the index property results and direct shear test results obtained, are discussed.

3.1 Description of the study area

Bishoftu, also known as Debre Zeit, is a town in Ethiopia located in the Oromia Region, approximately 47 kilometers southeast of the capital city of Addis Ababa. The town is situated in the Great Rift Valley and is known for its beautiful crater lakes, hot springs, and birdlife. Its geographical location is 8°45′N 38°59′E with an elevation of 1,920m (6,300 ft). The 2007 national census reported a total population for Bishoftu of 99,928, of whom 47,860 were men and 52,068 were women. The town is located within the Bishoftu volcanic field, an area of Holocene lava flows, cinder cones, tuff rings, and maars. Several of the maars are water-filled, forming five crater lakes. There are many important organizations and tourist attractions in Bishoftu. The town is home to a station for the Ethiopian Air Force. The crater lakes in Bishoftu are one of its major draws. Several large crater lakes, including Lake Hora, Lake Babogaya, and Lake Bishoftu, encircle the settlement. The lakes here are well-liked for boating, swimming, and wildlife viewing. Another well-liked draw in the town is its hot springs, which are renowned for their therapeutic qualities.

Vertisols are the type of soil that exists in Bishoftu. Vertisols are clayey soils with a high capacity for shrinkage and swelling. They stand out for having a lot of swelling clay minerals, which make the soil expand when it's wet and contract when it's dry. Vertisols typically have a dark color and a high capacity to retain nutrients, both of which are advantageous for agriculture. However, because the soil can become extremely hard when dry and can form deep cracks that can harm crops and infrastructure, their high potential for shrinking and swelling can also make them challenging to handle. The vertisols in Bishoftu are frequently found overlying volcanic rocks, which may influence their properties and make them more fertile. Additionally, the town is located in an area with moderate rainfall, which can help to sustain agriculture and support vegetation growth.

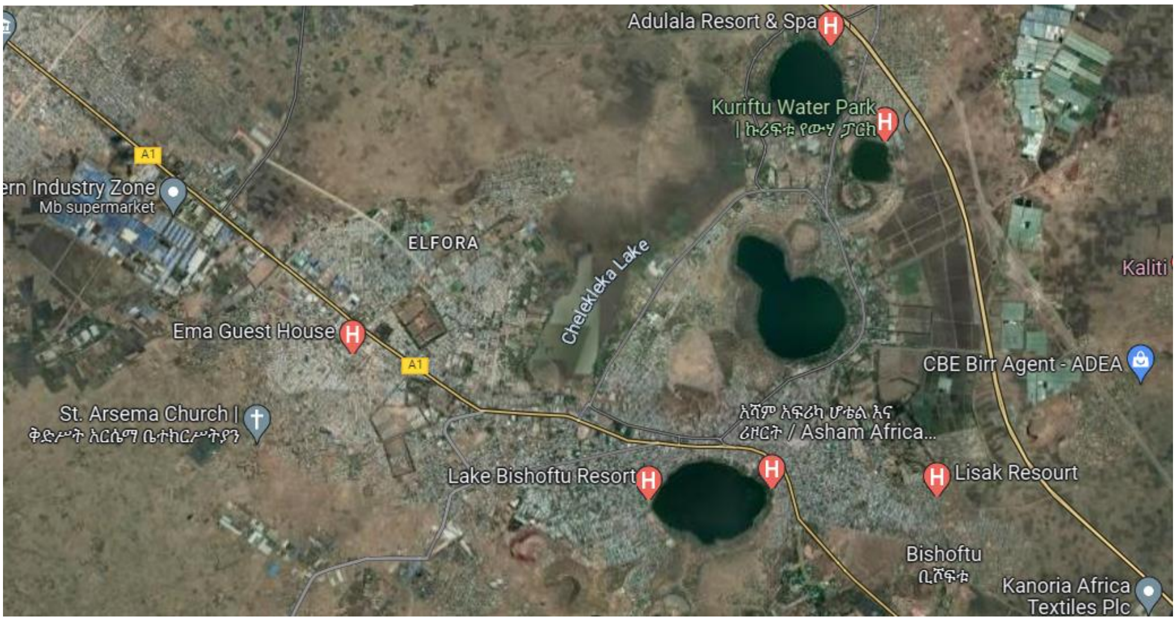

Figure 12: Location of Bishoftu town

3.2 Data collection and Sample size

A total of 316 soil sample laboratory test results were used in this research. The number of data points was determined by the artificial neural network's training requirements. Using a larger number of data to develop an artificial neural network is recommended to generate better generalization potential and minimize error. The 301 secondary data points were used to train the ANN models while the 15 primary data were used to cross validate the neural networks. Grain size distribution, Atterberg limits, and soil shear strength parameters are included in each soil test result.

3.2.1 Primary Data Collection

Before selecting primary data sample locations, visual site investigation was accomplished and necessary information was gathered regarding soil type and distribution throughout the town. Field identification of soils was carried out according to the ASTM D 2488 (Standard Practice for Description and Identification of Soil). Then the sample locations were selected in order to characterize the soil types found in the town including an industrialized and new construction area. The soil laboratory tests were done in ASTU (Adama Science and Technology University) and ARCON Design Build PLC geotechnical laboratories. All the tests were done according to the ASTM manual.

3.2.1.1 Sampling Area

The location of test pits was selected to characterize the soil types found in Bishoftu town. The sampling locations are Sunshine, Babugaya, Airforce, Ude/Denkaka, Kurkura, near Dukem, China sefer, Meda/Mesalemiya, Ashewa sefer, Indomie Factory, TVET and Adis sefer. These are residential areas, industrialized areas and new construction sites. The industrialized areas are places for factories like Crown packaging & plastics, Seven Hills Packaging solutions, SAWAYA Ethiopia Indomie Factory, Flower factory, Textile factory, and petrol station. The specific location of samples taken for the primary data and their depth is summarized on table 4.

Table 4: Sample Location and Depth of Primary Data Soil Samples

Locations	Test pit number	Latitude	Longitude	Sample depth(m)
Sunshine	Tp 1	8.734650	39.008535	1.5
Sunshine	Tp 2	8.73230	39.00991	1.5
Babugaya	Tp 3	8.7930	38.9909	1.5
Airforce	Tp 4	8.723886	38.992990	1.5
Ude/ Denkaka	Tp 5	8.681255	39.0345	1.5
Kurkura	Tp 6	8.7422873	38.9327956	1.5
Kurkura	Tp 7	8.7560845	38.9600119	1.5
Near Dukem	Tp 8	8.7774865	38.9327956	1.5
China sefer	Tp 9	8.72073	39.01019	1.5
Meda/Mesalemiya	Tp 10	8.71691	39.01350	1.5
Ashewa sefer	Tp 11	8.70556	39.02229	1.5
Indomie factory	Tp 12	8.6937	39.0329	1.5
TVET	Tp 13	8.78728	38.99817	1.5
Adis Sefer	Tp 14	8.7508467	38.9634737	1.5
Adis sefer	Tp 15	8.758992	38.949442	1.5

Figure 13: Google locations of sampling test pits

3.2.1.2 Soil Sampling and Preparation

For the study, a total of fifteen representative disturbed soil samples were taken from the selected sites. The samples were obtained at depth of 1.5m below the ground surface. The samples were selected by the standard sampling methods and techniques. For the determination of liquid limit, plastic limit, plasticity index, and grain size analysis disturbed samples were used. In contrast, remolded soil samples were used to determine shear strength parameters.

3.2.2 Laboratory Soil Tests and Test Standards

3.2.2.1 Grain size distribution

Grain size distribution or the percentage of various sizes of soil grains present in a given dry soil sample, is an important soil property. Grain size analysis of coarse grained soil is carried out by sieve analysis, whereas fine grained soil are analyzed by the hydrometer method. In general, as most soil contains both coarse and fine gained constituents, a combined analysis is usually carried out. This information is used to classify the soil in accordance with the Unified Soil Classification System (USCS). For grain size analysis, the disturbed soil samples were wet sieved through 75 µm (No. 200) sieve to determine the amount of material finer than the sieve in the soils. Particles with a size greater than 75 µm were then oven dried and sieved through a set of sieves ranging from number 3 to 200 (75 mm to 75 µm) sieves. Percent finer for different sizes of the particles retained on different sieves were calculated. Finally the soils were classified according to the Unified Soil Classification System (USCS) as shown in table 5.

Table 5: USCS Soil Classification

Class	**Grain size**
Gravel	4.75 mm to 75 mm
Sand	0.075 mm to 4.75 mm
Fine	<0.075 mm

3.2.2.2 Atterberg limits tests

Atterberg limits tests establish the moisture contents at which fine grained clay and silt soils transition between solid, semi solid, plastic and liquid states. These tests provide information regarding the effect of water content (w) on the mechanical properties of soil. Specifically, the effects of water content on volume change and soil consistency are addressed. There are three important Atterberg limits: Liquid limit (LL), Plastic limit (PL), and Shrinkage limit (SL). The liquid limit is defined as the water content, in percent, at which a part of soil in a standard cup and cut by a groove of standard dimensions will flow together at the base of the groove for a distance of 13mm (1/2 in.) when subjected to 25 shocks from the cup being dropped 10mm in a standard liquid limit apparatus operated at a rate of two shocks per second. The plastic limit is the water content, in percent, at which a soil can no longer be deformed by rolling into 3.2mm (1/8 in.) diameter threads without crumbling. From the Atterberg limit tests the liquid limit and plastic limit were determined and plasticity index which is the difference of the two was computed. Soil that passes through a sieve diameter of 0.425mm (425 µm) was used to perform the tests.

3.2.2.3 Direct shear test

Direct shear testing provides the strength properties of soils under conditions of drained loading, which is required for assessing different applications. Soil specimens are typically cylindrical, and are placed inside a square shear box. The minimum specimen diameter is

2in, but the diameter must be at least 10 times the maximum particle size. The thickness of the specimen must be at least 0.5in, and the minimum diameter: thickness ratio is 2:1. The direct shear test was performed in accordance with ASTM. The disturbed sample is used for the test and remolded soil which undergoes compaction is placed in to a metal square shear box of 62 mm x 62 mm x 20 mm undergoes a horizontal force.

ASTM manual of standard test methods were used for the laboratory soil tests of this study as presented in table 6.

Table 6: ASTM Manual of Standard Test Methods

Test Type	**ASTM Standard Manual**
Grain size distribution	D 4318-00
Atterberg limits	D 1140-14
Direct shear test	D3080-04
Field identification of soils	D 2488-00
Sample preserving and transporting	D 4220-95

3.2.3 Secondary Data Collection

For this research, three hundred one (301) soil test results were gathered from different soil investigation consulting firms. The secondary data were collected from Bishoftu Governmental Construction Office, Grace Engineering PLC, PIER Consulting Soil Test PLC, and ARCON Design Build PLC. The data comprises soil test results of different areas in Bishoftu. Therefore, the database was prepared to obtain a wide variety of soil types that represent Bishoftu town soil. Then, the data analyze the collected data in order to verify the input and output range so that the models' interval of confidence could be understood.

3.2.4 Input and Output Variables Description

The shear strength parameters of the soil, cohesion and internal friction angle are the desired output variables from the developed artificial neural network models. Choosing the right input variables that are well correlated with the desired outputs has an impact on a neural network when it comes to finding good prediction accuracy. The input variables must have a clear relationship with the output variables to influence the output's result. On former works related to ANN prediction of shear strength parameters, index properties were widely used as input parameters. Not only ANN prediction but also regression analysis often used index properties to show their correlation with shear strength parameters. In those researches it was proved that soil index properties have a good correlation with shear strength parameters of soil and can be used as input parameters for developing ANN models. The most commonly used soil index properties to predict strength parameters of soil were Grain size distribution and Atterberg limits. In the current study the input parameters used are also Grain size analysis and Atterberg limits. To ensure the correlation between the suggested input parameters with the desired output variables, a scatter plot was employed. A scatter plot is used to visually display the relationship between dependent and independent variables. The input variables were used as independent variables and the output variables as dependent variables. The correlation between the input and output variables was also done by using least square regression method to compare with other models.

3.3 ANN Modeling Procedure

3.3.1 Data Preprocessing

In machine learning, data quality is a major concern. To assure data quality, data preprocessing is required as a primary task before using raw data directly in any machine learning. In this study data integration, data cleaning, and data reduction were the methods used from the various data preprocessing techniques before developing the neural network models. Data integration is a way of merging data collected from different sources in the same format. This was the first challenge faced when dealing with the collected large-sized data structured differently. Even if it took some effort, it helped to avoid inconsistencies. In cases where collected data were incomplete, data cleaning was implemented. In this phase the data cleaning is done by eliminating the incomplete data since filling a missing data may decrease the quality of data and lead to a wrong value if not done properly. Data reduction was used to remove redundancy from the data set. This required careful observation of each line of data. In this study, all data integration, data cleaning and data reduction were done manually.

3.3.2 Modeling tool

The neural networks were developed using MATLAB R2018a. MATLAB is a programming language that can be used to analyze data, build algorithms and generate models. In this study, MATLAB was used for data analysis and model development using neural networks. There are some toolboxes in MATLAB that are collection of functions to address a certain type of problem. Neural networks are one of those functions with an available toolbox in MATLAB. In this study, the neural networks were modeled by directly coding a script into MATLAB. Script authoring allows more freedom to model neural networks the way needed than the neural network toolboxes. It is possible to change the architecture, training algorithm, learning methods and other aspects of the model as required while using script authoring for better performance.

3.3.3 Model Development

While developing the ANN models, the following steps were followed.

3.3.3.1 Data Division

The data sets were divided into training, validation and testing subsets randomly. Training data were used for learning. The testing data were used to measure the performance of the models on data that played no role in building the models. In order to obtain a consistent data division, several combinations of the training, validation and testing sets were considered. The best proportion was selected based on the resulting neural network performance. The proportion that gives a minimum value of mean squared error (MSE) and higher correlation coefficient R was taken as the best proportion to train the neural networks. For the neural networks, the proportion 70%, 15%, 15% was found to be the best proportion for training, validation and test sets respectively. Finally, for the neural network cross validation evaluation test 15 primary soils data were used. The number of input neurons was equal to the number of input variables and the number of output neurons was equal to the number of output variables. The number of hidden neurons in the hidden layer was determined by calculating the root mean squared error (RMSE). The number of hidden neurons that gives an output with minimum RMSE for the validation set was taken as the optimum number of hidden neurons.

3.3.3.2 Define Neural Network Architecture

In this Study, the Multilayer Perceptron Network (MLP) technique has been utilized to obtain a precise model relating shear strength parameters (c and ϕ) to index properties of soils. MLPs are classes of ANNs using feed forward architecture that are usually applied to perform supervised learning tasks, which involve iterative training methods to adjust the connection weights within the network. They are usually trained with Back Propagation (BP) algorithm. The number of nodes at the input layer is equal to the input parameters and the number of nodes at the output layer is equal to the output parameter.

3.3.3.3 Neural Network Training

A supervised learning method was used for both c and ϕ neural network models. Both the input and corresponding outputs values were provided while training the neural network models. The Levenberg-Marquardt algorithm (trainlm) training function was used to train the neural network models which is often the fastest back propagation algorithm and is suggested as a first choice supervised learning algorithm. Even though this training function takes more memory than other methods, it was chosen to train the neural networks because of its fast computation ability.

3.3.4 Model Cross Validation

The developed neural network models were validated using the 15 primary soil laboratory test results. The soil laboratory tests include grain size analysis, Atterberg limit and direct shear test. The result from the grain size analysis and the Atterberg limit tests were used as input variables to predict the shear strength parameters. Then the value of shear strength parameters cohesion and internal friction angle that was found by the experimental laboratory test was compared with the values from the prediction models' output. The comparison between the two values was used to show how well the artificial neural network models can predict the shear strength parameters value from soil index properties. The performance of the neural network models on the primary data was shown by calculating the mean squared error (MSE).

3.3.5 Model Performance Evaluation

To assess the performance of the developed neural network models the correlation coefficient (R), mean squared error (MSE) and root mean squared error (RMSE) were calculated. The correlation coefficient R was used to measure how well the predicted values using the created neural networks match the actual experimental results which value ranges from -1 to 1. As the R-value approaches 1 or -1, it indicates that the predicted values are well aligned with the actual values and when it approaches zero, it indicates that the model prediction is not well aligned with the actual or experimental values.

The mean squared error (MSE) is the difference between the original and predicted values, which is determined by squaring the average difference over the data set. It is a measure of the precision between the anticipated and original values, or how close the fitted line is to the actual data points. The less the MSE values, the closer the fitted line is to the original, indicating good precision between predicted and actual (experimental) values.

The error rate determined as the root of the mean squared error is called root mean squared error (RMSE). Because it has the same unit as the amount represented on the y-axis, RMSE is the most simply understood statics and is a good fit indicator.

$$\text{MSE}=\frac{1}{n}\sum(\text{Yi}-\text{yi})2 \qquad \text{Equation 3.1}$$

$$\text{RMSE}=\sqrt{\sum_{\text{i}=1}^{\text{n}}\frac{(Yi-yi)2}{n}} \qquad \text{Equation 3.2}$$

Where, Yi is the actual value and yi is the predicted value

An error histogram was also used to visually display the error ranges and their redundancies.

3.3.6 ANN Model Equation Derivation

The model equation for both of cohesion and internal friction angle prediction were derived by following the steps performed in creating the ANN models. The steps are normalizing input variables, calculating the weighted sum using weight and bias values and calculating the output using the activation function. These processes may be repeated a number of times based on the number of hidden layers used in the model. Finally, the output is transformed in to the original value from the normalized value. These steps are summarized on Figure 14.

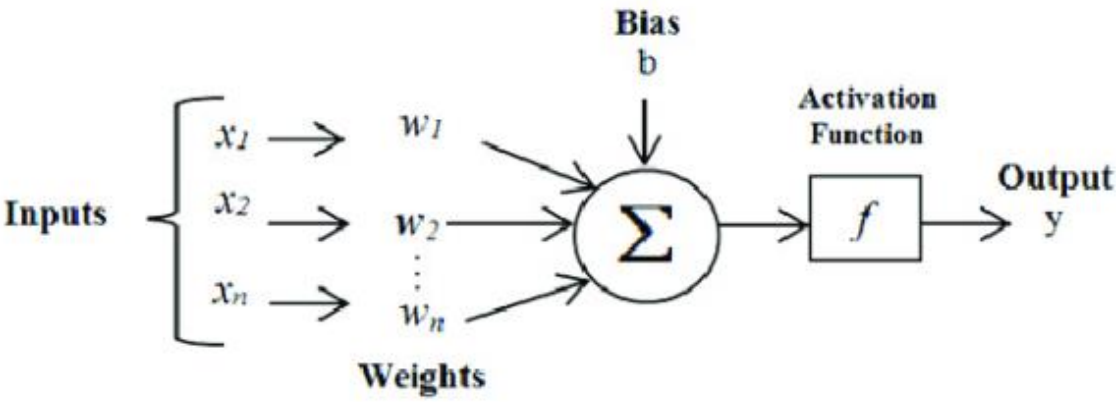

Figure 14: General Procedure in ANN Equation Derivation (Adugna, 2021)

4 RESULTS AND DISCUSSION

4.1 General

In this chapter the results of the soil laboratory test on primary data, the relationship between input and output parameters, the development of the ANN models by the secondary data with their structure and performance, model cross validation using experimental data, model equation derivation and their comparison with formerly formulated regression analysis and ANN models with common parameters are presented and discussed.

4.2 Laboratory Test Results

Laboratory tests were used to determine the index properties and shear strength parameters of soil samples. Three soil laboratory tests: grain size analysis, Atterberg limits and direct shear tests were done on 15 samples used as primary data. The primary data soil test results are summarized, as required for further analysis, below in the table.

Table 7: Summary of the Primary Data Soil Test Results

Test Pit No.	Grain size distribution		Atterberg limits			Shear strength parameters	
	% Sand	% Fine	LL	PL	PI	c	ϕ
TP 1	16.2	82.8	59.8	29.8	30	7	24
TP 2	5	94.1	83.4	36.2	47.2	21	18
TP 3	6	93.8	61.6	30.7	30.9	21	19
TP 4	4	95.5	89	35	54	15	19
TP 5	8	91.2	65.5	27	38.5	22	20
TP 6	13	86.6	57.2	33.4	23.8	10	28
TP 7	10.5	87.2	94.4	40.7	53.7	6	30
TP 8	4.6	94.4	90	37.8	52.2	23	19
TP 9	4	96	71	38	33	37	5
TP 10	7	93	72	35	37	35	4
TP 11	4	96	73	37	36	39	3
TP 12	6	94	75	37	38	38	3
TP 13	11	69	40.3	35.8	4.5	12	22
TP 14	20	56	42.4	35.2	7.2	14	22
TP 15	15	85	48.7	36.2	12.5	26	18

4.3 Secondary Data Analysis

Statistical descriptions of examined soils parameters are given below in Table 8. It can be seen from the table that the distributions of the median and average values of the soil properties are close together. This shows that soil experimental data are approximately normally distributed. This is further collaborated by the value of the skewness (-0.008 to 1.78). Also the standard deviation tells, on average, how far each value lies from the mean; this low standard deviation indicates that values are clustered close to the mean.

Table 8: Descriptive Statistics of the Secondary Data Soil Test Results

Parameter	% Sand	%Fine	LL	PL	PI	c	ϕ
Mean	18.596	76.732	54.449	29.791	24.680	23.830	14.255
Standard error	0.635	0.716	0.943	0.578	0.667	0.438	0.239
Median	16.77	75.32	52	33	23	24	15
Standard deviation	11.024	12.424	16.372	10.029	11.579	7.604	4.153
Sample variance	121.529	154.374	268.065	100.587	134.080	57.834	17.251
Skewness	1.785	-0.835	1.194	-0.484	1.574	0.006	-0.008
Range	72.14	68.09	89.81	42	71.32	49	22
Minimum	1	30.91	29	8	3.2	2	2
Maximum	73.14	99	118.81	50	74.52	51	24
Count (N)	301	301	301	301	301	301	301

The cohesion values had a mean of 23.8 kPa and standard deviation of 7.6 kPa. Also the values are in the range of 2 kPa to 51kPa. Meanwhile, friction angle statistics presented in the table show a mean value of 14.25° and distribution of gathered values in a range of 2° to 24°. That might represent a limitation on the prediction of values outside this range.

A correlation matrix was carried out on the soil parameters using Pearson's correlation. The correlation matrix is given in Table 9. The matrix indicated a high correlation between liquid limit and plasticity index. Except that there is no high positive or negative correlation between the variables; since high correlation coefficient between the pairs may lead to poor performance of the models and difficulty in interpreting the effects of the explanatory variables on the response. In the selection process of input parameters, it was tried to avoid multicollinearity. Also the correlation of cohesion and angle of internal friction with the other soil parameters did not give a high relationship, hence using regression analysis is likely to produce inappropriate models, but not for ANNs.

Table 9: Pearson's Correlation Matrix of the Variables

Soil Parameters	% Sand	% Fine	LL	PL	PI	c	Ø
% Sand	1						
% Fine	-0.88483	1					
LL	-0.06347	0.207216	1				
PL	-0.01169	0.217839	0.715986	1			
PI	-0.07885	0.105383	0.796042	0.148216	1		
C	-0.04602	0.10268	-0.09233	0.142356	-0.25876	1	
ϕ	0.014105	0.285149	0.645335	0.670724	0.334024	-0.0767	1

From the above graphs it may be stated that each input variable alone is not enough to predict c and ϕ.

4.4 Primary Data Analysis

The statistical analysis of the laboratory test results of the primary data is summarized below in Table 10. The cohesion values are ranged from 6 kPa to 39 kPa. Also as shown in the table the value of the friction angle ranges from 3° to 30°.

Table 10: Descriptive Statistics of the Primary Data Set

Parameters	% Sand	%Fine	LL	PL	PI	c	ϕ
Mean	8.953	87.64	68.22	34.986	33.233	21.8	15.666
Standard error	1.317	2.918	4.355	0.907	4.091	2.900	2.375
Median	7	93	71	35.8	36	21	19
Standard deviation	5.101	11.304	16.868	3.515	15.846	11.232	9.201
Sample variance	26.029	127.785	284.544	12.355	251.099	126.171	84.666
Skewness	0.905	-2.017	-0.127	-0.901	-0.492	0.307	-0.267
Range	16	40	54.1	13.7	49.5	33	27
Minimum	4	56	40.3	27	4.5	6	3
Maximum	20	96	94.4	40.7	54	39	30
Count (N)	15	15	15	15	15	15	15

4.5 ANN Prediction Model

After input and output data gathered and structured; training and test sets were established. A total of 301 secondary data were used to develop the models in this study, 70% used for the training, 15% for test and 15% for validation. After the models developed the 15 primary data used for cross validation of the selected best model. The general characteristic of the developed models is presented in the table below.

Table 11: Summary of the Developed Neural Network Models Characteristics

Parameters	Descriptions
Input parameters	Sand%, Fine%, LL, PL, and PI
Output parameters	c, ϕ
Number of hidden neuron	Trial and error(from 6 to 20)
Number of hidden layer	1
Learning method	Supervised learning
Network type	Feed forward Back propagation
Architecture	Multilayer Perceptron (MLP)
Data division	Random (dividerand)
Hidden layer activation function	Hyperbolic tangent Sigmoid function(tansig)
Output layer activation function	Linear function (purelin)
Training function	Levenberg-Marquardt (trainlm)
Performance function	MSE

4.5.1 Prediction to Cohesion

For prediction of cohesion values 20 models were developed. In the present case different architectures were developed for single hidden layer neurons. First the neuron was fixed as6in three layer architecture (input layer-hidden layer-output layer), then neurons were increased consecutively so as to study each architecture with increase in the neurons in hidden layer. Table 12 summarizes the different neural architectures and their accuracies in terms of correlation coefficient (R), mean squared error (MSE) and root mean squared error (RMSE) values.

Table 12: Prediction Models Developed for c

		Correlation Coefficient, R					
Model No.	**Network**	**Training**	**Validation**	**Test**	**All**	**MSE**	**RMSE**
1	5-6-1	0.74746	0.69639	0.72504	0.73455	26.02	5.1
2	5-7-1	0.95116	0.90815	0.68223	0.87421	8.48	2.91
3	5-8-1	0.75302	0.79148	0.6953	0.7427	25.02	5.001
4	5-9-1	0.96323	0.95851	0.88023	0.94954	3.99	1.99
5	5-9-1	0.95935	0.91906	0.87589	0.93422	11.39	3.37
6	5-10-1	0.95055	0.82408	0.82024	0.90464	22.01	4.69
7	**5-10-1**	**0.99929**	**0.99887**	**0.99725**	**0.99894**	**1.27**	**1.12**
8	5-10-1	0.94444	0.8826	0.8554	0.91624	10.83	3.29
9	5-10-1	0.95755	0.96581	0.82193	0.93477	3.13	1.76
10	5-11-1	0.93867	0.87302	0.84632	0.91207	12.58	3.54
11	5-11-1	0.96586	0.94359	0.94144	0.95697	6.73	2.59
12	5-12-1	0.996	0.98519	0.9752	0.99204	1.49	1.22
13	5-13-1	0.70719	0.45864	0.78273	0.65523	71.50	8.45
14	5-14-1	0.98559	0.92045	0.81711	0.9483	12.91	3.59
15	5-15-1	0.98405	0.95711	0.94925	0.97723	4.09	2.02
16	5-16-1	0.89291	0.82943	0.82372	0.87032	19.97	4.46
17	5-17-1	0.88486	0.9134	0.61214	0.85491	9.47	3.07
18	5-18-1	0.99209	0.93325	0.9297	0.97666	6.83	2.61
19	5-19-1	0.99609	0.97199	0.97262	0.99007	2.25	1.5
20	5-20-1	0.98204	0.85055	0.80104	0.92878	20.69	4.54

The training, validation and testing accuracies in terms of R values observed across different models are as follows: 0.70 to 0.99 for training 0.45 to 0.99 for validation and 0.61 to 0.99 for testing. R value close to 1 and MSE value near zero indicates a predicting capability. So a stable architecture can be reported among these architectures. Accordingly, a robust model selected among 20 architectures developed is model 7 of network 5-10-1.

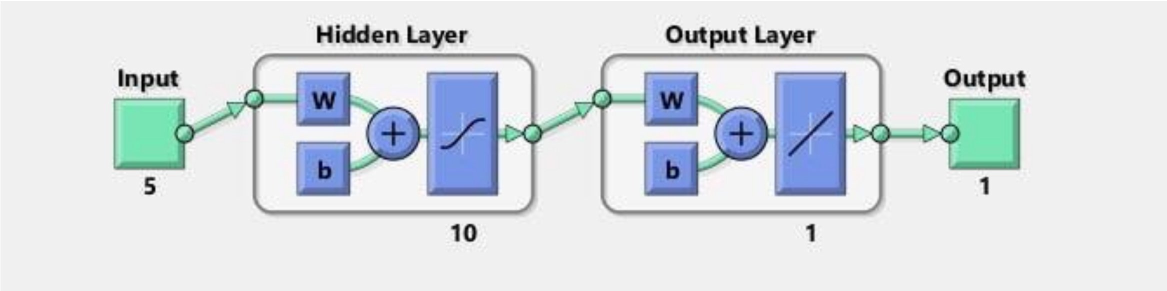

Figure 15: Neural Network Architecture Sample of the Model 7

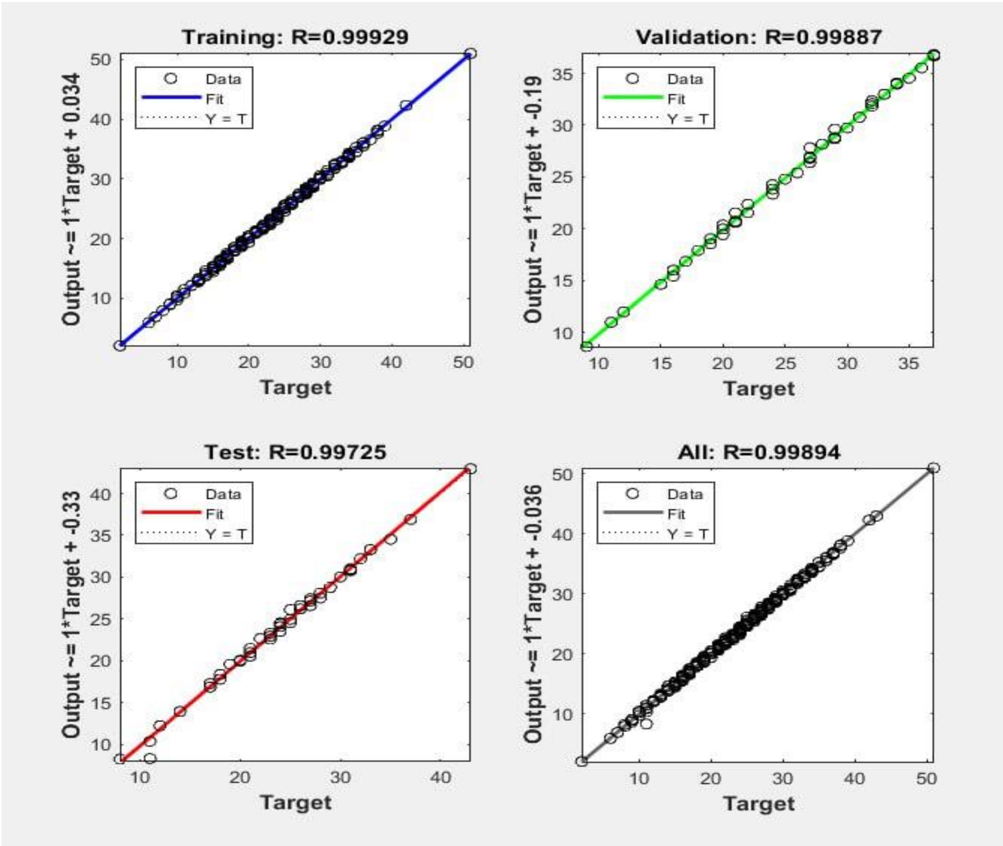

Figure 16: Regression Plot of Model 7

The regression plot describes the relationship between the response (output) variable, and the predictor (input) variables; also relationship between the actual (target) value and the predicted (output) value. As shown in Table 12 and Figure 16, Model 7 was determined to be the best structure to solve this problem. In order to examine the relationship between the values obtained as a result of the network and the actual values, the regression plot generated at the end of the process is looked at. In this study, R values were calculated as 0.999 for the training, 0.998 for the validation, 0.997 for the test, and 0.998 for all data as shown in Figure16.

4.5.2 Prediction to Internal Friction Angle

For prediction of Internal friction angle values 20 models were developed. In the present case different architectures were developed for single hidden layer neurons. First the neuron was fixed as 6 in three layer architecture (input layer-hidden layer-output layer), then neurons were increased consecutively up to 18, so as to study each architecture with increase in the neurons in hidden layer. Table 13 summarizes the different neural architectures and their accuracies in terms of correlation coefficient (R), mean squared error (MSE) and root mean squared error (RMSE) values.

Table 13: Prediction Models Developed for ϕ

		Correlation Coefficient, R					
Model No.	**Network**	**Training**	**Validation**	**Test**	**All**	**MSE**	**RMSE**
1	5-6-1	0.85878	0.74239	0.82233	0.8379	7.05	2.65
2	5-7-1	0.97153	0.87693	0.90529	0.95109	3.34	1.82
3	5-8-1	0.97133	0.98091	0.94532	0.96917	7.04	2.65
4	5-9-1	0.92348	0.88956	0.91779	0.91841	3.63	1.90
5	5-9-1	0.95282	0.74342	0.75285	0.88068	10.93	3.30
6	5-10-1	0.86552	0.78924	0.87272	0.85309	17.55	4.18
7	5-10-1	0.99066	0.98297	0.97752	0.98728	5.76	2.4
8	5-10-1	0.9742	0.93777	0.92502	0.96188	2.30	1.51
9	5-10-1	0.98775	0.96981	0.89589	0.97243	1.86	1.36
10	5-11-1	0.98605	0.97526	0.97786	0.98311	7.57	2.75
11	5-11-1	0.99271	0.94491	0.98311	0.98258	2.28	1.50
12	**5-11-1**	**0.98904**	**0.96517**	**0.94741**	**0.97941**	**1.15**	**1.07**
13	5-12-1	0.95195	0.80187	0.88126	0.91078	9.09	3.01
14	5-12-1	0.877	0.84375	0.87557	0.87004	6.07	2.46
15	5-13-1	0.9751	0.89656	0.76492	0.92877	3.02	1.73
16	5-14-1	0.5587	0.42432	0.53689	0.50061	40.99	6.40
17	5-15-1	0.97206	0.71885	0.96158	0.93092	6.61	2.57
18	5-16-1	0.66084	0.357	0.74773	0.51804	56.90	7.54
19	5-17-1	0.9314	0.75582	0.88673	0.86934	12.89	3.59
20	5-18-1	0.93978	0.69117	0.94289	0.84762	37.53	6.12

The training and testing accuracies in terms of R values observed across different models are as follows: 0.55 to 0.99 for training, 0.35 to 0.98 for validation and 0.53 to 0.98 for testing. R value close to 1 and MSE value near zero indicates a predicting capability. So a stable architecture can be reported among these architectures. Accordingly, a robust model selected among 20 architectures developed is model 12 of network 5-11-1 (five input neurons, eleven hidden neurons and one output neuron).

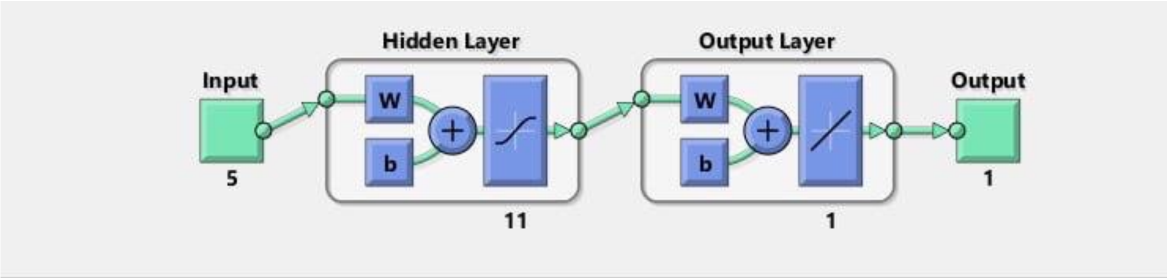

Figure 17: Neural Network Architecture Sample of the Model 12

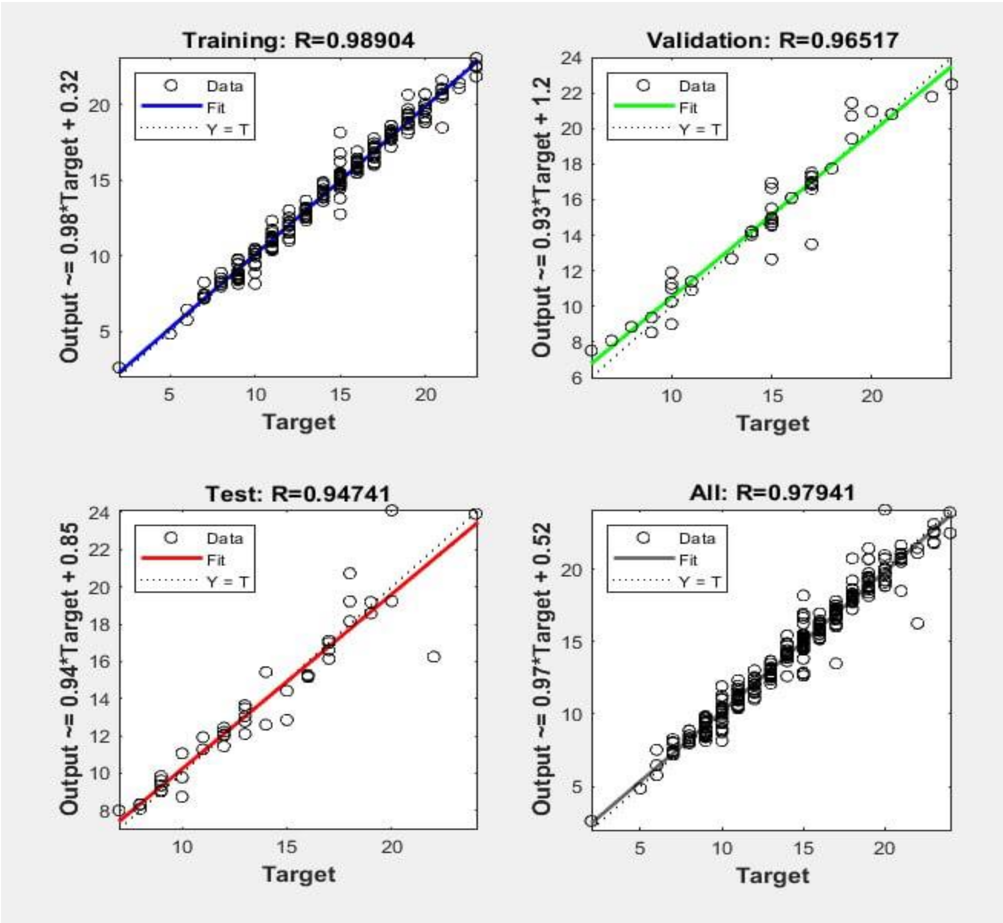

Figure 18: Regression plot of Model 12

As shown in Table 13 and Figure 18, Model 12 was determined the best structure to solve this problem. In order to examine the relationship between the values obtained as a result of the network and the actual values, the regression graph generated at the end of the process is looked at. In this study, adjusted R values were calculated as 0.98 for the training, 0.96 for the validation, 0.94 for the test, and 0.97 for all data as shown in Figure 18.

4.6 Cross Validation of the Model

4.6.1 Model Validation for c Prediction

The model was validated on primary soil test result data. The result indicates a very good prediction of cohesion (c) of the model with average difference value of 1.8, R value of 0.98 and RMSE value of 1.49, between experimental c and Predicted c values. Table 14 shows experimental and predicted values and of c for primary data set.

Table 14: Experimental and Predicted Values of c for Primary Data Set

Experimental c (kPa)	Predicted c(kPa)	Difference (kPa)
7	5.8	-1.2
21	21.6	0.6
21	18.3	-2.7
15	19.2	4.2
22	21.8	-0.2
10	11.1	1.1
6	6.1	0.1
23	25	2
37	36.7	-0.3
35	34.9	-0.1
39	38.3	-0.7
38	37.7	-0.3
12	10.4	-1.6
14	15	1
26	25.9	-0.1
Average difference (kPa)		**= 1.8**

The maximum difference showed between the experimental c and predicted c value was 4.2 kPa and the average difference was 1.8 kPa. The model showed very good prediction capacity on primary data set of the research.

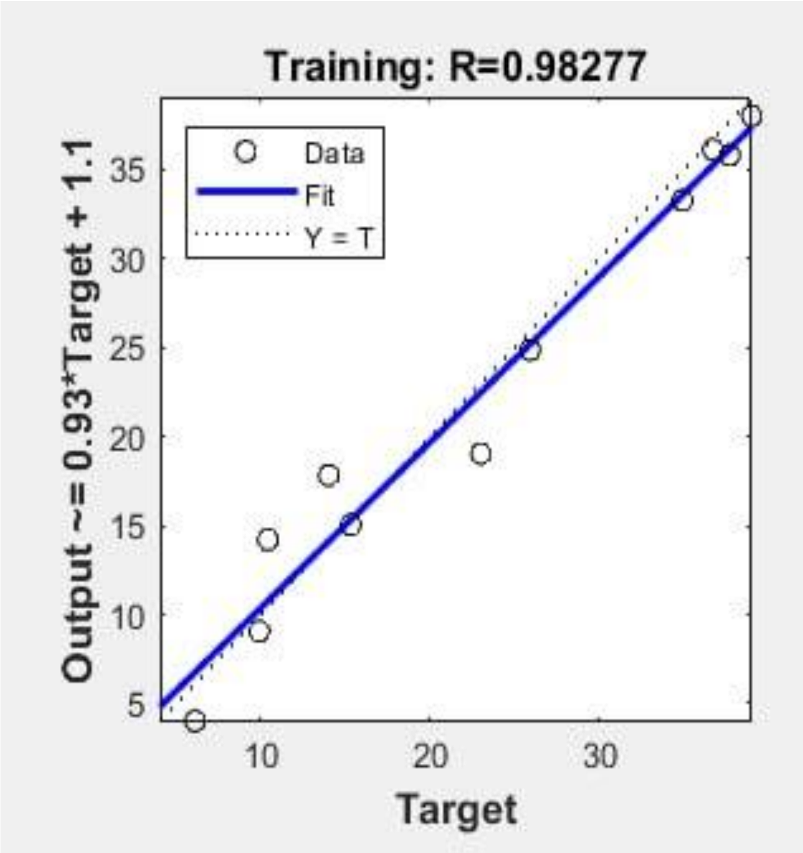

Figure 19: Regression Plot of Prediction of c Value for Primary Data Set

As can be seen from the regression graph in Figure 19, the data points are scattered near the line Y=T. the correlation coefficient R= 0.98277 indicates very good correlation between the actual and the predicted values of the primary data set.

4.6.2 Model Validation for ϕ Prediction

The model validation on primary soil test result data indicates an average difference value of 1.5, R value of 0.98 and RMSE value of 1.86, between experimental c and Predicted c values. The result shows a very good prediction of friction angle (ϕ) of the model. Table 15 shows the experimental and predicted values of ϕ for primary data set.

Table 15: Experimental and Predicted Values of Φ for Primary Data Set

Experimental ϕ (°)	Predictedϕ (°)	Difference ϕ (°)
24	24.6	0.6
18	15.5	-2.5
19	19.4	0.4
19	18.4	-0.6
20	20.1	0.1
28	24.4	-3.6
30	31.1	1.1
19	19.5	0.5
5	6.5	1.5
4	5	1
3	4.2	1.2
3	4.5	1.5
22	20.8	-1.2
22	21.8	-0.2
18	19.7	1.7
Average difference (°)		**1.5**

The maximum difference showed between the experimental ϕ and predicted ϕ value was 3.6° and the average difference was 1.5°. Generally the model showed very good prediction capacity on primary data set of the research. Also the regression graph in Figure 20 shows that, the data points are scattered near the line Y=T. the correlation coefficient R= 0.98786 indicates very good correlation between the actual and the predicted values of the primary data set of ϕ values.

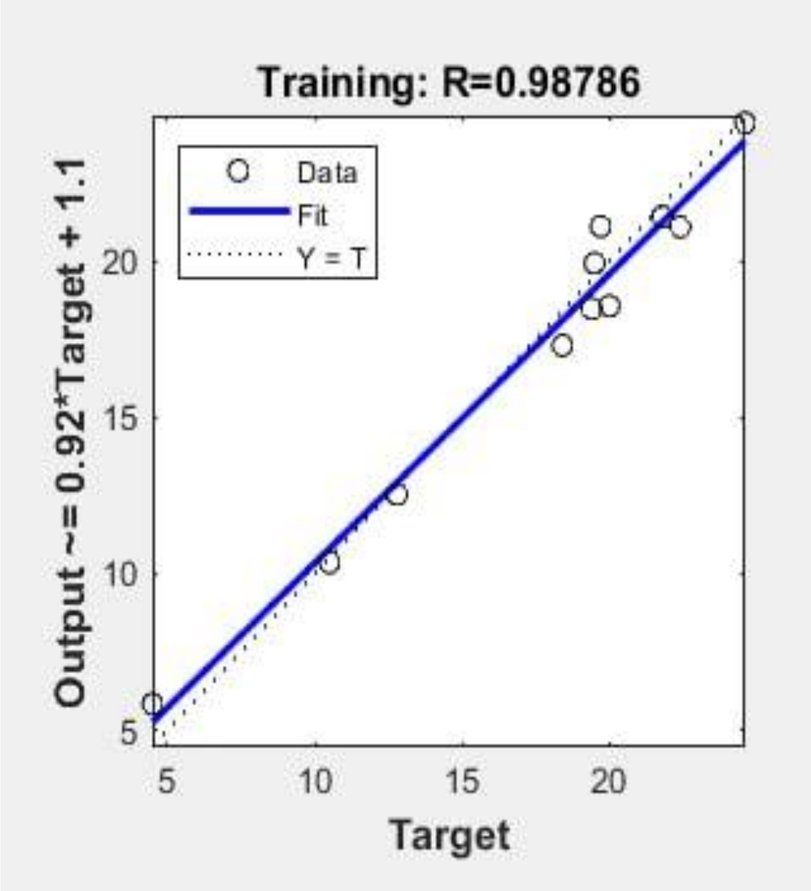

Figure 20: Regression Plot of Prediction of Φ Value for Primary Data Set

4.7 ANN Model Equations Model Performance Evaluation

4.7.1 Model Performance evaluation for c prediction

The model performance was evaluated by the coefficient of correlation (R) values of the test data and the combined data, Error histogram of the combined data and also MSE & RMSE values. The selected model, Model 7 (network 5-10-1) showed R value of 0.99 and 0.99 for testing and combined data sets respectively; also minimum values of MSE and RMSE, 1.27 and 1.12 respectively. The correlation coefficient R= 0.99 of the combined data indicates very good correlation between the actual and the predicted values of the entire data. R = 0.99 of the test data also indicates the performance of the model on new data sets. The comparison between the actual and predicted value of c using model 7, is plotted on Figure 21. The plot indicates good fitting and accuracy between experimental and predicted c values.

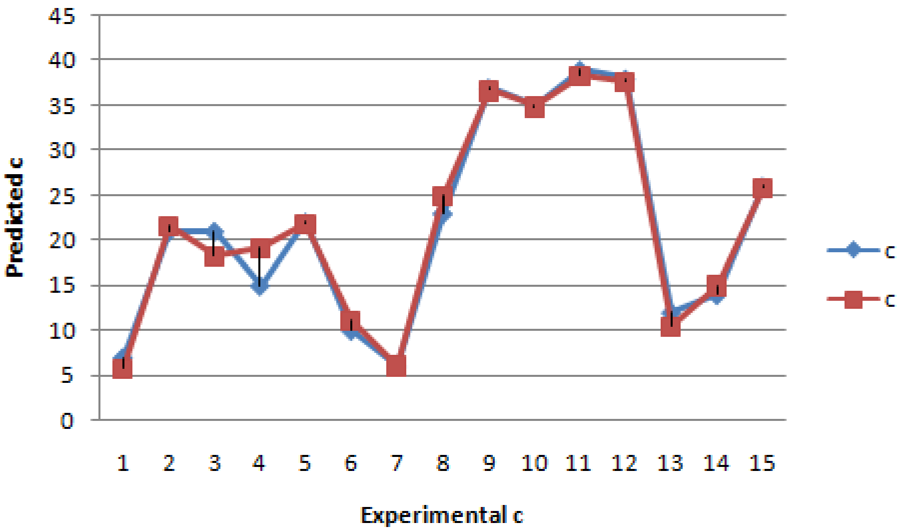

Figure 21: Comparison of Measured and Predicted c Value of Model 7

Error histogram indicates the errors between target values and predicted values of the model. As these error values indicate how predicted values are differing from the target values, hence these can be negative.

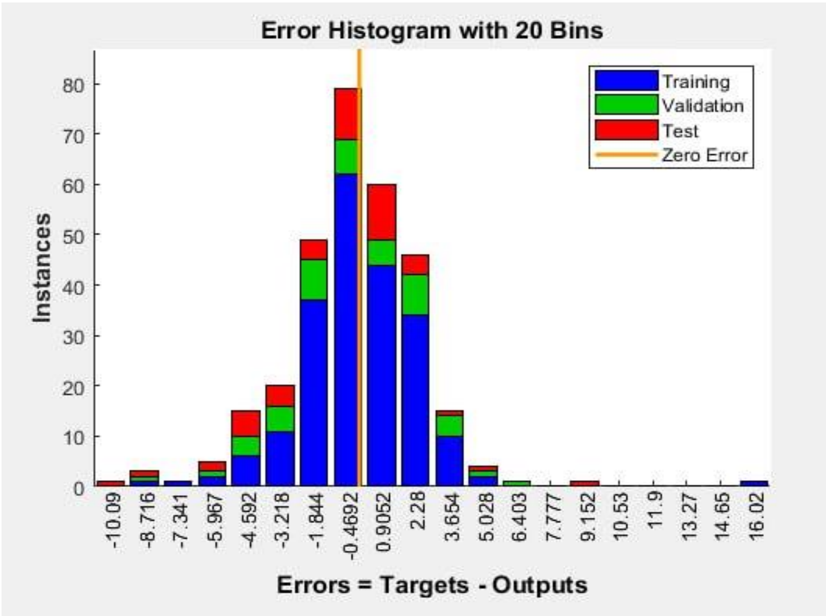

Figure 22: Error Histogram of Model 7 for Prediction of c

Error distribution of the entire data using model 10 is plotted on an error histogram graph of Figure 22. A significant concentration of error is seen at 0. The error histogram also shows that instances near zero error are higher than the rest indicating a minimum difference between actual and predicted values.

4.7.2 Model Performance Evaluation for ϕ Prediction

The model performance was evaluated by the coefficient of correlation (R) values of the test data and the combined data, Error histogram of the combined data and also MSE & RMSE values. The selected model, Model 12 (network 5-11-1) showed R value of 0.98 and 0.97 for testing and combined data sets respectively; also minimum values of MSE and RMSE, 1.15 and 1.07 respectively. The correlation coefficient R= 0.97 of the combined data indicates very good correlation between the actual and the predicted values of the entire data. R = 0.98 of the test data also indicates the performance of the model on new data sets. The comparison between the actual and predicted value of c using model 12, is plotted on Figure 23 and it showed good fitting and accuracy between experimental and predicted c values.

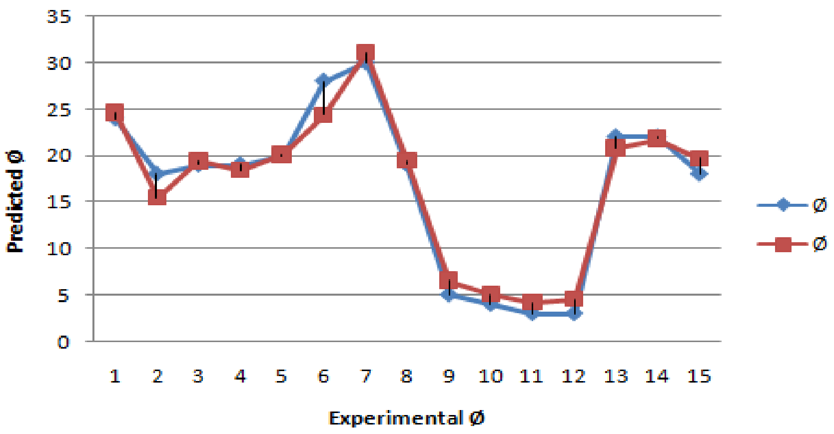

Figure 23: Comparison of measured and predicted ϕ value of model 12

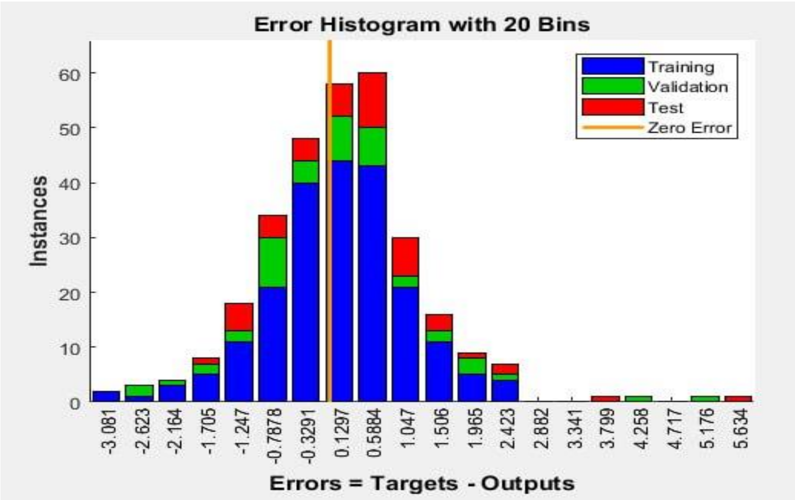

Figure 24: Error histogram of model 12 for ϕ prediction

Error distribution of the entire data using model 12 is plotted on an error histogram graph of Figure 24. A significant concentration of error is seen at 0, indicating a minimum difference between actual and predicted values.

4.8 ANN Equations

A sigmoid function is commonly used as a transfer function, while other differentiable nonlinear functions can also be used. Incorporating these functions allowed for the mapping of desirable nonlinear input–output relations. In this study, the hyperbolic tangent sigmoid function (tansig), which is represented by Equation 4.1, was chosen as the transfer function in the hidden neurons.

$$F\ tansig = f(x) = \frac{2}{1+e^{-2x}} - 1 \qquad \text{Equation 4.1}$$

4.8.1 ANN Model Equation for c

The most effective result for cohesion value prediction was achieved by Model 7 of the network 5-10-1 architecture. From the model equation, a model equation can be created that describes the weights and biases between input-hidden and hidden-output neurons. Table 16 presents the weight and bias matrices for the model.

Table 16: Weights and Biases of Model 7 (Network 5-10-1) for c Prediction

	Connection Weights (w_{ih})						Biases	
h	**LL(x1)**	**PL(X2)**	**PI(X3)**	**Sand%(x4)**	**Fine%(x5)**	**V_h**	**b_h**	**b_o**
1	-1.636	-0.484	-0.907	-0.367	1.028	2.162	-0.345	-0.345
2	0.307	-1.630	2.698	0.954	0.935	3.013	0.869	
3	-0.601	0.405	-1.337	3.741	-2.501	3.880	0.683	
4	-1.173	0.187	1.106	0.386	-1.019	0.115	-2.002	
5	1.139	-2.006	1.164	-2.646	0.356	-1.989	0.479	
6	-1.187	-1.834	-0.386	0.804	2.504	-0.031	-0.314	
7	1.793	0.116	0.897	0.221	-2.406	2.799	1.810	
8	-0.922	1.537	1.220	1.734	4.271	-0.351	-1.109	
9	-0.314	2.165	-2.354	3.775	1.461	-2.273	0.337	
10	-0.684	0.589	2.638	-2.005	-3.821	1.971	-2.478	

wih is a 10 by 5 connection weight between the input and hidden neurons; since i represents the input variables which is equal to 5, and 10 represents the number of hidden neurons that is equal to 10. vh is a 10 by 1 connection weight between h^{th} hidden layer and output layer of h equal to 10 hidden neurons, and 1 represents the number of output layer. bh is bias at the h^{th} neuron of hidden layer and b0 is a bias at output layer with one output c. The weighted sum, wh for each hidden neurons is calculated as:

$$wh = bh + \sum p\ i{=}1(wih * xi) \qquad \text{Equation 4.2}$$

xi represents the normalized value of the input variables. Min, max normalization was used in this research, given by:

$$xi = \left(\frac{Xnorm,max - Xnorm,min}{Xmax - Xmin}\right)(x - xmin) + xnorm,min \qquad \text{Equation 4.3}$$

Where, xmin is the minimum value of each input variables of the entire data set; xmax is the maximum value of each input variables of the entire data set; xnorm,min is the minimum value of the normalized data range; and xnorm,max is the maximum value of the normalized data range. The values used for normalizing each input variables are tabulated below in Table 17.

Table 17: Normalizing Values for Input Variables of c

X_{min}	$\frac{Xnorm,max - Xnorm,min}{Xmax - Xmin}$)	$X_{norm,min}$
29	0.0301	-1
8	0.0477	
3.2	0.0708	
1	0.0890	
30.91	0.1188	

The resulted value of a 10 by 1 weighted sum (wh), calculated by using Equation 4.2 was then inserted into the hyperbolic tangent sigmoid transfer function in Equation 4.4.

$$Th = Ftansig\ (wh) = \frac{2}{1 + e^{-2Wh}} - 1 \qquad \text{Eqaution 4.4}$$

The summation of the resulted a 10 by 1 matrix value of Th multiplied with corresponding values of vh 10 by 1 matrixes was then added with b0 value as shown in Equation 4.5 resulting normalized c value.

$$c\ norm = b0 + \sum_{h=1}^{n}(vh * Th) \qquad \text{Equation 4.5}$$

Finally, the real values of c then can be obtained by denormalizing the normalized c values with respect to the values given in Table 18 and by using Equation 4.6.

$$c = \frac{Cnorm - Ynormmin}{\left(\frac{Ynorm,max - Ynorm,min}{Ymax - Ymin}\right)} + Ymin \qquad \text{Equation 4.6}$$

Table 18: Normalizing Values for Output Variable c

Ynorm,min	-1
$\frac{Ynorm,max - Ynorm,min}{Ymax - Ymin}$	0.0311
Ymin	5

The formulation of c, based on the ANN result is as given in Equation 4.2 to 4.6. Using these mathematical equations output can be derived from input variables.

4.8.2 ANN Model Equation for ϕ

Model 12 of network 5-11-1 architecture gave the best result for prediction of ϕ values. A model equation can be formulated from the model equation in terms of weight and biases between input-hidden and hidden-output neurons.

Table 19: Weights and Biases of Model 12 (Network 5-11-1) for ϕ Prediction

	Connection Weights (w_{ih})						Biases	
h	**LL(x1)**	**PL(X2)**	**PI(X3)**	**Sand%(x4)**	**Fine%(x5)**	**V_h**	**b_h**	**b_o**
1	-0.950	-2.303	0.533	-1.468	0.772	1.723	-0.411	1.551
2	1.009	-1.397	1.498	-1.269	1.087	-1.284	0.070	
3	0.933	-1.210	0.506	0.707	-0.248	1.794	-1.650	
4	0.985	-2.457	1.954	-2.256	-0.208	0.211	0.800	
5	-0.823	-0.660	-0.159	-3.117	1.275	2.285	1.189	
6	0.388	-0.385	-0.732	1.794	0.959	-0.144	2.107	
7	0.544	-0.538	1.220	0.778	1.613	0.631	-0.450	
8	0.145	-0.280	2.029	-0.103	-0.599	1.104	0.617	
9	1.691	3.098	-0.853	0.802	0.241	3.589	0.314	
10	1.421	1.551	1.317	1.007	0.682	1.172	0.503	
11	0.443	1.249	-1.516	-0.644	-1.224	2.058	-0.435	

Table 20: Normalizing Values for Input Variables of ϕ

X_{min}	$\frac{Xnorm,max-Xnorm,min}{Xmax-Xmin}$)	$X_{norm,min}$
29	0.0294	-1
8	0.1322	
3.2	0.0497	
1	0.0680	
30.91	0.0416	

Following the same procedure for deriving model equation for c, by using Equations 4.2 to 4.5 and weight and bias values tabulated in Table 19, normalized ϕ shown in Equation 4.7 was obtained.

$$\phi norm = b0 + \sum n\ h{=}1(vh * Th) \qquad \text{Equation 4.7}$$

Finally, the real values of ϕ then can be obtained by denormalizing the normalized ϕ values with respect to the values given in Table 21 and by using Equation 4.8.

$$\Phi = \frac{\phi norm - Ynormmin}{\left(\frac{Ynorm,max-Ynorm,min}{Ymax-Ymin}\right)} + Ymin \qquad \text{Equation 4.8}$$

Table 21: Normalizing Values for Output Variable Φ

Ynorm,min	-1
$\frac{Ynorm,max - Ynorm,min}{Ymax - Ymin}$	0.0516
Ymin	5.8

4.9 Comparison of Current ANN Model with Existing Regression analysis and ANN Model Correlations

4.9.1 Regression Analysis

One of the main goals of the current study is to establish and develop a simple model that will allow analysts to predict responses for future observations with accuracy. Within the parameters of the investigation, the multivariable linear least square regression (LLSR) was used to conduct a regression analysis. Many assumptions are made regarding the predictor variables, the response variables, and their relationship in standard linear regression models (LLSR) using conventional estimate techniques. Each of these assumptions can be relaxed (i.e. reduced to a weaker version) by a number of extensions, and in some cases they can even be entirely eliminated. Depending on the method, it may be possible to relax multiple assumptions simultaneously. In other circumstances, this may be possible by combining several extensions. These expansions typically increase the complexity and length of the estimation process, and they may also require more data in order to build a model with an equivalent level of precision. The impact of geotechnical variables on shear strength parameters was investigated, including sand %, fine %, liquid limit, plastic limit, and plasticity index. The most influencing variables were chosen using a stepwise regression technique. Multiple regression models are developed in the equations below for the prediction of shear strength parameters by using excel.

$C = 20 + 2.18LL - 2.05PL - 2.36PI + 0.06F + \varepsilon$ Equation 4.9

$\emptyset = -29.51 + 0.45F + 0.46S + \varepsilon$ Equation 4.10

The multiple regression (R) values for both c and ϕ are 0.35 and 0.64 respectively. The R^2 values are 0.12 and 0.41 for c and ϕ respectively.

4.9.2 Comparison of Current Regression and ANN Model with Existing Regression analysis

For Bishoftu town, no specific equation has been developed for obtaining shear strength parameters from index properties. However, the literature presents a variety of empirical methods for predicting soil shear strength values. Four of these have been selected in order to evaluate the relative effectiveness of the ANN model. These techniques were chosen because both the models were created for fine-grained soils and the database used in this work includes the majority of the parameters needed to determine shear strength parameters by these methods. The selected existing regression and ANN models are illustrated in the tables below.

Table 22: Comparison of ANN Model and Existing Correlations for c Prediction

Existing Models	Equation for c	R	MSE	RMSE
Roy, (2014)	c= 224.032- 2.272 PL- 2.485 PI	0.036	72.65	8.52
Ersoy et al., (2013)	c= 0.265(PI/LL) $^{2.78}$	0.108	134.50	11.60
Goktepe et al., (2008)	c= 1.61- 0.03 ω- 0.01PI	0.592	94.17	9.70
Current Regression	20+2.18LL-2.05PL-2.36PI+0.06F	0.35	50.471	7.104
Current ANN	ANN	0.982	1.27	1.12

Table 23: Comparison of ANN Model and Existing Correlations for Φ Prediction

Existing Models	**Equation for ϕ**	**R**	**MSE**	**RMSE**
Roy,(2014)	ϕ= -29.604 + 34.220 BD	0.296	175.92	13.26
Ersoy et al., (2013)	ϕ= -204.5(PI/LL) + 56.3(PI/LL) +31	0.309	123.52	11.11
Goktepe et al., (2008)	ϕ= -6.38 + 0.58 ω + 0.05 PI	0.503	295.93	17.20
Current Regression model	-29.51+ 0.45 F+ 0.46 S	0.64	10.173	3.189
Current ANN model	ANN	0.987	1.15	1.07

4.9.3 Comparison of Current ANN Model with Existing ANN models

The following ANN models are models that includes database of the majority of the parameters needed to determine shear strength parameters by the methods. And also the table illustrated below is to show that the effect of the number of dataset have on the ANN modeling method. The current study is the largest dataset that developed the ANN model to estimate the shear strength parameters of soil from index properties.

Table 24: Comparison of existing ANN models with the current model for c prediction

ANN Models	No. of datasets	Soil types	R	MSE	RMSE
Lyeke et al., (2016)	83	Tropical lateritic soil	0.861	MAE=6.08	8.33
Kiran & Lal, (2016)	200	Sandy silt	0.942	3.97	11.68
Yoseph, (2022)	284	Fine grained	0.974	2.82	1.68
Current model	316	Black cotton soil	0.982	1.27	1.12

Table 25: Comparison of existing ANN models with the current model for ϕ prediction

ANN Models	No. of datasets	Soil types	R	MSE	RMSE
Lyeke et al., (2016)	83	Tropical lateritic soil	0.805	MAE=4.34	4.77
Kiran & Lal, (2016)	200	Sandy silt	0.981	5.65	6.04
Yoseph, (2022)	284	Fine grained	0.965	1.72	1.31
Current model	316	Black cotton soil	0.987	1.15	1.07

5 Conclusion and Recommendation

5.1 Conclusion

The goal of the research was to develop ANN models that could predict the values of the soil shear strength parameters (cohesion and angle of internal friction) based on the properties of the soil index. Three hundred one secondary and fifteen primary soil test result data a total of 316 were used for the purpose of this study to generate better generalization potential and minimize error. A Pearson correlation analysis was carried out to study the relative relationship of the factors that affect shear strength parameters. Artificial neural network models for c and ϕ were developed and separately validated using the test data. The feed-forward architecture of the multilayer perceptron (MLP) with the back propagation technique was used. The following conclusions are taken from the study's findings:

- As determined by prior literature, the most suitable input parameters for this study are liquid limit, plastic limit, plasticity index, sand percentages, and fine percentages. And less interdependence exists between the parameters.
- The optimum architecture for the ANN network for cohesion was found to be 5-10-1 (five inputs, ten hidden layer nodes, and one output node) with a correlation coefficient of R=0.99 for testing data and MSE= 1.27. While the angle of friction had an optimal ANN geometry of 5-11-1 (five inputs, eleven hidden layer nodes, and one output node) with a correlation coefficient R= 0.98 for testing data and MSE= 1.15.
- The selected best models for both cohesion and friction angle were used to predict the shear strength parameters of soil of primary data from their index properties for validation. And the results between the experimental and predicted shear strength parameters obtained by the models showed a good performance with a regression value of R= 0.98 for both cohesion and angle of friction.
- The ANN models were compared to currently formulated regression model in the study area and also three previously formulated traditional methods that has common input parameters. The results obtained demonstrated that the ANN method outperforms the empirical methods considered.
- Equations for the ANN models were derived.

- According to the results, it can be said that the developed ANN models perform the best in terms of accuracy in prediction and generalization. This indicates that the suggested models are accurate and reliable in describing soil shear strength parameters using the input ranges taken into consideration in this study. Therefore, the developed ANN models can be used to predict the values of shear strength parameters from soil index properties for the study area Bishoftu and places with similar soil types as Bishoftu.

5.2 Recommendation

1) Further studies can be done to improve the accuracy and generalization capacity of the soil shear strength parameters prediction by further increasing the size and diversity of the training dataset. It can be achieved by collecting data from various soil types, geological formations, and regions.
2) While this study focused on utilizing index properties as input parameters, incorporate additional input parameters would be beneficial to explore the inclusion of other relevant factors that influence soil shear strength parameters. For instance, parameters such as organic content, compaction characteristics, and stress history could potentially improve the predictive capabilities of the ANN models.
3) The soils of Bishoftu town were the only ones used for the purpose of this study. In the future, efforts can broaden the scope and parameters. Due to the fact that soil properties vary from location to location and periodically, it is advised to do frequent soil studies.

REFERENCES

Abdulabbas, A. A.., & Bind, Y. (2014). Estimation of Shear Strength Parameters of Soils Using ANN. *International Journal of Civil, Structural, Environmental and Infrastructure Engineering*, *4*(3), 1–10.

Adugna, H. (2021). *Use of Artificial Neural Network To Predict Compaction Characteristics of Soil From Soil Index Properties (Case of Addis Ababa)*. Addis Ababa Institute of Technology.

Aslay, F., & Ustun, O. (2013). Estimating Soil Temperature With Artificial Neural Networks Using Meteorological Parameters. *Journal of Ploytechnic*, *16(4)*, 139–145.

Bakala, T. T., Quezon, E. T., & Yasin, M. (2021). Statistical Analysis on Shear Strength Parameter from Index Properties of Fine-grained Soils. *Journal of Engineering Research and Reports*, *April*, 15–28.

Balasubramanian, A. (2017). Soil Forming Processes and Factors. In *Centre for Advanced Studies in Earth Science*. University of Mysore, Mysore.

Das, Sarat Kumar. (2013). 10 Artificial Neural Networks in Geotechnical Engineering : Modeling and Application Issues. In *Metaheuristics in Water, Geotechnical and Transport Engineering* (First Edit, Issue 1994). Elsevier Inc.

Das, Sarat Kumar, & Basudhar, P. K. (2008). Prediction of residual friction angle of clays using artificial neural network. *Engineering Geology*, *100*(3–4), 142–145.

Dipo Theophilus Akomalfe, and O. S. E. (2013). Comparative study of the biological and artificial neural networks. *European Journal of Applied Engineering and Scientific Research, Pp. 36-46*.

El-Maksoud, M. A. F. (2006). Laboratory determining of soil strength parameters in calcareous soils and their effect on chiseling draft prediction. *Proceedings of Energy Efficiency and Agricultural Engineering International Conference*, *1*(1), 1–13.

Ersoy, H., Betül Karsli, M., Çellek, S., Kul, B., Baykan, I., & Parsons, R. L. (2013). Estimation of the soil strength parameters in Tertiary volcanic regolith (NE Turkey) using analytical hierarchy process. *Journal of Earth System Science*, *122*(6), 1545–

1555.

Foram S. Panchal & Mahesh Panchal. (2014). Review on Methods of Selecting Number of Hidden Nodes in Artificial Neural Network. *International Journal of Computer Science and Mobile Computing*, *3(11)*, 455–464.

Gallo, C. (2018). Artificial Neural Networks tutorial. *Encyclopedia of Information, Science and Technology*, *Third Edit*, 6369–6378.

Gevrey, M., Dimopoulos, I., & Lek, S. (2003). Review and comparison of methods to study the contribution of variables in artificial neural network models. *Ecological Modelling*, *160*(3), 249–264.

Goktepe, A. B., Altun, S., Altintas, G., & Tan, O. (2008). Shear strength estimation of plastic clays with statistical and neural approaches. *Building and Environment*, *43*(5), 849–860.

Gopal Ranjan. A S R Rao. (2011). *Basic and Applied Soil Mechanics* (Third edit). New Age International.

Hamzacebi, C. (2011). Artificial neural networks: predictive use of MATLAB and Neurosolutions applied. *Neural Computing and Applications*, 17–31.

Harini, H., & Naagesh, S. (2014). Predicting CBR of fine-grained soils by artificial neural network and multiplelinear regression. *Internat. Jour. Civil Engg. Tech. (IJCIET), v.5(2)*, 119–126.

Harsh Kukreja, B. N. & K. S. (2016a). An Introduction to Artificial Neural Network. *International Journal Of Advance Research And Innovative Ideas In Education*, *1*, 27–30.

Haykin, S., & Network, N. (2004). *Neural Networks A comprehensive foundation: Vol. Second edi*. McMaster University.

Jiawei Han, M. K. & J. P. (2012). Data Mining Concepts and Techniques. *Academic Press, Morgan Kaufmann*, 50.

Juwaied, N. S. (2018). Applications of artificial intelligence in geotechnical engineering. *ARPN Journal of Engineering and Applied Sciences*, *13(8)*, 2764–2785.

Khanlari, G. R., Heidari, M., Momeni, A. A., & Abdilor, Y. (2012). Prediction of shear strength parameters of soils using artificial neural networks and multivariate regression methods. *Engineering Geology*, *131–132*, 11–18.

Kiran, S., & Lal, B. (2016). Modelling of soil shear strength using neural network approach. *Electronic Journal of Geotechnical Engineering*, *21*(10), 3751–3771.

Korayem, A., Ismail, K., & Sehari, S. (1996). Prediction of soil shear strength and penetration resistance using some soil properties. *Journal of Agricultural Research*, *13(4)*, 119–140.

Lee, S. J., Lee, S. R., & Kim, Y. S. (2003). An approach to estimate unsaturated shear strength using artificial neural network and hyperbolic formulation. *Computers and Geotechnics*, *30*(6), 489–503.

Lek, S., Delacoste, M., Baran, P., Dimopoulos, I., Lauga, J., & Aulagnier, S. (1996). Application of neural networks to modelling nonlinear relationships in ecology. *Ecological Modelling*, *90*(1), 39–52.

Lyeke, Eze, Ehiorobo, & O. (2016). The Estimation of Shear Strength Parameter of Lateritic Soils Using Artificial Neural Network. *Canadian Geotechnical Journal*, *15*(34), 315–321.

Michele Scardi, Lawerence W, H. J. (1999). Developing empirical model of a neural network case study. *Ecological Modelling*, *4*(1), 88–100.

Mollahasani, A., Alavi, A. H., Gandomi, A. H., & Rashed, A. (2011). Nonlinear neural-based modeling of soil cohesion intercept. *KSCE Journal of Civil Engineering*, *15*(5), 831–840.

Mousavi, S. M., & Alavi, A. H. (2011). Nonlinear genetic-based simulation of soil shear strength parameters. *Journal of Earth System Science*, *6*, 1001–1022.

Murthy, V. (2002). *Geotechnical engineering: principles and practices of soil mechanics and foundation engineering*. CRC press.

Obasi, N. L., & Anyaegbunam, A. J. (2005). Correlation of the Undrained Shear Strength and Plasticity Index of Tropical Clays. *Nigerian Journal of Technology*, *24*(2), 1–11.

Olden, J. D., & Jackson, D. A. (2002). Illuminating the “black box”: A randomization approach for understanding variable contributions in artificial neural networks. *Ecological Modelling*, *154*(1–2), 135–150.

P. Kim. (2017). MATLAB Deep Learning With Machine Learning, Neural Networks, and Artificial Intelligence. In *Apress*.

Roy, S. (2014). Statistical models for the prediction of shear strength parameters. *International Journal of Civil and Structural Engineering*, *4*(4), 483–498.

S. Karsoliya. (2012). Approximating Number of Hidden layer neurons in Multiple Hidden Layer BPNN Architecture. *International Journal of Engineering Trends and Technology*, *3(6)*, 714–717.

Shahin, M. A., Jaksa, M. B., & Maier, H. R. (2001). Artificial Neural Network Applications in Geotechnical Engineering. *Australian Geomechanics*, *36(1)*, 49–62.

Shahin, M. A. (2013). Artificial Intelligence in Geotechnical Engineering: Applications, Modeling Aspects, and Future Directions. In *Metaheuristics in water, geotechnical and transport engineering* (First Edit). Elsevier Inc.

Shahin, M. A., Jaksa, M. B., & Maier, H. R. (2009). Recent Advances and Future Challenges for Artificial Neural Systems in Geotechnical Engineering Applications. *Advances in Artificial Neural Systems*, *2009*, 1–9.

Shahin, M. A., Maier, H. R., & Jaksa, M. B. (2004). Data Division for Developing Neural Networks Applied to Geotechnical Engineering. *Journal of Computing in Civil Engineering*, *18*(2), 105–114.

Shooshpasha, I., Amiri, I., & MolaAbasi, H. (2015). An investigation of friction angle correlation with geotechnical properties for granular soils using GMDH type neural networks. *Scientia Iranica*, *22*(1), 157–164.

Vanneschi, L., & Silva, S. (2023). Artificial Neural Networks. In *Natural Computing Series*.

Yoseph, H. (2022). *Estimation of Soil Shear Strength Parameters From Index Properties Using Ann the Case of Addis Ababa*. Addis Ababa Institute of Technology.

Zumrawi, M. M. E., & Mohammed, L. A. D. (2016). Correlation of Placement Conditions and Soil Intrinsic Properties with Shear Strength of Cohesive Soils. *In 7th Annual Conference for Postgraduate Studies and Scientific Research- Khartoum*, 7.

APPENDIX A: DETAILS OF SECONDARY DATA

	Atterberg limits			Grain size		Shear strength parameters	
1	LL	PL	PI	Sand%	Fine%	c	Ø
2	58	34.7	23.3	26.16	40.98	8	5
3	53.5	32.9	20.6	44.97	43.22	14	13
4	54.4	34.7	19.7	33.56	44.77	10	6
5	46.5	33.8	12.7	35.32	50.85	8	10
6	30	13	17	20.74	70.45	9	10
7	32	20	12	28	65	14	7
8	32	8	24	20.74	69.12	10	9
9	32	11	21	19.51	70.67	11	9
10	32	12	20	18.9	71.22	12	9
11	32	20	12	21	72	19	10
12	32	19	13	20.69	70.89	15	10
13	32	14	18	16.77	72.33	13	9
14	32	10	22	15.4	72.8	14	7
15	33	14	19	18.9	65.77	11	8
16	33	9	24	16.77	70.22	16	8
17	33	12	21	13.2	73.4	14	7
18	33	11	22	13	74.56	14	7
19	34	14	20	18.9	69.88	16	9
20	34	10	24	20.74	70	15	9
21	34	8	26	16.77	73.44	20	8
22	35	15	20	15.8	69.88	19	9
23	35	17	18	13.2	69.9	19	9
24	35	13	22	18.9	70.88	17	9
25	35	11	24	16.77	71.22	19	8
26	35	13	22	15.8	72.31	18	8
27	35	16	19	20.74	72.33	18	11
28	35	14	22	22.12	75.46	17	13
29	35	15	20	12.01	85.86	30	11
30	36	20	16	36.23	30.91	2	2
31	36	11	25	20.74	69.44	18	10
32	36	12	24	15.8	73.4	20	8
33	36	14	22	13.7	84.36	27	11
34	36	13	23	11.45	85.67	25	9
35	37	17	20	14.53	80.94	22	12
36	37	14	23	19.77	75.12	21	11
37	37	16	21	15.8	73.4	20	9
38	37	13	24	16.77	73.44	22	9
39	37	12	25	17.31	78.65	24	10

40	37	15	23	16.77	79.11	18	11
41	37	16	21	12.67	85.86	29	12
42	38	11	26	19.51	70.67	24	9
43	38	16	22	10.33	87.89	26	11
44	38	15	23	18.9	72.33	22	10
45	38	12	26	16.77	73.44	24	8
46	42	25.6	16.4	17.65	75.44	24	9
47	41.4	28.6	12.8	16.77	77.98	24	7
48	51.2	35.5	15.7	16.54	81.22	29	12
49	38	17	21	12.11	85.42	25	12
50	39	15	24	15.4	69.67	28	9
51	39	14	25	13.2	70.5	28	8
52	39	16	23	19.8	71.73	23	10
53	39	13	26	16.77	72.31	25	9
54	39	18	21	20	74.5	22	12
55	39	17	22	11.31	85.16	20	11
56	39	19	20	10.11	87.02	22	13
57	40	17	23	21	69.49	24	11
58	40	12	28	16.77	71.22	28	9
59	40	16	24	19	73.12	24	11
60	40	13	27	20.74	74.56	24	11
61	40	25	15	18.79	79.32	30	10
62	57.5	36.4	21.1	22.09	76.33	28	13
63	41.1	27.4	13.7	16.81	75.5	21	7
64	61.2	35.8	25.4	14.4	79.05	26	14
65	71.4	42.3	29.1	13.7	84.36	27	17
66	41	18	23	13.2	68.55	34	9
67	41	19	22	18.9	69.9	28	11
68	41	21	20	21	71.32	25	11
69	41	20	21	13.2	71.45	29	10
70	41	15	26	10.56	87.56	21	10
71	41.13	27	14	17.85	74.52	22	7
72	41.6	34.8	6.8	26.25	68.65	27	15
73	42	17	25	18.9	68.38	30	10
74	42	21	21	15.4	69.4	32	11
75	42	19	23	15.4	72.12	29	10
76	42	22	20	22	72.33	26	12
77	42	15	27	18.79	72.33	27	10
78	42	13	29	16.77	78.65	26	10
79	42	28	14	18.44	80.56	32	8
80	43	25	18	28	62.86	24	6
81	43	22	21	22	66.6	28	11
82	43	20	23	18.9	69.8	30	11
83	43	16	27	13.2	72.31	31	9

84	43	19	24	21	72.32	26	12
85	44	23	21	23.11	65.87	28	10
86	44	21	23	21	69.9	29	12
87	44	20	24	21	72.12	27	13
88	44	20	24	21	72.12	27	13
89	44	21	23	15.8	72.33	31	11
90	44	21	23	15.8	72.33	31	11
91	44	27	17	12.74	85.76	28	12
92	45	22	23	28	69.86	27	15
93	45	21	24	15.8	71.54	33	11
94	45.8	23	22.8	28	65	28	12
95	46	32	14	69.45	45.07	30	19
96	46	33	13	73.14	47.63	43	18
97	46	23	23	28	65	28	12
98	46	24	22	28	65	28	10
99	46	31	15	21.25	69.58	24	6
100	46	22	24	13.2	69.87	39	11
101	46	21	25	15.4	72	34	11
102	46	34	12	19.89	74.68	21	10
103	47	21	26	15.4	70.78	37	11
104	47	22	25	22	70.83	29	13
105	47	31	16	8.3	94	35	12
106	47.1	30	17.1	8.29	91	24	13
107	48	23	25	18.6	69.6	36	12
108	49	20	29	27.15	62.31	24	14
109	49	25	24	21	73.5	28	13
110	50	25	25	17.9	70.6	37	13
111	51	28	23	23.6	71.6	29	11
112	52	23	29	45	49	9	17
113	53	22	31	18.85	69.34	38	13
114	53	32	21	24.4	70.9	29	9
115	53	28	25	20.97	71.23	32	12
116	54	29	25	22.7	70.6	31	11
117	55	33	22	23.89	66.87	32	9
118	56	29	27	21	70.25	35	13
119	56	17	39	10.96	83.24	18	11
120	57	16	41	11.33	85.67	19	12
121	59	35	24	24.56	59.87	36	9
122	60	37	23	11.2	86.9	24	15
123	60	39	21	11.9	90.9	42	17
124	60.1	37.1	23	11.16	85.29	21	15
125	60.15	37	23	14.23	85.29	32	14
126	60.47	39	21	12.2	87.9	37	16
127	60.5	39.5	21	11.9	86.14	29	16

128	61	40	21	33.54	50.54	19	13
129	63	42	21	28	65	25	18
130	68	45	23	35.46	49.77	23	19
131	69	45	24	21	72	21	18
132	79	21	58	8.66	85.54	11	22
133	88	47	42	3.28	93.72	7	23
134	99.77	41.84	57.93	10.89	87.75	16	19
135	100	42	58	1	99	19	21
136	103	41	62	1	99	20	20
137	106	43	63	1	99	21	19
138	107.77	41.84	65.93	8.69	90.54	20	15
139	108	42	66	7.59	89.89	17	15
140	82	39	43	22.09	76.32	21	18
141	76	40	36	22.12	72.33	29	15
142	63	32	31	16.77	76.55	26	17
143	29	18	11	10.3	88.45	51	15
144	74	42	32	15.8	73.44	34	16
145	71	40	31	10.78	88.33	22	19
146	83	39	44	19	72.45	27	19
147	82	49	33	9	91	25	17
148	85	50	35	18.9	69.6	34	17
149	65	34	31	27	62.31	36	11
150	66	39	27	21	73.5	28	14
151	77	41	36	18	70.6	38	15
152	49	30	18	24	71.6	32	8
153	91.7	40.01	51.69	45	49	22	11
154	69.8	32.5	37.3	32.5	69.8	12	19
155	73.29	29.69	43.6	13.63	73.29	23	17
156	106.61	40.31	66.3	2	98	22	18
157	118.81	44.29	74.52	1	99	27	17
158	112.8	43.47	69.33	3	97	24	16
159	86	43	43	40	50	27	15
160	84	43	41	42	59	21	20
161	83	43	40	45	55	21	20
162	78	40	38	49	48	16	15
163	73	39	34	39	68.9	18	20
164	67	35	32	28	70	22	15
165	63	36	27	22	73	28	13
166	84	44	40	33	67.84	17	21
167	81	41	40	16.58	74.21	29	18
168	76	40	36	11.87	81.89	16	21
169	71	37	34	17	76	27	17
170	68	35	33	10.5	88	15	20
171	62	31	31	22.45	74.55	24	16

172	63	32	31	19	71.97	35	16
173	96.67	36.9	59.8	4	95.67	17	20
174	94	39.2	55	6.2	93.89	16	21
175	67	31	36	14.4	85.4	17	19
176	81	37	44	6.5	93.3	14	24
177	78	35.5	42.5	5.7	94.1	15	23
178	65	29	36	27.2	72.11	16	20
179	63	32	31	27	73.94	19	16
180	72	31	41	35.8	63.77	16	20
181	70	33	37	27.2	68.59	24	17
182	72	30	42	21.6	77.24	16	21
183	73	35	38	14.2	85.09	16	22
184	74	29	45	24.8	75.56	15	23
185	73	31	41	25.8	73.65	17	22
186	68	31	37	33.4	66.57	17	19
187	64	33	31	36.2	73.66	21	21
188	76	29	47	28.2	71.77	13	23
189	65	34	31	16.2	82.65	22	17
190	62	29	33	30.8	68.8	19	18
191	62	31	31	21.4	78.38	23	17
192	64	30	34	24.8	75.64	18	19
193	62	32	30	24.8	74.76	22	15
194	54.8	36.16	18.64	13	85	28	13
195	48.3	28.64	19.66	24	74	29	9
196	45.26	28.24	17.02	26	71	31	8
197	68.8	26.31	42.49	21	79	16	20
198	61.5	33.6	27.9	56	42	18	16
199	57.4	30.1	27.3	6	94	17	17
200	63.2	40.31	22.89	58	41	20	16
201	72.1	42.23	29.87	9	91	25	19
202	47	31.3	15.7	5	94	19	14
203	57	31.6	25.4	10	89	18	16
204	42	25.6	16.4	5	95	29	15
205	41.4	28.6	12.8	6	94	29	13
206	51.2	35.5	15.7	5	95	20	15
207	57.5	36.4	21.1	10	90	27	14
208	41.1	27.4	13.7	11	83	21	10
209	61.2	35.8	25.4	8	87	9	18
210	71.4	42.3	29.1	11	89	28	18
211	68.6	39.6	29	10	90	25	19
212	62.4	34.9	27.5	7	91	12	19
213	63.1	36.1	27	14	84	24	15
214	64.5	35.2	29.3	11	88	20	18
215	65.2	37	28.2	11.5	85	18	17

216	65.4	36.3	29.1	9.88	85	13	19
217	50.2	28.5	21.7	12.55	79	21	13
218	43.9	30.5	13.4	58.89	41	18	19
219	51.7	39	12.7	5.99	91	13	15
220	57.1	31.1	26	49.78	42	16	15
221	71.5	39.5	39	26.52	79	11	18
222	58	25	33	39.65	56	14	19
223	42	20	22	9.89	86	15	12
224	59	22	37	10.21	89	15	13
225	37.5	15.5	22	49.77	48	7	21
226	45	22	23	6.87	91	15	13
227	48	20	28	8	92	19	12
228	41	17	24	20	80	26	14
229	61	39	22	18.7	80.74	34	16
230	52.6	39.7	12.9	14.79	84.77	33	19
231	53.4	38.8	14.6	8.44	90.11	24	17
232	57	27	30	11.38	86.91	15	16
233	61.7	33.7	28	4.33	93	6	20
234	58.6	37.5	21.1	9.94	89.1	26	15
235	53.6	37.5	16.1	11.49	87.34	29	15
236	47.9	36.2	11.7	11.5	87.41	30	14
237	59.5	39.7	19.8	18.9	77.46	27	16
238	48.6	37.3	11.3	50.85	46.79	18	21
239	63.6	41.3	22.3	58.37	39.59	21	17
240	52.7	36.4	16.3	8	91	23	14
241	51.7	38.2	13.5	8.57	89.51	23	17
242	45.4	36.3	9.1	5.65	94.35	21	17
243	51.3	38.7	12.6	3	97	13	20
244	56.2	38.4	17.8	11.04	87.44	28	15
245	57.4	39.5	17.9	25.73	72.58	27	18
246	49.7	37.5	12.2	9.53	89.6	28	16
247	43.6	36.6	7	25.7	72.6	33	19
248	46.6	37.5	9.1	12.25	86.37	27	18
249	53.6	37.5	16.1	15.44	77.7	20	13
250	43.6	36.6	7	24.93	69.68	24	17
251	53.6	37.5	16.1	24.27	74.31	29	16
2512	43.6	35.9	7.7	11.69	88	31	17
253	58.7	39.4	19.3	15.4	83	33	16
254	40.4	37.2	3.2	12.4	87	21	23
255	52.7	37.4	15.3	21.55	75.32	25	15
256	50.7	37.5	13.2	14.14	75.27	11	14
257	57.5	37.4	20.1	10.26	84.09	17	15
258	52.4	37.1	15.3	11.74	85.85	26	14
259	55.4	37.7	17.7	23.08	74.34	27	15

260	49.4	38.6	10.8	22.62	70.96	19	17
261	52.7	37.2	15.5	10.77	85.99	23	14
262	53.7	37.6	16.1	10.8	87.34	26	15
263	44.7	35.2	9.5	14.87	83	27	14
264	59.7	39.5	20.2	16.16	77.1	25	15
265	60.4	40.7	19.7	14.15	72.78	23	16
266	50.3	36.5	13.8	10.86	82.63	15	13
267	50.4	37.6	12.8	10.71	82.35	12	15
268	53.4	37.5	15.9	9.22	89.4	25	15
269	56.2	39.4	16.8	2.91	96	10	20
270	68.6	39.6	29	2.51	97.24	17	24
271	62.4	34.9	27.5	11.02	88.79	23	17
272	63.1	36.1	27	14.19	82.75	24	15
273	64.5	35.2	29.3	14.1	85.9	25	17
274	65.2	37	28.2	10	90	23	18
275	48.5	37.4	11.1	19	81	31	17
276	51.4	37.4	14	11.3	88.7	33	15
277	58.7	36.4	22.3	10.9	89.1	28	14
278	50.3	37.4	12.9	10.7	89.3	32	16
279	52.3	38.5	13.8	12.3	87.7	34	17
280	45.7	37.3	8.4	12.3	86	26	18
281	48.4	36.5	11.9	27.8	72.2	38	18
282	52.7	37.3	15.4	14.3	85.7	36	15
283	48.6	37.3	11.3	19.8	80.2	31	17
284	52.2	37.4	14.8	12.5	87.5	34	15
285	51.3	38.7	12.6	24.3	75.7	32	20
286	53.9	37.4	16.5	19.1	80.9	34	15
287	55.7	38.2	17.5	21.2	78.8	32	16
288	55.4	38.3	17.1	14.7	85.3	37	16
289	53.3	39.5	13.8	25.7	74.3	32	21
290	51.3	36.6	14.7	17.2	82.8	35	14
291	58.7	39.2	19.5	12.6	87.4	35	17
292	50.9	37.5	13.4	11.1	88.9	32	16
293	51.3	36.2	15.1	26.1	73.9	34	16
294	56.4	37.5	18.9	17.9	82.1	36	14
295	54.4	37.5	16.9	30.1	69.9	34	19
296	45.7	37.2	8.5	11.7	88.3	30	18
297	45.2	35.6	9.6	13.5	86.5	33	15
298	54.4	38.2	16.2	12.1	87.9	34	16
299	56.4	37.5	18.9	21	79	32	15
300	54.4	37.5	16.9	13.8	86.1	35	15
301	57.7	38.5	19.2	6.8	93.2	23	17

APPENDIX B: DETAILS OF GRAIN SIZE ANALYSIS TEST RESULTS

Table 26: Dry sieve analysis for TP 1

Testpit 1					
Sieve *ASTM*	Sieve Opening(*mm*)	WeightRetaine doutof1000*g*	%Retained	Cumulative %Retained	%Finer
3/8"	9.50	0	0.00	0	100.00
No.4	4.75	9	0.90	0.90	99.10
No.8	2.36	4	0.40	1.30	98.70
No.10	2.00	2	0.20	1.50	98.50
No.16	1.18	2	0.20	1.70	98.30
No.30	0.600	5	0.50	2.20	97.80
No.40	0.425	6	0.60	2.80	97.20
No.50	0.300	6	0.60	3.40	96.60
No.100	0.150	13	1.30	4.70	95.30
No.200	0.075	12	1.20	5.90	94.10

Table 27: Hydrometer analysis for TP 1

ElapsedTime,T(min)	ActualHydrometerReading,Ra	Corrected Hydrometer reading,Rc	Effective DepthL(cm)	√(L/T)	Coefficient, K fromTable	Diameter ofparticle,D (mm)	% Finer	Adjustpercent PA
0.5	46	44.35	8.8	4.1952	0.01253	0.053	88.10	82.90
1	45	43.35	8.9	2.9833	0.01253	0.037	86.12	81.03
2	44	42.35	9.1	2.1331	0.01253	0.027	84.13	79.17
5	42	40.35	9.4	1.3711	0.01253	0.017	80.16	75.43
10	40	38.35	9.7	0.9849	0.01253	0.012	76.18	71.69
20	38	36.35	10.1	0.7106	0.01253	0.009	68.24	67.95
40	36	34.35	10.4	0.5099	0.01253	0.006	68.24	64.21
80	33	31.35	10.9	0.3691	0.01253	0.005	62.28	58.60
120	29	27.35	11.5	0.3096	0.01253	0.004	54.33	51.13
240	25	23.35	12.2	0.2255	0.01253	0.003	46.39	43.65
480	21	19.35	12.9	0.1639	0.01253	0.002	38.44	36.17
1440	14	12.35	14	0.0986	0.01253	0.001	24.53	23.09

Table 28: Dry sieve analysis for TP 4

Testpit4					
Sieve *ASTM*	Sieve Opening(*mm*)	WeightRetained outof1000*g*	%Retained	Cumulative %Retained	%Finer
3/8"	9.50	0	0.00	0	100.00
No.4	4.75	5	0.50	0.50	99.50
No.8	2.36	0	0.00	0.50	99.50
No.10	2.00	2	0.20	0.70	99.30
No.16	1.18	3	0.30	1.00	99.00
No.30	0.600	5	0.50	1.50	98.50
No.40	0.425	4	0.40	1.90	98.10
No.50	0.300	6	0.60	2.50	97.50
No.100	0.150	9	0.90	3.40	96.60
No.200	0.075	11	1.10	4.50	95.50

Table 29: Hydrometer analysis for TP 4

Elapsed Time,T(min)	ActualHydrometerReading,Ra	CorrectedHydrometerreading, Rc	EffectiveDepthL(cm)	√(L/T)	Coefficient, K fromTable	Diameter ofparticle,D (mm)	% Finer	Adjust percent PA
0.5	47	45.35	8.6	4.1473	0.01253	0.052	90.29	86.23
1	46	44.35	8.8	2.9665	0.01253	0.037	88.30	84.33
2	45	43.35	8.9	2.1095	0.01253	0.026	86.31	82.42
5	43	41.35	9.2	1.3565	0.01253	0.017	82.33	78.62
10	41	39.35	9.6	0.9798	0.01253	0.012	78.34	74.82
20	38	36.35	10.1	0.7106	0.01253	0.009	66.40	69.11
40	35	33.35	10.6	0.5148	0.01253	0.006	66.40	63.41
80	31	29.35	11.2	0.3742	0.01253	0.005	58.43	55.81
120	27	25.35	11.9	0.3149	0.01253	0.004	50.47	48.20
240	23	21.35	12.5	0.2282	0.01253	0.003	42.51	40.59
480	17	15.35	13.5	0.1677	0.01253	0.002	30.56	29.19
1440	9	7.35	14.8	0.1014	0.01253	0.001	14.63	13.98

Table 30: Grain size distribution for TP 1, 2, 3, and 4

Testpit 1		Testpit 2		Testpit 3		Testpit 4	
SieveOpening,(*mm*)	%Finer	SieveOpening,(*mm*)	%Finer	SieveOpening,(*mm*)	%Finer	SieveOpening,(*mm*)	%Finer
9.500	100.000	9.500	100.000	9.500	100.000	9.500	100.000
4.750	99.000	4.750	99.100	4.750	99.800	4.750	99.500
2.360	96.000	2.360	98.700	2.360	99.800	2.360	99.500
2.000	95.300	2.000	98.500	2.000	99.800	2.000	99.300
1.180	93.400	1.180	98.300	1.180	99.800	1.180	99.000
0.600	91.700	0.600	97.800	0.600	99.800	0.600	98.500
0.425	90.100	0.425	97.200	0.425	99.200	0.425	98.100
0.300	88.000	0.300	96.600	0.300	98.200	0.300	97.500
0.150	85.100	0.150	95.300	0.150	95.400	0.150	96.600
0.075	82.800	0.075	94.100	0.075	93.800	0.075	95.500
0.052	72.886	0.053	82.904	0.049	93.613	0.052	86.227
0.037	71.256	0.037	81.035	0.035	91.754	0.037	84.326
0.027	69.625	0.027	79.166	0.025	89.894	0.026	82.424
0.017	66.364	0.017	75.427	0.016	88.035	0.017	78.622
0.012	63.103	0.012	71.688	0.012	84.317	0.012	74.819
0.009	59.842	0.009	67.950	0.008	80.598	0.009	69.115
0.006	54.950	0.006	64.211	0.006	76.880	0.006	63.411
0.005	50.058	0.005	58.603	0.005	69.443	0.005	55.805
0.004	45.167	0.004	51.126	0.004	62.006	0.004	48.200
0.003	38.644	0.003	43.649	0.003	52.710	0.003	40.594
0.002	30.492	0.002	36.171	0.002	43.413	0.002	29.186
0.001	19.078	0.001	23.086	0.001	28.539	0.001	13.975

Table 31: Grain size distribution for TP 4, 5, 6, 7, and 8

Testpit 5		Testpit 6		Testpit 7		Testpit 8	
SieveOpening,(*mm*)	%Finer	SieveOpening,(*mm*)	%Finer	SieveOpening,(*mm*)	%Finer	SieveOpening,(*mm*)	%Finer
9.500	100.000	9.500	100.000	9.500	100.000	9.500	100.000
4.750	99.200	4.750	99.600	4.750	97.700	4.750	99.000
2.360	98.700	2.360	98.700	2.360	97.000	2.360	98.900
2.000	98.700	2.000	98.300	2.000	96.600	2.000	98.800
1.180	98.300	1.180	97.100	1.180	95.700	1.180	98.500
0.600	97.500	0.600	95.300	0.600	94.000	0.600	98.000
0.425	96.400	0.425	93.800	0.425	92.600	0.425	97.200
0.300	94.900	0.300	92.000	0.300	90.500	0.300	96.200
0.150	92.900	0.150	88.800	0.150	88.400	0.150	95.100
0.075	91.200	0.075	86.600	0.075	87.200	0.075	94.400
0.052	83.873	0.053	78.448	0.053	79.334	0.051	90.728
0.037	82.077	0.038	76.743	0.038	77.609	0.037	88.865
0.027	80.281	0.027	75.038	0.027	75.884	0.026	87.002
0.017	78.485	0.017	73.332	0.017	74.160	0.017	85.139
0.012	74.893	0.012	71.627	0.012	72.435	0.012	83.276
0.009	73.097	0.009	68.216	0.009	70.710	0.008	81.413
0.006	69.505	0.006	64.805	0.006	67.261	0.006	77.687
0.005	64.117	0.005	59.689	0.005	60.363	0.005	73.961
0.004	56.933	0.004	52.867	0.004	53.464	0.004	68.372
0.003	49.749	0.003	46.046	0.003	46.565	0.003	60.920
0.002	40.769	0.002	37.519	0.002	39.667	0.002	53.468
0.001	24.605	0.001	23.876	0.001	25.870	0.001	36.701

Gravel(>4.75)

Sand(0.075-4.75)

Silt(0.005-0.075)

Clay (< 0.005)

Figure: Grainsizedistribution curveforTP 1 up to 8 tests

100

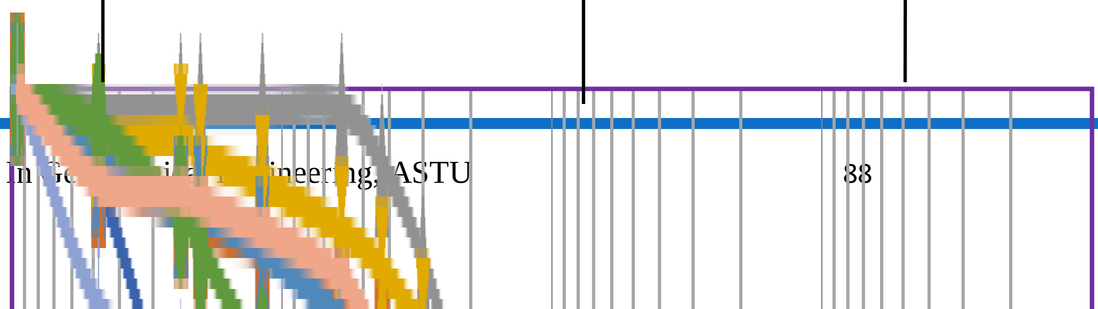

Table 32: Grain size distribution of TP 9

Sieve Size (mm.)	% Passed
4.750	100
2.000	100
0.425	99
0.075	96

%COBBLE	%GRAVEL	%SAND	%FINE
	NiL	4	96

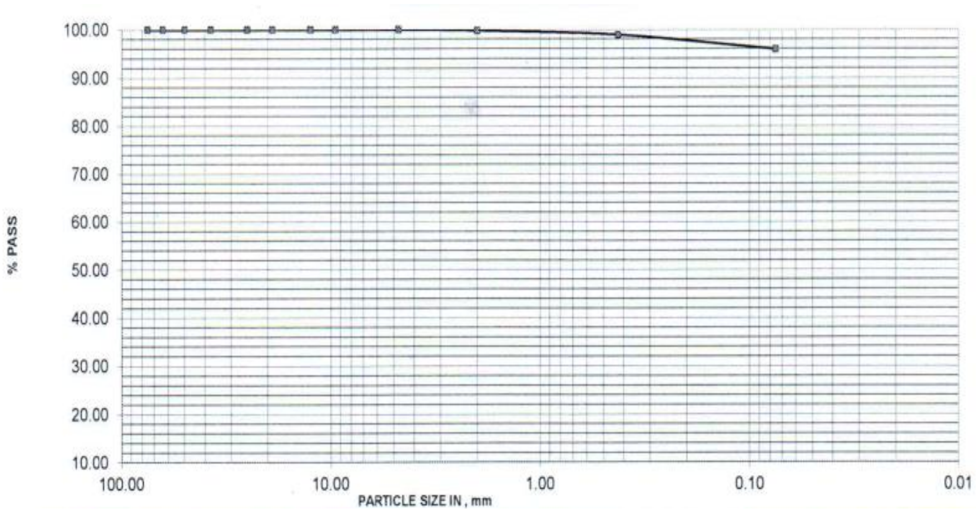

Figure 25: Grain size distribution curve of TP 9

Table 33: Grain Size Analysis of TP 10

Sieve Size (mm.)	% Passed
4.750	100
2.000	100
0.425	99
0.075	93

%COBBLE	%GRAVEL	%SAND	%FINE
	NiL	7	93

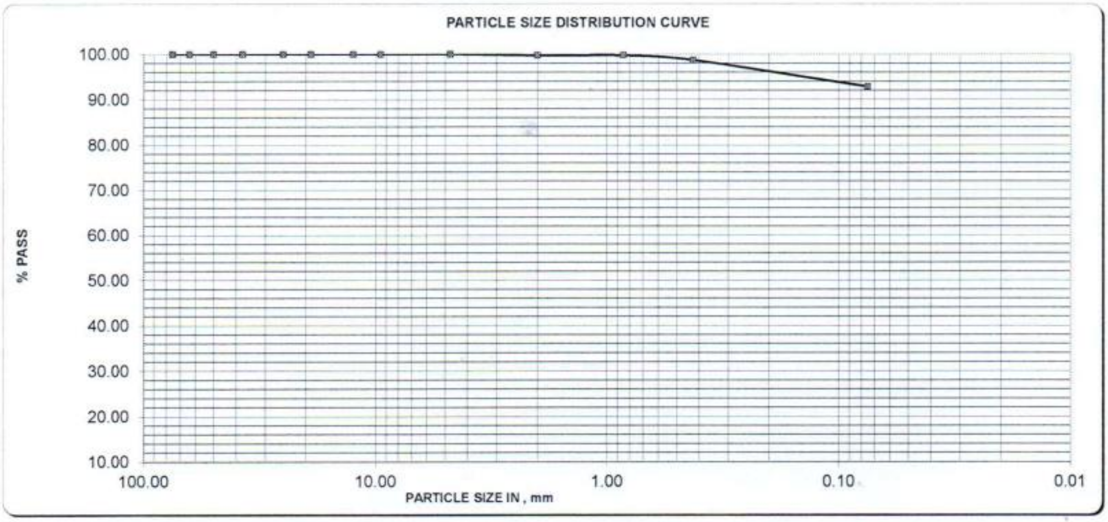

Figure 26: Grain Size Distribution Curve of TP 10

Table 34: Grain Size Analysis of TP 11

Sieve Size (mm.)	**% Passed**
4.750	100
2.000	100
0.425	99
0.075	96

%COBBLE	%GRAVEL	%SAND	%FINE
	NiL	4	96

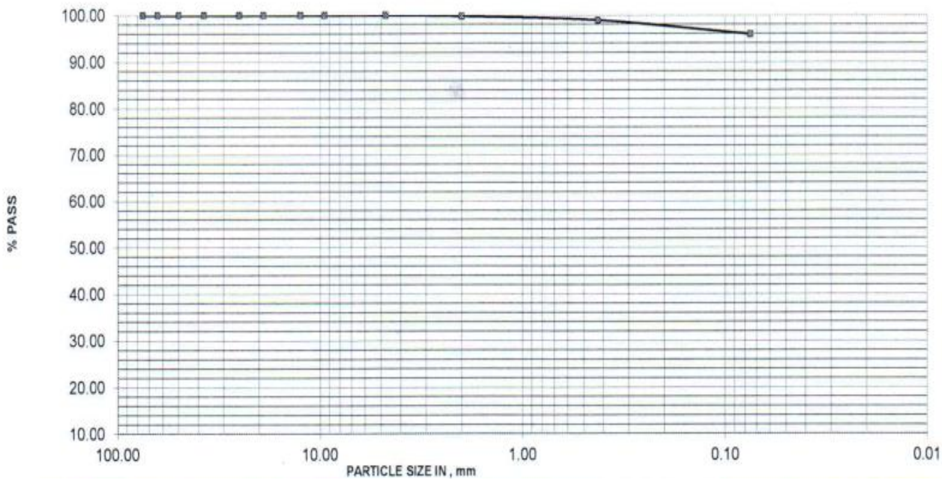

Figure 27: Grain Size Distribution Curve of TP 11

Table 35: Grain Size Analysis of TP 12

Sieve Size (mm.)	% Passed
4.750	100
2.000	100
0.425	98
0.075	94

%COBBLE	%GRAVEL	%SAND	%FINE
	NiL	6	94

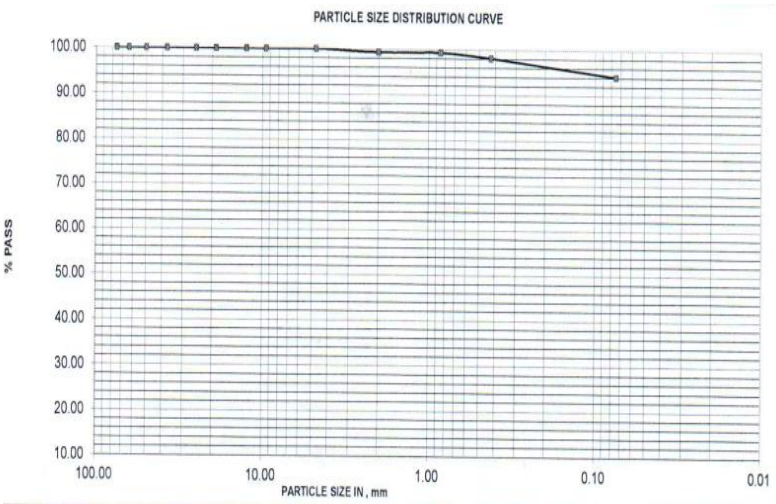

Figure 28: Grain Size Distribution Curve of TP 12

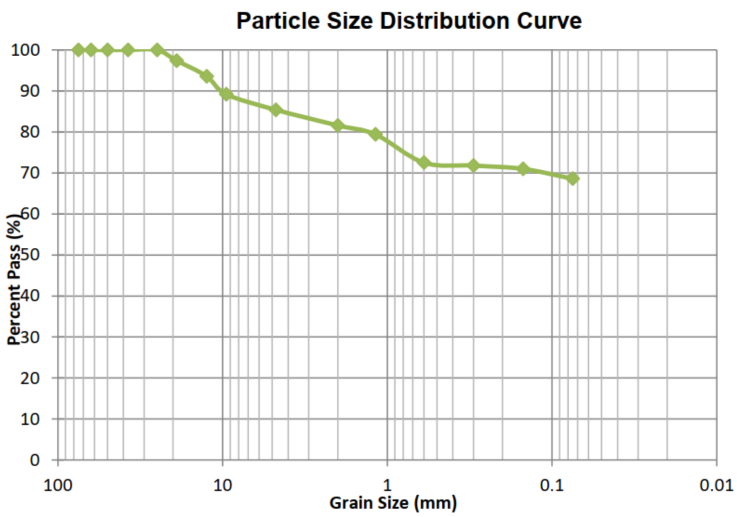

Figure 29: Grain Size Distribution Curves of TP 13

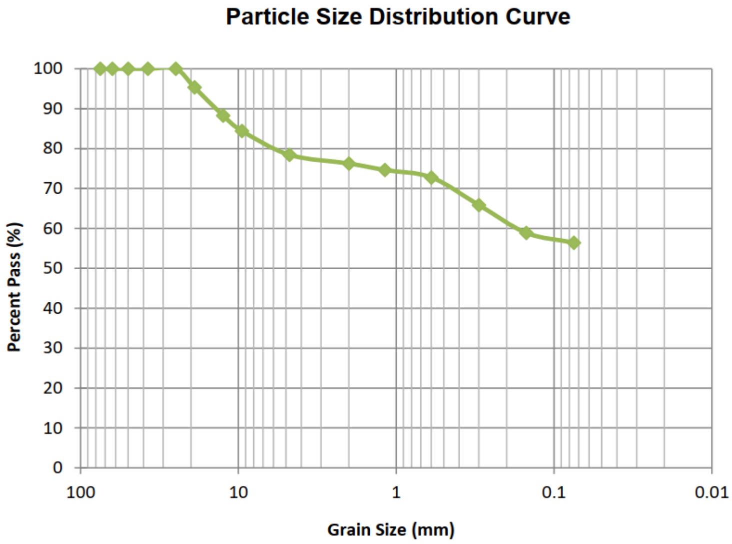

Figure 30: Grain Size Distribution Curves of TP 14

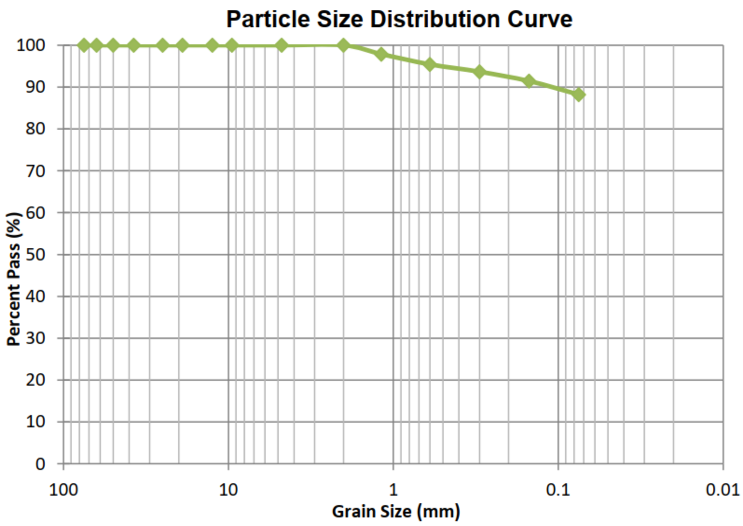

Figure 31: Grain Size Distribution Curves of TP 15

APPENDIX C: ATTERBERG LIMIT TEST RESULTS

Table 36: Atterberg Limits Analysis of TP1

Testpit 1@1mdepth	LiquidLimit(LL)			PlasticLimit(PL)		
TrialNo	1	2	3	1	2	3
Can No	A_1	A_2	A_3	B_1	B_2	B_3
Massofwet soil+ can,A(g)	42.15	42.53	43.71	41.09	41.14	40.91
Mass ofdrysoil + can,B(g)	37.96	37.89	38.43	38.79	38.69	38.26
Massofwater,C =(A–B)	4.19	4.64	5.28	2.30	2.45	2.65
Massofcan,D(g)	30.35	30.21	30.16	30.51	30.37	29.99
MassofdrysoilE=(B-D), (g)	7.61	7.68	8.27	8.28	8.32	8.27
Watercontent %(C /E x100)	55.06	60.42	63.85	27.78	29.45	32.04
Numberofblows	32	24	19			
Result,%	**59.8**			**29.8**		
PlasticityIndex(PI)=LL -PL	**30**					

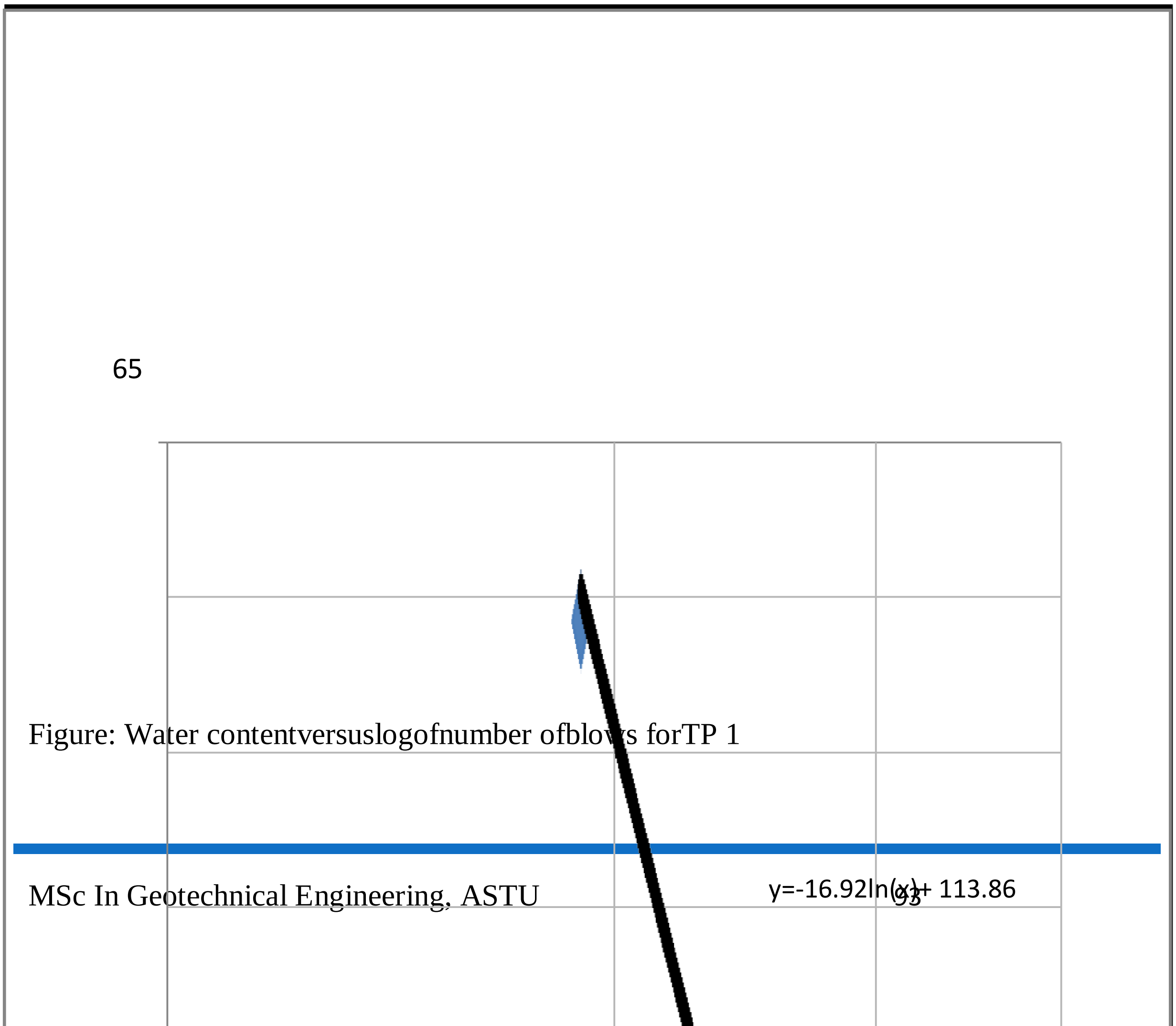

Figure: Water contentversuslogofnumber ofblows forTP 1

Table 37: Atterberg Limits Analysis of TP3

Testpit 2@1.5mdepth	LiquidLimit(LL)			PlasticLimit(PL)		
TrialNo	1	2	3	1	2	3
Can No	C_1	C_2	C_3	D_1	D_2	D_3
Massofwet soil+ can,A(g)	33.30	32.92	32.45	29.38	30.09	28.58
Mass ofdrysoil + can,B(g)	28.21	27.88	27.32	27.15	27.74	26.28
Massofwater,C =(A–B)	5.09	5.04	5.13	2.23	2.35	2.30
Massofcan,D(g)	19.48	19.69	19.44	19.73	19.69	19.29
MassofdrysoilE=(B-D), (g)	8.73	8.19	7.88	7.42	8.05	6.99
Watercontent %(C /E x100)	58.30	61.54	65.1	30.05	29.19	32.90
Numberofblows	35	24	15			
Result,%	**61.6**			**30.7**		
PlasticityIndex(PI)=LL -PL	**30.9**					

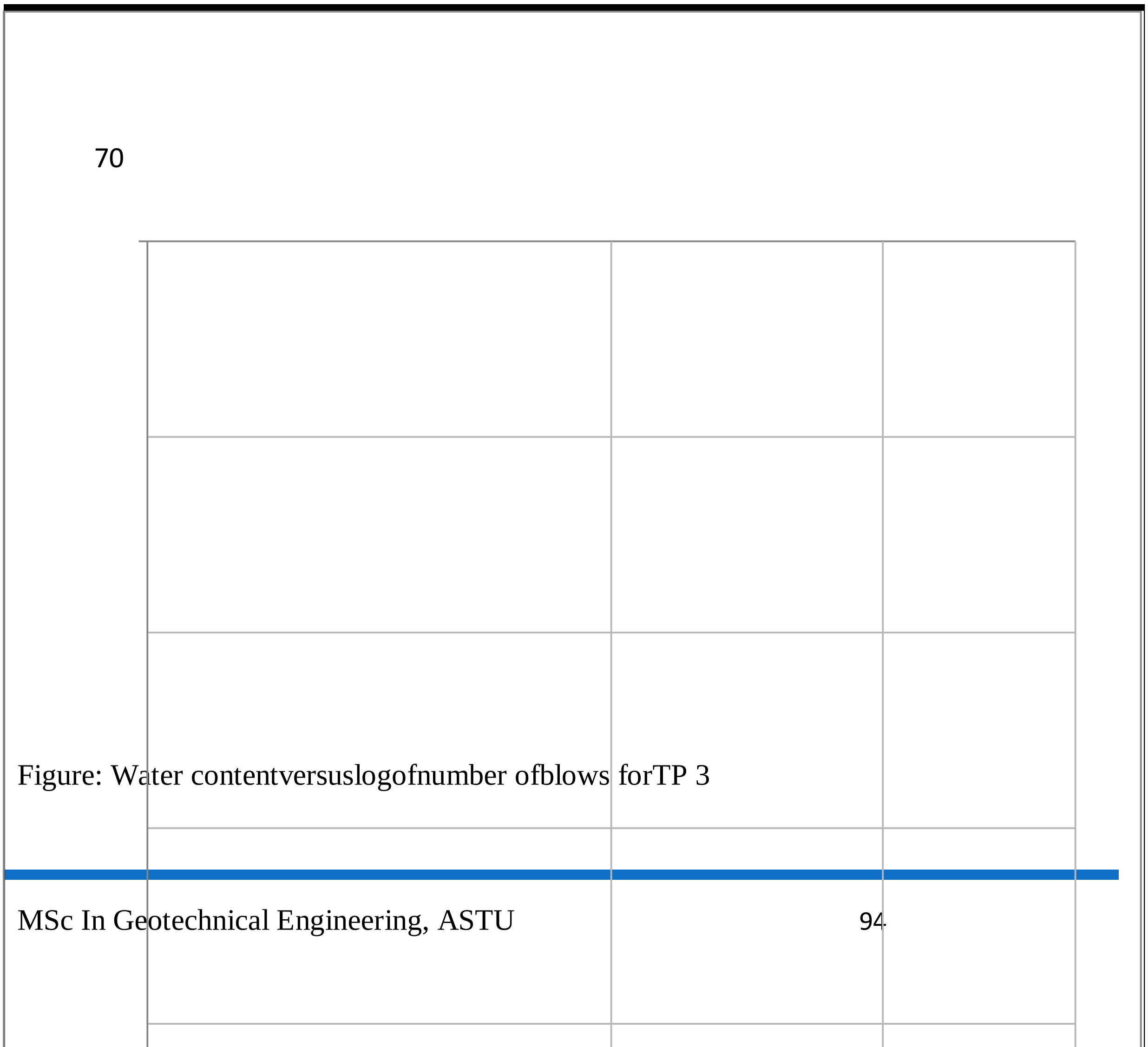

Figure: Water contentversuslogofnumber ofblows forTP 3

Table 38: Atterberg Limits Analysis of TP 5

Testpit 4@1.5mdepth	LiquidLimit(LL)			PlasticLimit(PL)		
TrialNo	1	2	3	1	2	3
Can No	C_1	C_2	C_3	D_1	D_2	D_3
Massofwet soil+ can,A(g)	33.42	35.22	34.34	42.18	44.32	43.41
Mass ofdrysoil + can,B(g)	28.16	28.86	28.3	39.73	41.44	40.53
Massofwater,C =(A–B)	5.26	6.36	6.04	2.45	2.88	2.88
Massofcan,D(g)	19.46	19.22	19.68	30.52	30.63	30.28
MassofdrysoilE=(B-D), (g)	8.7	9.64	8.62	9.21	10.81	10.25
Watercontent %(C /E x100)	60.46	65.98	70.07	26.60	26.64	28.10
Numberofblows	32	23	18			
Result,%	**65.5**			**27**		
PlasticityIndex(PI)=LL -PL	**38.5**					

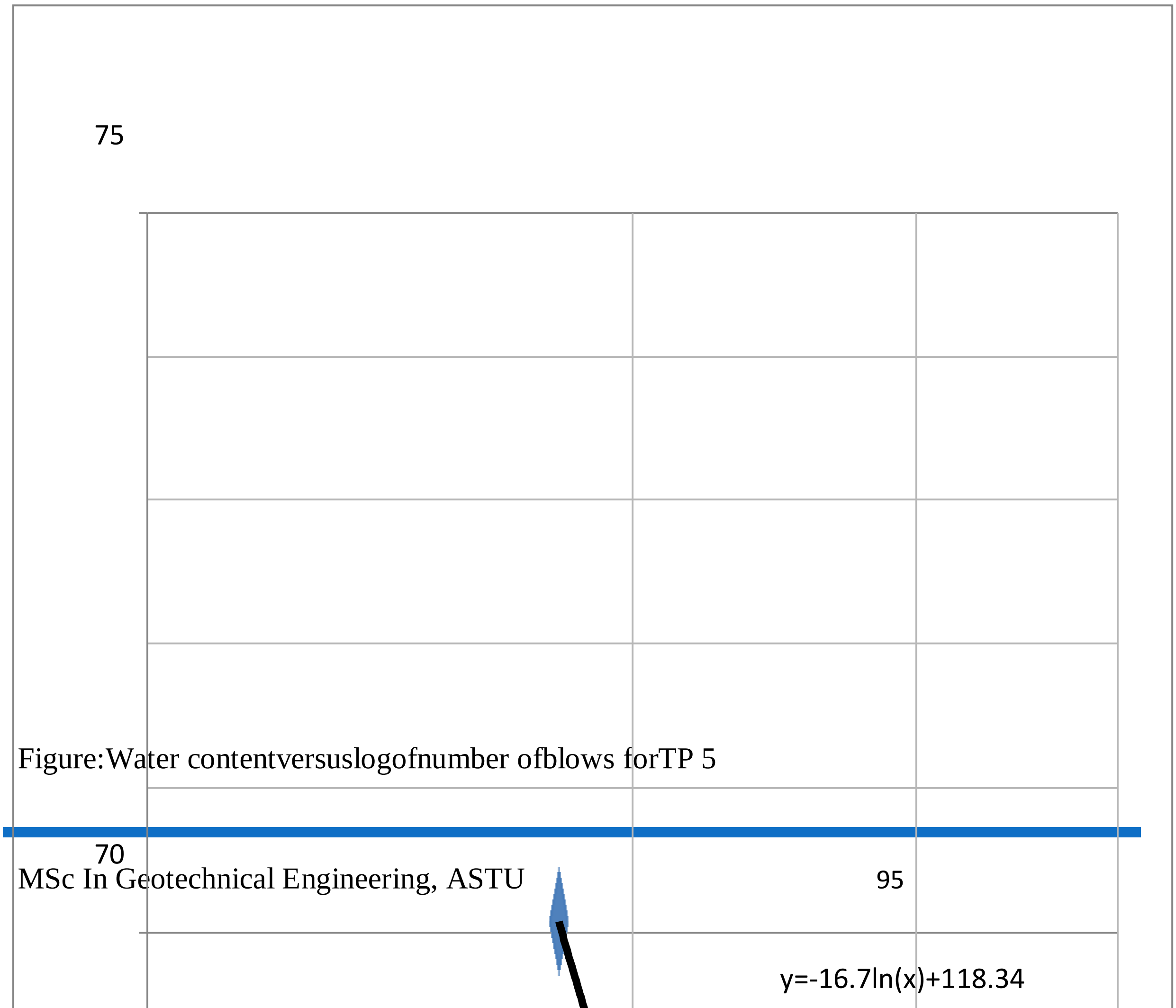

Figure:Water contentversuslogofnumber ofblows forTP 5

Table 39: Atterberg Limits Analysis of TP 6

Testpit 5@1mdepth	LiquidLimit(LL)			PlasticLimit(PL)		
TrialNo	1	2	3	1	2	3
Can No	P	Q	R	S	T	U
Massofwet soil+ can,A(g)	40.55	41.13	40.32	42.38	43.80	40.40
Mass ofdrysoil + can,B(g)	36.77	37.14	36.68	39.22	40.49	37.74
Massofwater,C =(A–B)	3.78	3.99	3.64	3.16	3.31	2.66
Massofcan,D(g)	29.84	30.24	30.53	29.86	30.67	29.58
MassofdrysoilE=(B-D), (g)	6.93	6.90	6.15	9.36	9.82	8.16
Watercontent %(C /E x100)	54.55	57.83	59.19	33.76	33.71	32.60
Numberofblows	35	25	20			
Result,%	**57.2**			**33.4**		
PlasticityIndex(PI)=LL -PL	**23.8**					

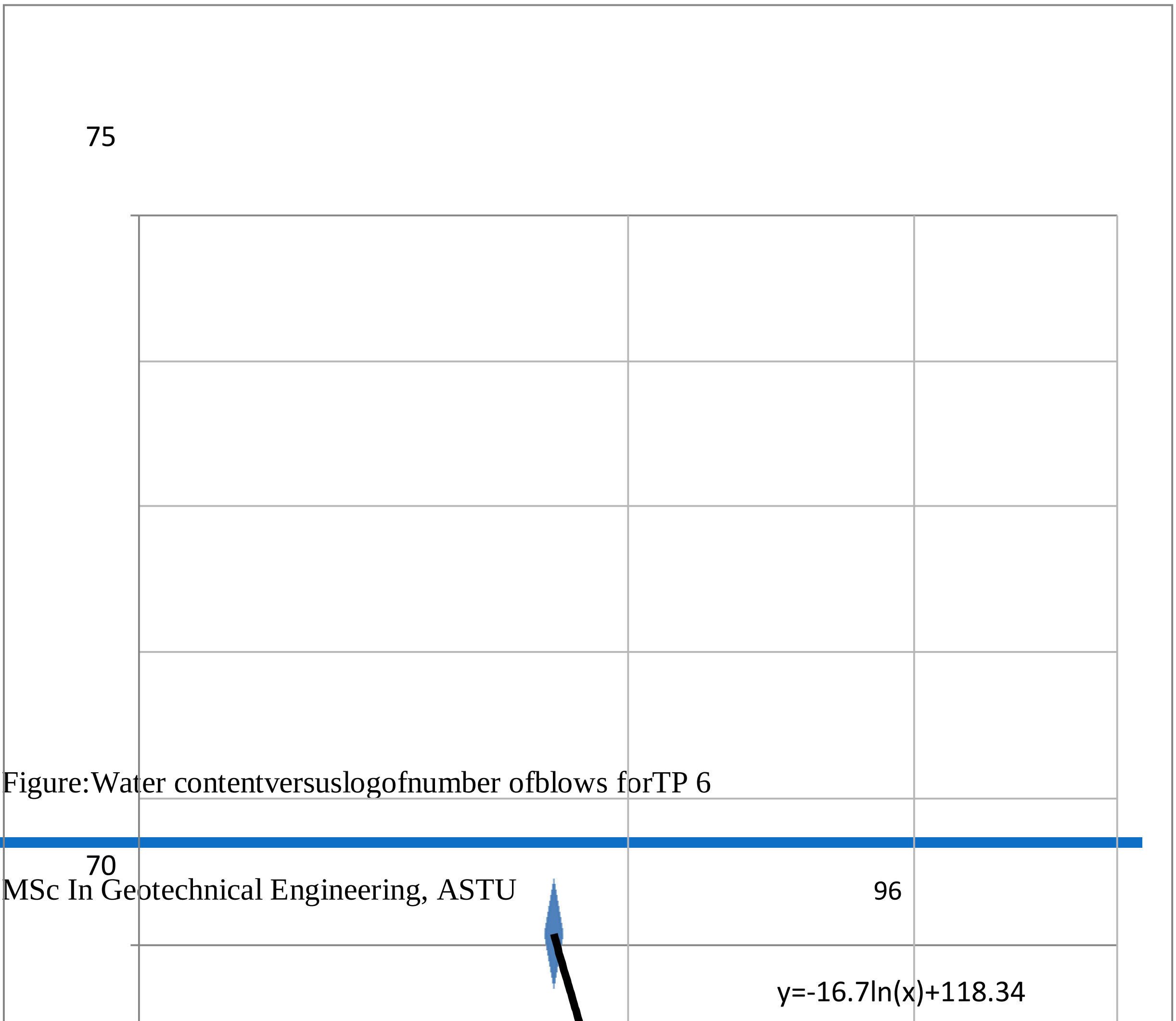

Figure:Water contentversuslogofnumber ofblows forTP 6

Table 40: Atterberg Limits Analysis of TP 9

	LIQUID LIMIT			PLASTIC LIMIT	
No. Blows	32	28	24		
Wt. wet soil (g.)	16.81	16.84	17.16	2.32	2.55
Wt. dry soil (g.)	9.98	9.90	10.02	1.68	1.84
Moisture content (%)	68.44	70.06	71.26	38.10	38.59
				AV. PL (%)	38.3

Liquid Limit LL(%)	Plastic Limit PL(%)	Plasticity Index PI	WET SEIVE ANALYSIS, % PASS		
			2mm	0.425mm	0.075mm
71	38	33			

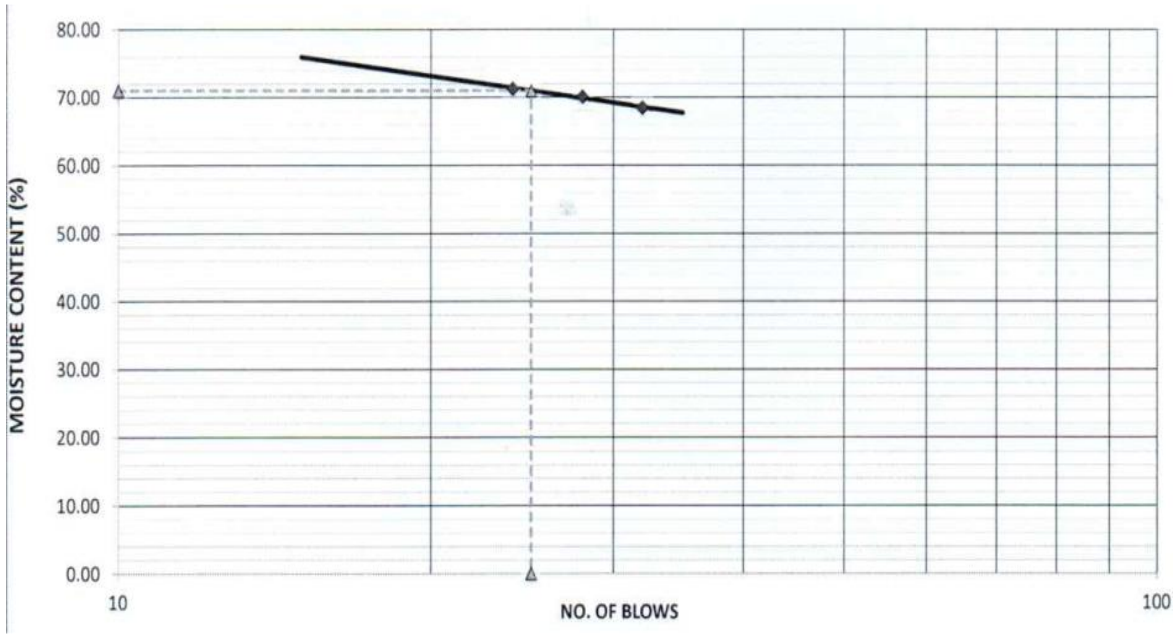

Figure 32: Water content versus log of number of blows for TP 9

Table 41: Atterberg Limits Analysis of TP 12

	LIQUID LIMIT			PLASTIC LIMIT	
No. Blows	35	30	24		
Wt. wet soil (g.)	16.04	16.86	16.89	2.95	2.53
Wt. dry soil (g.)	9.36	9.74	9.66	2.15	1.86
Moisture content (%)	71.37	73.10	74.84	37.21	36.02
				AV. PL (%)	36.6

Liquid Limit LL(%)	Plastic Limit PL(%)	Plasticity Index PI	WET SEIVE ANALYSIS, % PASS		
			2mm	0.425mm	0.075mm
75	37	38			

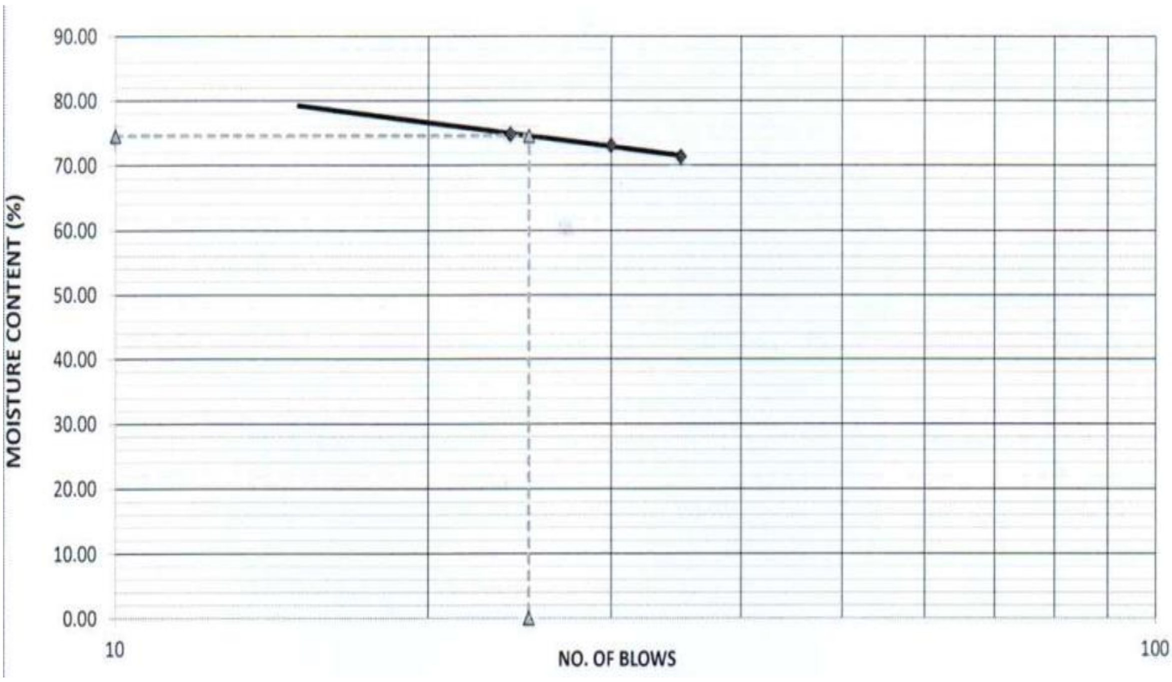

Figure 33: Water content versus log of number of blows for TP 12

Table 42: Atterberg Limits Analysis of TP 15

	LiquidLimit			**PlasticLimit**	
No. Blows	30	25	20		
Wt.ofcont. +wet soil(gm)	43.40	43.80	43.87	16.340	16.481
Wt.of cont.+ drysoil (gm)	35.64	35.83	35.87	15.693	15.846
Wt.ofwater(gm)	7.76	7.97	8.00	0.65	0.38
Wt.container(gm)	21.72	21.88	22.00	14.046	14.878
Wt. drysoil (gm)	13.92	13.95	13.87	1.65	0.97
Water(%)	55.76	57.11	57.68	38.80	38.20
	LL=56.2			**PL=38.4**	

APPENDIX D: DIRECT SHEAR TEST GRAPHS

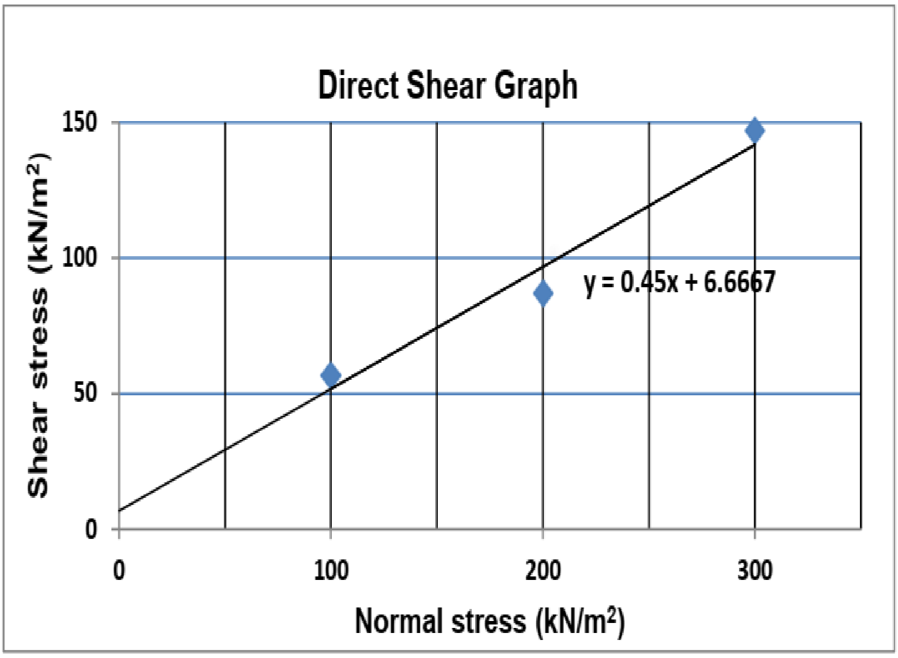

Figure 34: Direct shear test graph of TP1

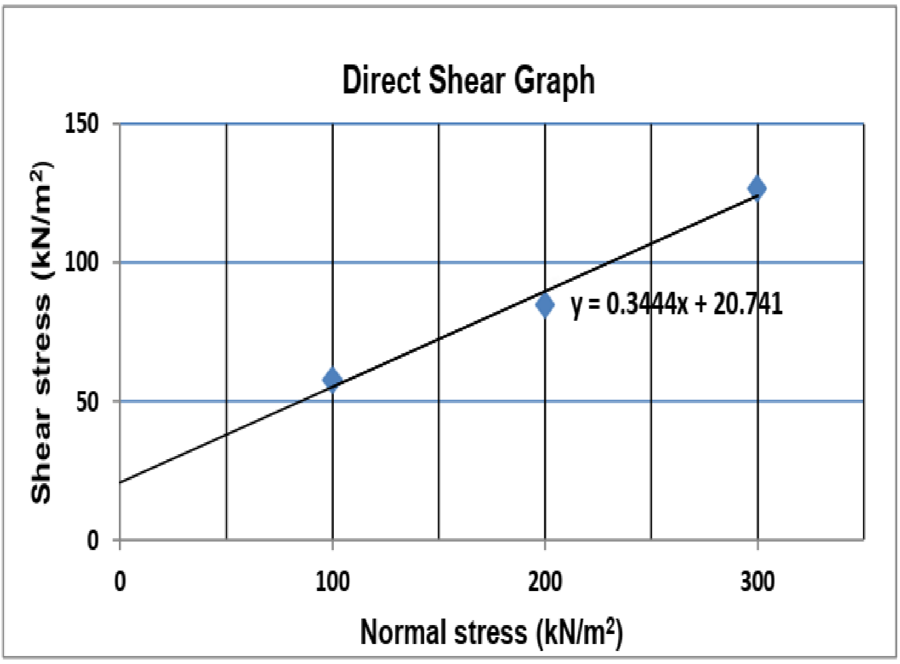

Figure 35: Direct shear test graph of TP3

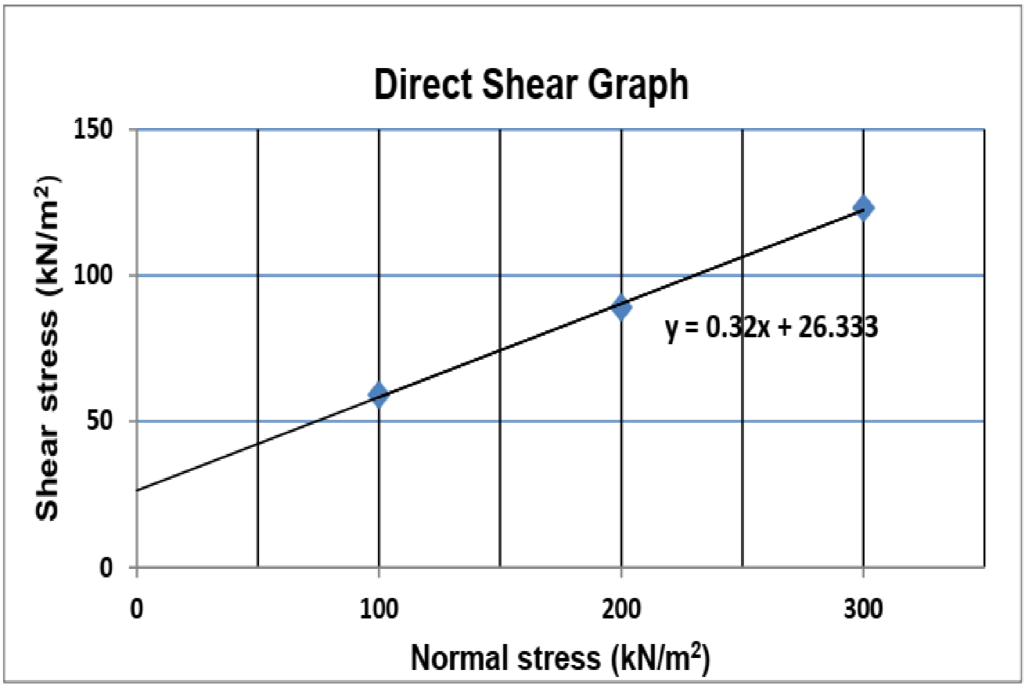

Figure 36: Direct shear test graph of TP6

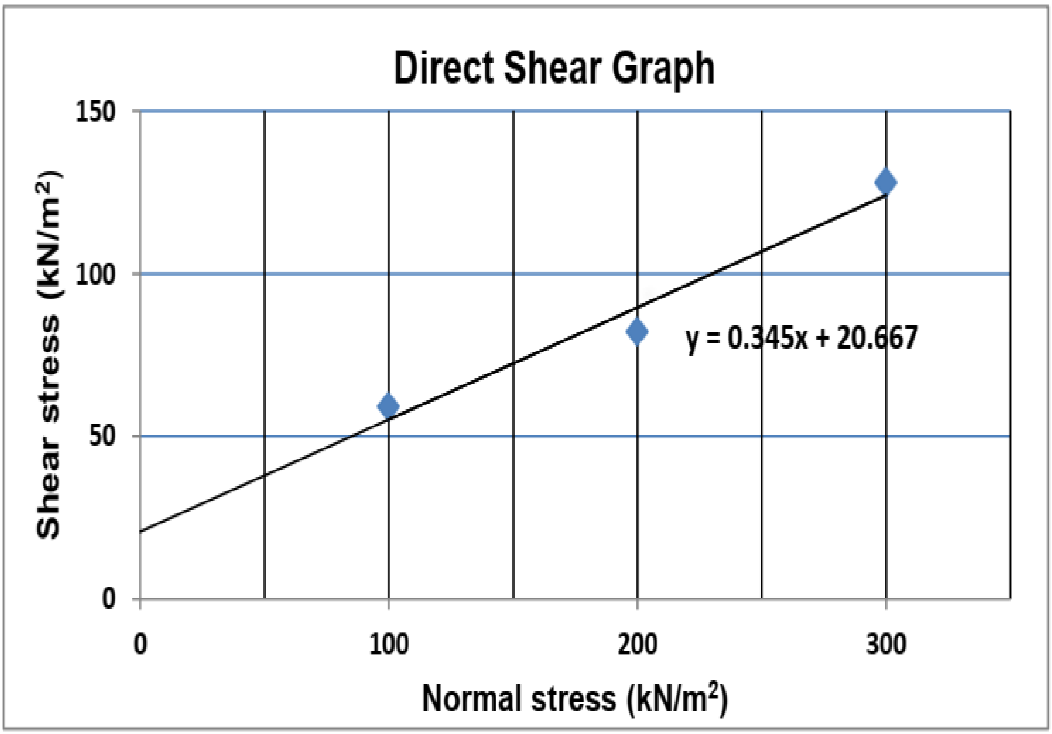

Figure 37: Direct shear test graph of TP8

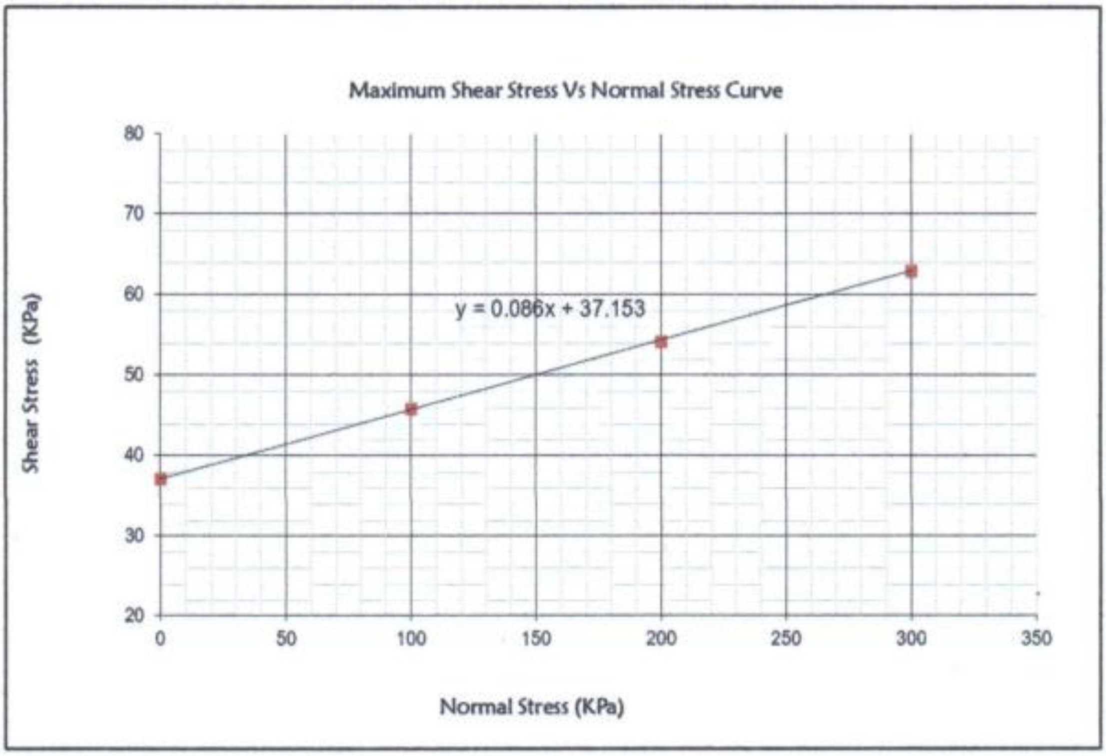

Figure 38: Direct shear test graph of TP9

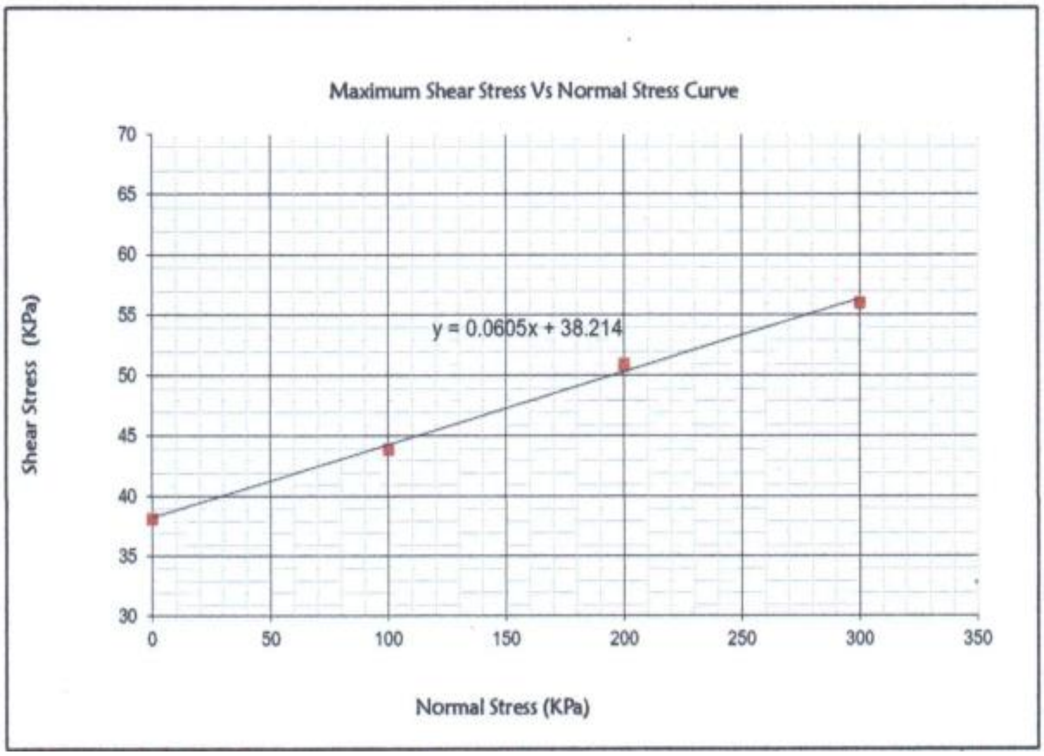

Figure 39: Direct shear test graph of TP12

APPENDIX C: MATLAB SCRIPT FILE FOR COHESION

```
Solve an Input-Output Fitting problem with a Neural Network
% Script generated by Neural Fitting app
% This script assumes these variables are defined:
%   data - input data.
%   data_1 - target data.

x = data';
t = c;

% Choose a Training Function
% For a list of all training functions type: help nntrain
% 'trainlm' is usually fastest.
% 'trainbr' takes longer but may be better for challenging problems.
% 'trainscg' uses less memory. Suitable in low memory situations.
trainFcn = 'trainlm';  % Levenberg-Marquardt backpropagation.

% Create a Fitting Network
hiddenLayerSize = 10;
net = fitnet(hiddenLayerSize,trainFcn);

% Setup Division of Data for Training, Validation, Testing
net.divideParam.trainRatio = 70/100;
net.divideParam.valRatio = 15/100;
net.divideParam.testRatio = 15/100;

% Train the Network
[net,tr] = train(net,x,t);

% Test the Network
y = net(x);
e = gsubtract(t,y);
performance = perform(net,t,y)

% View the Network
view(net)
view(net)
op = NEWINPUT1';
a=net(op)
% Plots
% Uncomment these lines to enable various plots.
%figure, plotperform(tr)
%figure, plottrainstate(tr)
```

```
%figure, ploterrhist(e)
%figure, plotregression(t,y)
%figure, plotfit(net,x,t)
```

APPENDIX D: MATLAB SCRIPT FILE FOR FRICTION ANGLE

```
% Solve an Input-Output Fitting problem with a Neural Network
% Script generated by Neural Fitting app
% This script assumes these variables are defined:
%
%   data - input data.
%   data_1 - target data.

x = data';
t = phi';

% Choose a Training Function
% For a list of all training functions type: help nntrain
% 'trainlm' is usually fastest.
% 'trainbr' takes longer but may be better for challenging problems.
% 'trainscg' uses less memory. Suitable in low memory situations.
trainFcn = 'trainlm';  % Levenberg-Marquardt backpropagation.

% Create a Fitting Network
hiddenLayerSize = 11;
net = fitnet(hiddenLayerSize,trainFcn);

% Setup Division of Data for Training, Validation, Testing
net.divideParam.trainRatio = 70/100;
net.divideParam.valRatio = 15/100;
net.divideParam.testRatio = 15/100;

% Train the Network
[net,tr] = train(net,x,t);

% Test the Network
y = net(x);
e = gsubtract(t,y);
performance = perform(net,t,y)

% View the Network
view(net)
op = Primaryinput2';
a=net(op)
% Plots
% Uncomment these lines to enable various plots.
%figure, plotperform(tr)
```

```
%figure, plottrainstate(tr)
%figure, ploterrhist(e)
%figure, plotregression(t,y)
%figure, plotfit(net,x,t)
```

Research Fund Acknowledgement

This research thesis was funded by Adama Science And Technology University under the grant number of ASTU/SM-R/841/23, Adama, Ethiopia.